

CENTRAL LIBRARY
TEZPUR UNIVERSITY
Accession No. 789
Date 26/02/13

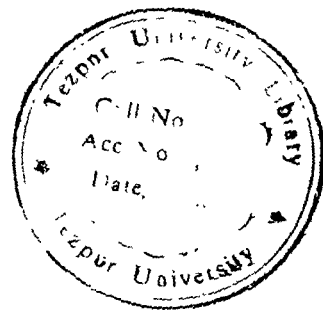


REFERENCE BOOK
NOT TO BE RETURNED
TEZPUR UNIVERSITY

Tezpur University Library



30024



REFERENCE BOOK
NOT TO BE ISSUED
TEZPUR UNIVERSITY LIB. 7

004.66
NEO

ABSTRACT

Key words: Microstrip patch antenna, horn-shaped, triangular notch, thin Substrate, Inverted-L microstrip patch antenna, parasitically coupled, multi-slots, hole-coupled, Artificial Neural Networks, tunneling, resonant frequency, radiation pattern, wide bandwidth and material loading.

The principal contribution of this study includes the development of new design of probe-fed microstrip patch antennas on thin substrate for wide band width, high gain along with multi frequency operation and development of formula for calculation of resonance frequency of designed antenna as well as implementation of Artificial Neural Network code for the calculation of design parameters of the designed antennas.

The art of antenna miniaturization is a compromise among volume, bandwidth and efficiency. Contribution of the thesis addresses the limitations of miniaturization, large band width, High gain, simplicity in design, low cost and accurate computation-technique for design of microstrip antenna to be used in wireless environment. In this thesis, new designs are introduced that can be used for the most sought after probe-fed Microstrip patch antenna on thin substrate.

A Horn shaped Microstrip patch antenna has been designed on thin substrate and characteristics are studied for substrate of dielectric constant 2.2 and also for air dielectric. This Horn shaped antenna gives wide band width and high gain without any design complexities. Variation of slot length and width to control the bandwidth gives flexibility to control the bandwidth for varied applications. A coax-fed inverted-L shaped microstrip patch antenna, a parasitically coupled inverted-L microstrip patch antenna and a parasitic coupled T- shaped microstrip patch antenna have been designed on thin substrate and characteristics are studied. The wider bandwidth and dual band of frequency of operation are the special features of these antennas. In another new design, a multi-slot hole-coupled microstrip patch antenna on substrate of thickness 2mm has been designed and the characteristics are studied. This antenna is a wide band, multi-frequencies antenna. It has the attractive features of simplicity and flexibility of controlling the bandwidth with high isolation between

band of frequencies. And with almost omni directional radiation patterns, the multi slots hole coupled microstrip patch antenna seems to be a good antenna for wireless communications especially for cellular telephone applications.


In this thesis, a generalized method is presented to determine the resonance frequency of slot coupled rectangular microstrip patch antenna. In this implementation a modified formula is used to calculate the edge extension of an equivalent rectangular patch antenna of the slot loaded microstrip patch antenna. Then modified resonance frequency formula is used for calculation of resonance frequency of the slot loaded microstrip patch antenna. The suggested method gives reasonable accurate result without any complicated mathematical functions or operations.

In this thesis, Artificial Neural Networks (ANNs) have been implemented to find accurately the slot length and width of horn shaped antenna for wide band width without involving high experimental cost, time and tedious theoretical calculations. The back propagation algorithm has been used to train the network, which learns using gradient descent method. Again, tunnel based Artificial Neural Network has been used for determination of radiation pattern of the multi-slot hole-coupled microstrip patch antenna. The tunnel based Artificial Neural Networks can save considerable computational time while giving accurate results. The calculation of radiation pattern using the ANNs is a new and interesting part of the work that reflects the simplicity and accuracy of the method.

DECLARATION

I here by declare that the thesis entitled “**ARTIFICIAL NEURAL NETWORKS (ANNs) BASED TECHNIQUE TO DESIGN AND DEVELOP WIDE BAND, HIGH GAIN MINIATURISED MICROSTRIP ANTENNAS FOR CELL-PHONE AND WIRELESS HAND HELD DEVICES**” submitted by me in partial fulfillment of the requirements for the degree of Doctor of Philosophy is a record of my bonafide research work carried out under the guidance of *Professor(Dr.) Malay Dutta*, Computer Science and Information Technology Department, Tezpur University, India, and *Professor(Dr.) Shyam S. Pattnaik*, Educational Television Centre and Electronics and communication Engineering Department, National Institute of Technical Teachers Training and Research(NITTTR), Chandigarh, India.

The research work included in the thesis has not been submitted to any other university or institute for the award of any other degree.


17.05.2018
(Dipak Kr. Neog)


TEZPUR UNIVERSITY
SCHOOL OF SCIENCE AND TECHNOLOGY
COMPUTER SCIENCE AND INFORMATION TECHNOLOGY DEPARTMENT
ASSAM, INDIA.

This to certify that the thesis entitled “ARTIFICIAL NEURAL NETWORKS (ANNs) BASED TECHNIQUE TO DESIGN AND DEVELOP WIDE BAND, HIGH GAIN MINIATURISED MICROSTRIP ANTENNAS FOR CELL-PHONE AND WIRELESS HAND HELD DEVICES” submitted to the Tezpur University in the department of Computer Science and Information Technology, under the school of Science and Technology in partial fulfillment for the award of the degree of **Doctor of Philosophy in Computer Science and Information Technology** is a record of research work carried out by Sri Dipak Kr. Neog under our personal supervision and guidance.


All the helps received by him from various sources have been duly acknowledged.

No part of this thesis has been reproduced elsewhere to award of any other degree.

Date. 24-05-2006
Place: Tezpur university,
INDIA.


Dr. Malay Dutta.
(Principal Supervisor)
Professor,
School of science and Technology,
Computer Science and Information Technology Department.

Date: 17-05-2006
Place: NITTTR, Chandigarh,
INDIA.


17-05-06
Dr. Shyam S. Pattnaik,
(Co-Supervisor)
Professor,
ETV and Electronics and Communication Engineering Department.

ACKNOWLEDGEMENT

I would like to express my indebted gratitude to my supervisor, *Professor(Dr.) Malay Dutta*, Computer Science and Information Technology Department, Tezpur University for his constant cooperation, guidance and suggestions during the work. His scholarly support and constant encouragement have been great source in completion of my work.

I would like to extend my indebtedness and deepest gratitude to my other supervisor, *Professor(Dr.) Shyam S. Pattnaik*, Head, Educational Television Centre and Electronics and Communication Engineering Department, National Institute of Technical Teachers' Training and Research, Chandigarh for his profound suggestion and skillful guidance throughout the progress of the research work. He has been always there with constant cooperation, guidance, advice, inspiration during the research work. He has a sharp eye for details and superb analytical skill. These have been instrumental in the success of the thesis.

I am also grateful to Mrs Swapna Devi, Dhruba C. Panda and Bonomali Khuntia for their companionship throughout the work. Thanks are due to Dr. P.N.Bora, Retired Principal, Dhemaji College and Dr. Budhin Boruah, Principal, Dhemaji College for all their support and positive approach to encourage research. I am thankful to Dr.O. P. Bajpai, Director, NITTTR, Chandigarh, India and North Eastern Regional Institute of Science and Technology(NERIST), India, for providing the necessary infrastructure.

I am thankful to all the members of my research committee of Tezpur University for their timely guidance, suggestions and support during the thesis work.

My gratitude also goes to all the family members and well wishers who were concerned for my progress and for my well being. I express my sincere gratitude to my wife, Bobby. She knows more than anyone else about the sacrifices that had to be made. I would like to thank her for her love, encouragement, patience and understanding throughout all of my studies. Finally, my two small kids Adrija and Abhijyan are deserve appreciation as during my study many times they have to sacrifices the love of father.

Table of Contents	page
-------------------	------

A. Title page.....	I
B. Abstract.....	II
C. Declaration.....	IV
D. Certificate of supervisor.....	V
E. Acknowledgement.....	VI
F. Table of contents.....	VII
G. List of tables.....	X
H. List of figures	XI
I. List of abbreviation.....	XV
J. List of common symbols used.....	XVI
CHAPTER 1: Introduction and Overview of the Thesis	1
1.1 Introduction.....	2
1.1 Scope of the thesis.....	7
1.2 General overview of the thesis.....	8
CHAPTER 2: Microstrip Patch Antenna and Modeling Techniques	12
2.1 Introduction.....	13
2.2 Choice of substrate of microstrip patch antenna.....	14
2.3 Feeding Techniques of microstrip patch antenna.....	16
2.3.1 Microstrip line feed	17
2.3.2 Co-axial feed.....	18
2.3.3 Aperture coupling.....	19
2.3.4 Proximity coupling.....	20
2.4 Wide-Band Probe Fed Microstrip Patch Antennas.....	21
2.4.1 Impedance matching network.....	22
2.4.2 Edge coupled patch.....	24
2.4.3 Stacked-coupled patch.....	25
2.4.4 Capacitance coupled patch.....	27
2.4.5 Slot coupled patch.....	28

2.5. Modeling Techniques of Microstrip Patch Antennas.....	30
2.5.1 Introduction.....	30
2.5.2 Transmission line model.....	32
2.5.3 Cavity model.....	37
2.5.4 Full wave method- moment method.....	42
CHAPTER 3: A Brief Review of Artificial Neural Networks	48
3.1 Introduction.....	49
3.2 Biological motivation of neural network.....	49
3.3 Model of a neuron	50
3.4 Activation function and characteristics.....	52
3.5 Learning rules	55
3.6 Multilayer neural networks	58
3.7 Implementation procedures and issues involved in training neural network.....	59
3.8 Background for Development of ANN Codes.....	61
3.8.1 Introduction.....	61
3.8.2 Backpropagation algorithm.....	62
3.8.3 Tunnel based backpropagation algorithm.....	72
CHAPTER 4: Horn Shaped Microstrip Patch Antenna	77
4.1 Introduction.....	78
4.2 Design specification and antenna structure.....	78
4.3 Computational and measured results.....	82
4.4 Conclusion.....	93
CHAPTER 5: Inverted-L, Parasitic Coupled Inverted-L Shaped and T-Shaped Microstrip Patch Antenna	94
5.1 Introduction.....	95
5.2 Design specification and antenna structure of inverted-L microstrip patch antenna and parasitic coupled inverted L-shaped microstrip antenna.....	96
5.3 Computational and measured results of inverted-L microstrip patch antenna and parasitic coupled inverted-L shaped microstrip patch antenna.....	97

5.4 Design specifications and antenna structure of T-shaped microstrip patch antenna.....	101
5.5 Computational and measured results of T-shaped microstrip patch antenna.....	102
5.6 Conclusion.....	106
CHAPTER 6: Multi-Slot Hole Coupled Microstrip Patch Antenna.....	107
6.1. Introduction.....	107
6.2. Design specifications and antenna structure.....	108
6.3. Computational and measured results.....	110
6.4. Conclusion.....	114
CHAPTER 7: Generalised Formula for Determination of Resonance Frequency of Slot Coupled Microstrip Patch Antenna.....	115
7.1 Introduction.....	116
7.2 Theoretical model.....	117
7.3 Calculated and measured results of slot loaded microstrip patch antenna.....	123
7.4 Determination of two resonance frequencies of E-shaped microstrip patch antenna.....	124
7.4 Conclusion.....	127
CHAPTER 8: Applications of Artificial Neural Networks on Designed Microstrip Patch Antennas.....	128
8.1 Introduction.....	129
8.2 Determination of resonance frequency and impedance bandwidth.....	129
8.3 Calculation of radiation pattern.....	133
8.4 Conclusion.....	136
CHAPTER 9: Conclusions, Future Scope and Publications.....	149
9.1 General conclusions.....	150
9.2 Future scope.....	152
9.3 Publications of the scholar.....	154
CHAPTER 10: References.....	158

LIST OF TABLES

page

Table No.7.1 Comparison of Resonant Frequencies.....	124
Table No.7.2 Comparison of Resonant Frequencies.....	126
Table No.8.1 Network Parameters(width variation).....	131
Table No.8.2: Network Parameters(Length variation).....	131
Table No.8.3: Training data for slot width variation(W_s) for $L_s = 06\text{mm}$	138
Table No.8.4: Training data for variation of slot length(L_s) at $W_s=6\text{mm}$	145

LIST OF FIGURES	page
Figure 2.1. Variation of efficiency and band width with substrate height at constant resonance frequency for two different substrates.....	16
Figure 2.2 Microstrip Patch antenna with microstrip line feed.....	17
Figure 2.3 Microstrip Patch antenna with coaxial line feed.....	18
Figure 2.4 Aperture coupled fed microstrip patch antenna.....	19
Figure.2.5 Proximity couple fed microstrip patch antenna.....	20
Figure 2.6 Geometry of a microstrip patch antenna with a impedance matching network.....	22
Figure 2.7 Edge coupled microstrip patch antenna.....	25
Figure.2.8 Stacked patch microstrip patch antenna.....	26
Figure 2.9 Capacitive coupled microstrip patch antenna.....	27
Figure 2.10 Slot coupled microstrip patch antenna.....	29
Figure 2.11 Microstrip line and its electric field lines.....	33
Figure 2.12 Microstrip patch antenna.....	34
Figure 2.13 Physical and effective lengths of rectangular microstrip patch antenna.....	35
Figure 2.14 Side View of microstrip patch with electric field component.....	35
Figure 2.15 Charge distribution and current density creation on the microstrip patch.....	38
Figure 3.1 (a) Structure of biological neuron.....	50
Figure 3.1 (b) Model of biological neuron.....	51
Figure 3.1 (c) Model of Artificial Neuron.....	51
Figure 3.2 Activation functions.....	53
Figure 3.3 Generalised learning rule.....	57

Figure 3.4 Multilayer neural network structure.....	59
Figure 3.5 Flow Chart of Backpropagation algorithm.....	69
Figure 3.6 Flow chart of tunnel based backpropagation algorithm.....	76
Figure 4.1 Horn Shaped microstrip patch antenna	81
Figure 4.2 Measured and calculated return loss of horn-shaped microstrip patch antenna with 2mm thick substrate.....	83
Figure 4.3 Return loss of horn-shaped microstrip patch antenna with 2mm and 3.175mm thickness.....	84
Figure 4.4 Calculated S_{11} of horn-shaped microstrip patch antennas with different notch length (L_s).....	85
Figure 4.5 Calculated S_{11} of horn-shaped microstrip patch patch antenna with different notch widths (W_s).....	85
Figure 4.6(a) Azimuth pattern of horn-shaped microstrip patch antenna of 2mm thick substrate.....	86
Figure 4.6(b) Elevation pattern of horn-shaped microstrip patch antenna of 2mm thick substrate.....	86
Figure 4.7(a) Azimuth pattern of horn-shaped antenna of 3.175mm thick substrate.....	87
Figure 4.7(b) Elevation pattern of horn-shaped patch microstrip patch Antenna of 3.175mm thick substrate.....	87
Figure 4.8 Calculated return loss of horn-shaped microstrip patch antenna with 2mm thick air substrate.....	88
Figure 4.9 Calculated return loss of horn-shaped microstrip patch antenna with 2mm and 3mm thick air substrate.....	89
Figure 4.10 Elevation pattern of horn-shaped microstrip patch antenna of 2mm thick air substrate.....	90
Figure 4.11 Azimuth pattern of horn-shaped microstrip patch antenna of 2mm thick air substrate.....	91
Figure 4.12 Elevation pattern of horn-shaped microstrip patch antenna of 3mm thick air substrate.....	91
Figure 4.13 Azimuth pattern of horn-shaped microstrip patch antenna of 3mm thick air substrate.....	92

Figure 5.1	Inverted L-shaped microstrip patch antenna.....	97
Figure 5.2	Measured and calculated return loss of inverted-L microstrip patch antenna with 2mm thick substrate.....	98
Figure 5.3	Parasitic coupled inverted-L shaped microstrip patch antenna.....	99
Figure 5.4(a)	VSWR plot of inverted-L shaped microstrip patch antenna....	100
Figure 5.4(b)	VSWR plot of parasitically coupled inverted-L shaped microstrip patch antenna.....	100
Figure 5.5(a)	Azimuth pattern of inverted-L shaped microstrip patch antenna.....	100
Figure 5.5(b)	Elevation pattern of inverted-L shaped microstrip patch antenna.....	100
Figure 5.6(a)	Azimuth pattern of parasitically coupled inverted-L shaped microstrip patch antenna.....	101
Figure 5.6(b)	Elevation pattern of parasitically coupled inverted-L shaped microstrip patch antenna.....	101
Figure 5.7	T-Shaped microstrip patch antenna.....	102
Figure 5.8	Return loss of T-shaped microstrip patch antenna.....	103
Figure 5.9	Measured and calculated return loss plot of T-shaped microstrip patch antenna.....	103
Figure 5.10	Elevation pattern of T-shaped microstrip patch antenna.....	104
Figure 5.11	Azimuth pattern of T-shaped microstrip patch antenna.....	105
Figure 5.12	Variation of resonant frequency with the variation of feed position of T-shaped antenna.....	105
Figure 6.1	Geometry of the Multi-Slots Hole-Coupled Microstrip patch Antenna.....	109
Figure 6.2	Calculated and measured return loss plot of multi-slots hole coupled microstrip patch antenna with 2mm thick substrate.....	111
Figure 6.3	Azimuth pattern of multi-slots-hole-coupled microstrip patch antenna of 2mm thick substrate.....	112
Figure 6.4	Elevation pattern of Multi-slots-hole-coupled microstrip patch antenna of 2mm thick substrate.....	113

Figure 6.5 Return loss of the multi-slots hole-coupled microstrip patch antenna with varying L_s and W_s	113
Figure 7.1 (a) E-shaped microstrip patch antenna.....	118
Figure 7.1 (b) H-shaped microstrip patch antenna.....	118
Figure 7.1 (c) Horn-shaped microstrip patch antenna.....	119
Figure 7.1 (d) L-Shaped microstrip patch antenna.....	119
Figure 8.1 Network architecture showing slot width(W_s)/slot length(L_s) and frequency as input and return loss(dB) as output.....	130
Figure 8.2 No of iterations vs error plot.....	132
Figure 8.3 (a) Comparisons of returnloss of horn shaped microstrip patch antenna for slot width(W_s) variations	132
Figure 8.3 (b) Comparisons of returnloss of horn shaped microstrip patch antenna for slot length(L_s) variations.....	133
Figure 8.4 Network architecture showing frequency and angle as input and gain as output.....	134
Figure 8.5 Radiation pattern for E-Total, theta=0 at 6 GHz and 10.5GHz.....	135
Figure 8.6 Radiation pattern for E-Total, theta=0 at 6.5GHz and 12.0GHz.....	135

List of Abbreviation

PTFE	Polytetrafluoroethylene
SRFT	Simplified Real Frequency Technique
FDTD	Finite Difference Time Domain
FEM	Finite Element Method
MoM	Method of Moments
VSWR	Voltage Standing Wave Ratio
RMSPA	Rectangular Microstrip Patch Antenna
ERMSPA	Equivalent Rectangular Microstrip Patch Antenna
ANNs	Artificial Neural Networks
MLP	Multi Layer Percptrons
NBP	Normal Backpropagation
MSE	Mean Square Error
LMS	Least Mean Square
E_{abs}	Absolute Error
E_{rms}	Root Mean Square Error
TBP	Tunnel Based Back Propagation
PSO	Particle Swarm Optimization

List of Common Symbols Used

μ	Permeability
μ_r	Relative Permeability
μ_{eff}	Effective Permeability
λ	Wavelength
ϕ	Activation Function
ϵ	Permittivity
ϵ_r	Dielectric Constant
ϵ_{eff}	Effective Dielectric Constant
L	Length of Rectangular Microstrip Patch Antenna
L_s	Slot length of the Microstrip patch Antenna
W	Width of Microstrip Patch Antenna
W_s	Slot Width of the Microstrip patch Antenna
h	Height of Dielectric Substrate
f_r	Resonant Frequency
f	Operating Frequency
ϵ	Small Perturbation for Tunnel based neural networks
λ	Steepness of Activation Function for Neural Networks
α	Learning Constant
α	Momentum Factor
(m,n)	Mode of Resonant Frequency
ρ	Strength of Learning

CHAPTER 1

INTRODUCTION AND OVERVIEW

OF THE THESIS

1.1 Introduction

The wireless communications have become an important part of everyday life. During recent years, there have been an enormous growth in the area of wireless communications with the introduction of new applications like; tagging, wireless computer links, wireless microphones, remote control, wireless multimedia links, satellite mobile phone, wireless internet etc[1]. Present day demand is for a wireless device of more practicable and easily transportable. Now need is for a wireless device of light weight, small size, having low energy consumption and have an appealing design. The evolving technology has able to satisfy the need of electronics to reduce the size of wireless devices with the incorporation of small chips which consume less current and are more efficient with a large functionality but at the same time placing a demand for optimal antennas for these devices[1]. The commercial applications in communication, sensing, position location, messaging etc. continue to challenge antenna designer. Advances in technology associated with signal processing, R.F. components and batteries have stimulate more innovative applications in wireless that has in turn stimulate for extensive research to find new solutions to the problems in the antenna engineering. Thus, it is safe to say that the 21st century will certainly be one of active research development and production of antenna for various agencies.

The field of antenna engineering is of course central to all wireless technologies and plays a significant role in the successful deployment and optimization of such systems. Antenna type is based on fundamental operation of

antennas but also aligns closely to major performance specification i.e. gain, bandwidth, radiation efficiency, input impedance etc. For wireless communications, the basic requirement is that the antenna should be relatively cheap, lightweight, robust and easy to manufacture. They should have a minimum impact on environment. The microstrip patch antenna is the best candidate that fulfills all the requirements of antenna to be implemented in handsets as well as in wireless devices. Again, if the number of published journal articles, symposia papers, workshops and short term courses are considered as the parameters, it can be undoubtedly said that microstrip patch antennas are one of the most innovative areas of research work at present day.

The basic form of microstrip patch antenna is a metallic patch printed on a thin grounded dielectric substrate. Although, microstrip patch antenna was suggested back in 1953[2] but serious work started in 1972[3][4]. Still after 33 years, major researches are going on to improve antenna to meet with present day demands of industries and government agencies. From the survey of literature, it is found that the major disadvantages of the microstrip patch antennas are: low efficiency, low power handling, high quality factor, poor polarization purity, poor scan performance, spurious feed radiations, vary narrow frequency band width and the progressive stage of analysis tools for complicated structures.

In commercial world, size reduction of microstrip patch antenna is the biggest demand. To achieve additional progress is to view the antenna not as separate device, but as integrate device in to the system. The antenna must be designed along with the entire communication unit. The size reduction of antenna is difficult as it is

associated with the aim of achieving high gain and large band width. Again for multifunction purposes, a number of antennas are used in a common platform (example: dual mode radios, satellite and terrestrial communications). So, thrust area of focused is to develop wide band and multifunctional microstrip patch antennas, which will reduce the number of antenna used in a single platform.

The microstrip patch antennas are inherently narrow bandwidth structure due to their resonant nature and the confinement of fields between the patch metalisation and ground plane. The impedance bandwidth with $VSWR < 2$ for a microstrip patch antenna increases almost linearly with substrate thickness “h”[5]. To manipulate the impedance curve, the suggested techniques that are commonly used are: use of the substrate thickness with low relative dielectric constant ϵ_r [5], choice of suitable feeding technique[5,6,7,8,9,10], introduction of coupled mode[11,12,13], impedance matching[14,15,16,17], resistive loading [18,19], selection of different geometries[6,8,9,20,21], use of shorting pins[22,23], addition of active circuits i.e. design active antenna[24], stub loading, slot and notch loading, short circuit via, parasitic coupling, superstrate cover[6,8,9,21].

There are four fundamental feeding techniques to excite the patch[3-9]. These are Microstrip line feed, Co-axial Probe feed, Aperture coupled feed and Proximity coupled feed. Each one of these techniques has its own advantages and disadvantages. However, the probe feed has a number of characteristics that make it suitable to be used in wireless system. In probe-fed technique the probe is directly connected to the patch, the antenna structure is quit robust. The probe feed is also less prone to alignment errors, which can significantly affect the performance of the

aperture coupled and proximity coupled feeds. As the feed is separated from the patch, there is less spurious radiation from the feed network as compared to that of the microstrip feed line and the proximity coupled feed. The probe feed has the advantage that it can directly excite via a coaxial cable, for which it does not require an additional substrate layer to support the feed network. There are various approaches that have been suggested to enhance the bandwidth of probe-fed microstrip patch antenna. These include, use of impedance matching network, edge coupled probes, Stacked Coupled probes, Shaped Probes, capacitive coupled and slot coupled. However, all the solutions given to the problems faced in microstrip patch antennas are not sufficient to fulfill the need of modern wireless systems[1,4,83,286-294]. Even from the number of recent published articles on microstrip antennas it is safe to say that research in to wide band probe-fed microstrip patch antennas, is still a very important topic[1,5,9-78].

Another area of research related to the advances of microstrip patch antenna technology is the modeling technique used to analysis of the microstrip patch antenna. With the present trend of development of microstrip patch antenna, many new models have been developed for the analysis. They fall in to two broad categories: approximate methods and full wave methods. The approximate method include the transmission line model[6,7,8,10], cavity model[6,7,8,10] and segmentation model[8]. The full wave methods that can be used to model microstrip patch antennas are the method of moments (MoM), the finite element method(FEM), and the finite-difference time-domain(FDTD)method[80,81,82,].

The model based techniques maintain simplicity at the expense of

accuracy. They suffer from various limitations. These include: thin substrate approximation, isotropic substrate and single mode analysis approximation[84, 85]. Also the microstrip patch antenna structure is becoming complex due to its inherent inhomogeneous dielectric, multi layered dielectric structure, periodic loading of the substrate to prevent surface waves, aperture coupling of the feed to the antenna, use of stacked configuration to achieve larger bandwidth, loading of the antenna to achieve the desired antenna characteristics and integration of circuit function with antenna function[1,4,8,9,10,86]. Form the consideration of the design complexity of microstrip patch antenna; it is found that there is lack of accurate theory to analysis the microstrip patch antenna and also there exit considerable deviation between the theoretical result and experimental findings. It is difficult to find exact feed point for proper impedance matching. There is no available accurate theory to design microstrip patch antenna for the cellular phone in realistic users' conditions.

As the microstrip patch antennas become more complex, the more sophisticated numerical methods such as full wave modeling techniques has become inevitable. However, applications of full wave modeling are more computationally expensive and can easily exceed the capabilities of most personal computers. Therefore, the search for techniques that can reduce the computational complexity of modeling of an antenna is currently a very important research area.

The aim of this thesis is therefore, firstly to design of new wide band probe-fed microstrip patch antenna elements to fulfill the requirements of modern-day wireless communication system and development of simple method to calculate the resonance frequency of designed antenna. The second objective of the thesis is to use

Artificial Neural Network as alternative to the modeling technique to support the newly designed antenna without any computational complexities as well as to reduce the use of excessive computational resources.

1.2 Scope of the Thesis

In this thesis focus is given mainly on the development of new design of wide band probe-fed microstrip patch antenna of single resonance frequency and multi resonance's. In addition, to develop simple method to calculate the resonance frequency of designed antenna and use of Artificial Neural Network(ANN) code to analysis the microstrip patch antenna. The specific objectives of the thesis are:

- The first phase of this research is the development and design of wide band probe fed microstrip patch antenna for modern wireless communication systems. To reduce the size of the antenna to be suitable for compact wireless system, it is decided to consider only the thin substrate and single layer antenna with finite ground plane while still retaining the benefits of low cost, light weight, low profile and wideband & high gain. It is also tried to make the design, very simple so that it can be implemented easily.
- The second objective is to verify the performance of the new antenna elements and to study the characteristics for practical applications. This is achieved through numerical calculation /simulation and through actual experimental measurements of the designed microstrip patch

antenna elements.

- Third phase of this study is aimed at formulation and implementation of an efficient modeling technique for calculation of parameters of the newly designed microstrip patch antennas. Here the primary importance is given to make easy implementation and consumption of less computational time for the parameter calculation of the microstrip patch antenna.
- The final objective is to develop an accurate simulation code based on Artificial Neural Networks(ANNs) to calculate the design parameters of the newly designed microstrip patch antenna elements.

1.3 General Overview of the Thesis

The general back ground of the microstrip patch antenna is included in this chapter 1. It is briefly outlined the needs of present days wireless systems and problems of the microstrip patch antennas so far developed. The fact to select the probe feed technique is mentioned here. It is also briefly pointed out the problems of wide band probe-fed microstrip patch antennas in terms of design as well as modeling techniques. The formulated objective of the thesis is included, which is in short is to design new wide band probe fed microstrip patch antenna and to develop the Artificial Neural Network(ANN) code to calculated the design parameter of the newly designed microstrip patch antennas.

Chapter 2 introduces a brief overview on choice of substrate and the

feeding technique of microstrip patch antennas with their advantages and disadvantages for practical applications. Overviews of the various techniques that have been used so far for the bandwidth enhancement of probe-fed microstrip patch antennas are presented in this chapter 2. Then chapter 2, gives an overview of various modeling technique used for the analysis and design of probe-fed microstrip patch antennas. This includes the approximate methods and full wave methods. Out of all methods, only transmission line method, Cavity method and the Method of Moments are discussed.

Chapter 3 includes an overview of Artificial Neural Network(ANN). It includes the brief analysis of biological motivation of neural network, Model of a neuron, activation functions, learning rules, multilayer neural network along with issues involved in implementation in neural network training. In this chapter, the ANN code development & its application in microstrip patch antenna problems is discussed i.e. it contains the mathematical details of back propagation and tunnel based back propagation algorithm.

Chapter 4 deals with the new design of microstrip patch antenna i.e. probe-fed horn shaped microstrip patch antenna. The detail design specification of the probe-fed horn shaped microstrip patch antenna is pointed out. The experimental as well as calculated parameters of the probe-fed horn shaped microstrip patch antennas are included in this chapter 4. The studied characteristics of the probe-fed horn shaped microstrip patch antennas for two different heights and for two different substrates i.e. for one of dielectric constant 2.2 and another for air dielectric are also included in this chapter. The chapter 4 also contains the study of variation of band

width with the variation of slot length of the probe-fed horn shaped microstrip patch antennas.

The chapter 5 contains the design of a coax fed-inverted-L shaped microstrip patch antenna, a parasitically coupled inverted-L microstrip patch antenna and a parasitic coupled T- shaped microstrip patch antenna that have been designed on thin substrate. The experimental and theoretical results of the characteristics of coax fed-inverted-L shaped microstrip patch antenna, parasitically coupled inverted-L microstrip antenna and parasitic coupled T- shaped antenna are given in the chapter. The coax fed-inverted-L shaped microstrip patch antenna, and parasitically coupled inverted-L microstrip patch antenna show wide band properties and the parasitic coupled T- shaped antenna shows the dual bands frequency of operation.

Chapter 6 presents another new design, a multi-slot hole-coupled microstrip patch antenna that has been designed on a substrate of thickness of 2mm. The wide band and multi frequency characteristics of the designed antenna, has the attractive features of simplicity and flexibility of controlling the bandwidth with high isolation among bands of frequencies. The notable features of designed multi-slot hole-coupled microstrip patch antenna is the variation of slot parameters, hole size and positions that give the flexibility to shift the frequency and match the impedance of the antenna, are mentioned in this chapter.

Chapter 7 contains a generalized method used to determine the resonance frequency of slot coupled probe fed rectangular microstrip patch antenna. The details implementation technique of the generalized method on the slot loaded probe-fed rectangular microstrip patch antenna to calculate the edge extension with a

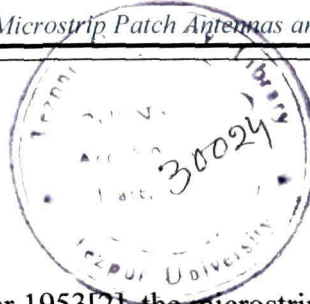
modified formula and use of modified resonance frequency formula for calculation of resonance frequency of the slot loaded probe-fed rectangular microstrip patch antenna are included in the chapter 7. In the chapter 7, the comparative analysis of results of different slot coupled probe fed rectangular microstrip patch antennas calculated with different methods and the present suggested method are compare, It is shown that the suggested method gives accurate result without any complicated mathematical functions or operations.

Chapter 8 contains the implementation of Artificial Neural Networks (ANNs) code to accurately find the slot length and width of horn shaped antenna without involving high experimental cost, time and tedious theoretical calculations. The developed code of back propagation algorithm that has been used to train the network, that learns using gradient descent method, is mentioned in the chapter 8. Again, the use of tunnel based Artificial Neural Networks that has been used for determination of radiation pattern of the multi-slot hole-coupled probe-fed microstrip patch antenna is included in the chapter. It is pointed out that the calculation of radiation pattern using the Artificial Neural Networks(ANNs) is a new and interesting part of the work that reflects the simplicity and accuracy of the method.

Chapter 9 contains general conclusions regarding this study and concludes the thesis with some recommendations that can be considered for future work.

CHAPTER 2

**MICROSTRIP PATCH ANTENNAS
AND MODELING TECHNIQUES**



2.1 Introduction

Being conceived in the year 1953[2], the microstrip Patch Antenna has matured considerably over last 33 years with starting of serious work in 1972[2,3]. The major progresses in the Microstrip Patch Antennas are included; success in bandwidth enhancement, combating surface wave effects, development of compact antennas, active antennas and development in the analysis tools.

Microstrip Patch Antennas use radiating elements of a wide variety of shapes: square, rectangle, circle, ring, triangle, ellipse, star, L, semi-circle etc. More complex geometrical figures and combinations of simple shapes are also used for some particular applications [7,8,87]. The selection of a particular shape depends on the parameters one wishes to optimize: bandwidth, sidelobes, cross polarization, and antenna size.

Microstrip antennas are inherently narrowband structure due to their resonant nature and confinement of fields between the patch metallization and ground plane[4]. Hence narrow bandwidth is one of the principal disadvantages of microstrip patch antenna. In recent years, significant research contributions have been devoted to the band width enhancement technique of the microstrip patch antenna in general. The various techniques that have been suggested and tried to manipulate the impedance curve includes: use of thick substrate with low relative dielectric constant (ϵ_r)[4,8],

choice of suitable feeding technique[8,9,86], introduction of coupled modes[8,9,86], impedance matching and resistive loading [4,86]. There exists a large amount of open literature related to bandwidth enhancement technique and related solution that have been suggested [5,6,9-125].

In this chapter, a brief overview on the choice Substrate of microstrip patch antenna is included in the section 2.2. In section 2.3, discussion is included on feeding technique of microstrip patch antennas while an overview of wideband probe fed microstrip patch antenna is given in section 2.4. Section 2.5 gives an insight of modeling techniques that are currently available.

2.2 Choice of Substrate of Microstrip Patch Antenna

The dielectric substrate provides a stable support for the conductor strip and patches that make up connecting lines, resonator, and antennas. It ensures that the components that are implemented are properly located and firmly held in place, just as in printed circuits for electronics at lower frequencies. The substrate plays an important role in determining the electrical characteristics of the Microstrip Patch Antenna. There is no one ideal substrate; the choice rather depends on the application. For instance, conformal microstrips require flexible substrates,

while low frequency applications require high dielectric constant to keep size small[6]. Microstrip Patch Antennas use low dielectric substrates i.e. generally substrate of dielectric constant $\epsilon_r < 2$. The use of higher value of dielectric constant (ϵ_r), affects the confinement of field and reduces the radiation efficiency of the Microstrip Patch Antenna. The bandwidth and efficiency variation with substrate height at centre frequency for rectangular microstrip patch for two different substrate are shown in Figure 2.1[5]. From the figure it is clear that the bandwidth increases almost linearly with substrate height and the bandwidth decreases with the increase of dielectric constant of the substrate.

Most commonly used substrate for microstrip patch antennas are: alumina or high dielectric (ϵ_r) substrate, composite material substrates, and honey-comb substrate. Honey-comb material is light-weight, sturdy and low ϵ_r and is generally preferred for aerospace applications. Composite materials are obtained by adding fiberglass, quartz or ceramic in suitable proportion to the organic or synthetic materials to obtain the desired permittivity and the electrical and mechanical properties. The most commonly used combination is that of PTFE and glass and the resulting substrate have ϵ_r between 2.17 and 2.55. Combination of PTFE and ceramic is used to produce flexible substrates with ϵ_r near 10. These high ϵ_r substrate or alumina are used for miniaturization of microstrip antennas often at the cost of bandwidth.

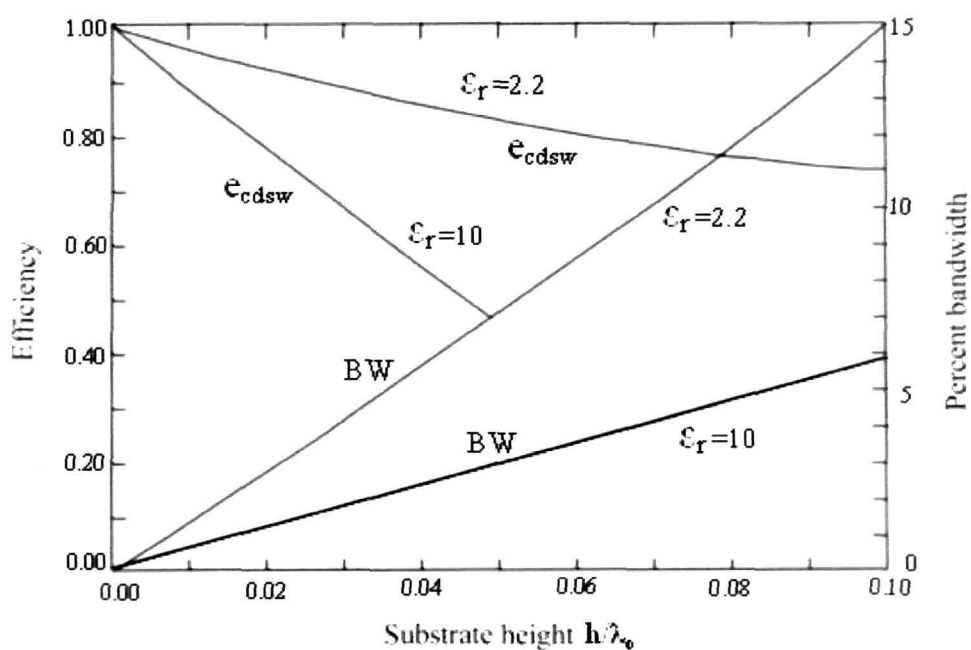


Figure 2.1 Variation of efficiency and band width with substrate height at constant resonance frequency for two different substrates[5].

2.3 Feeding Techniques of Microstrip Patch Antenna

The excitation of the radiating element is an essential and important factor, which requires careful consideration in designing a most appropriate antenna for a particular application. A wide variety of feed mechanisms are available, not just for coupling energy to individual elements, but also for the controlled distribution of energy to linear or planar array elements. The feed element may be either co-planer with the radiating elements, or situated in a separate transmission-line layer. Now there is available ample literature on the feeding technique [6,7,8,9,87]. Therefore, a brief over view of only four most popular Microstrip Antenna Feed techniques are given. These are namely: Microstrip line, Co-axial Probe, Aperture coupling and Proximity coupling.

2.3.1 Microstrip Line Feed

Microstrip line feed is based on the principle that cutting an inset in the patch does not significantly affect the resonant frequency but that it modifies the input impedance. By properly selecting the depth of the inset, one can match the path to the transmission line without additional matching elements [87]. The feed was the first used for practical applications [88] and is the simplest way to feed a microstrip patch is to connect a microstrip line directly to the edge of the patch, with both elements located on the same substrate. A microstrip line feed is shown in figure.2.2.

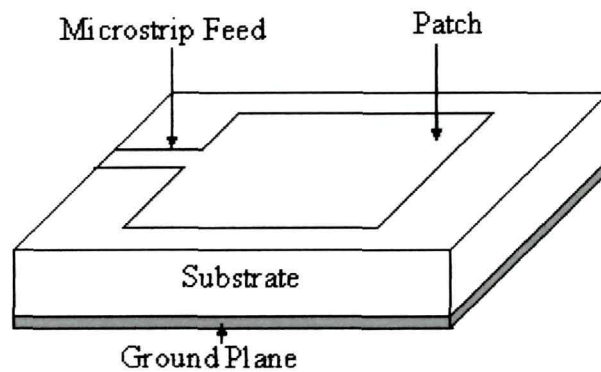


Figure 2.2 Microstrip patch antenna with microstrip line feed.

The microstrip line feed though simple in nature but a microstrip structure with the line and patch cannot be optimized simultaneously as an antenna and a transmission line. There must be some compromise between the two so that feed line does not radiate too much at the discontinuities [89]. The spurious radiation and the accumulated reactive power below the patch (cavity effect), degrades the antenna performance and reduces its bandwidth[8].

2.3.2 Co-axial Line Feed

Co-axial line feed was among the first considered and even today one of the most popular in many application of microstrip patch antenna. In co-axial line feed, the inner conductor of the coax is extends across the dielectric substrate and is connected to the patch while the outer conductor is connected to the ground plane as shown in the figure 2.3.

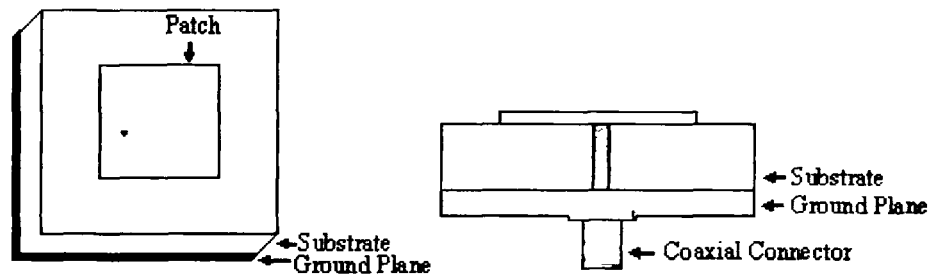


Figure 2.3 Microstrip Patch antenna with coaxial line feed.

In case of coaxial line feed the intrinsic radiation from the feed is small and can be neglected for thin substrates but becomes significant with thicker substrates. Now, most of the theoretical developments consider coaxial feeds and models were developed to characterize the injection of current in to patch accurately [84,90]. However, coaxial feeds are difficult to realize in practice because drilling or punching holes through the substrate in a particular specific point is critical task, generally this operation would like to avoid. Again introducing the conductor through the holes and soldered to the patch are delicate operations that require careful handling, and mechanical control of the connection is difficult, especially for very high frequencies[86].

2.3.3 Aperture Coupling

In a conventional aperture coupling, the microstrip patch antenna consists of two substrate layers separated by a common ground plane. The radiating microstrip layer on the top of the substrate is fed through an aperture in the ground plane by a microstrip feed line lying on the bottom of the lower substrate. The important requirement is that the common ground plane should contain etched apertures accurately positioned below the microstrip patch and above the feed line [8]. Figure 2.4. shows an Aperture coupled feed microstrip patch antenna.

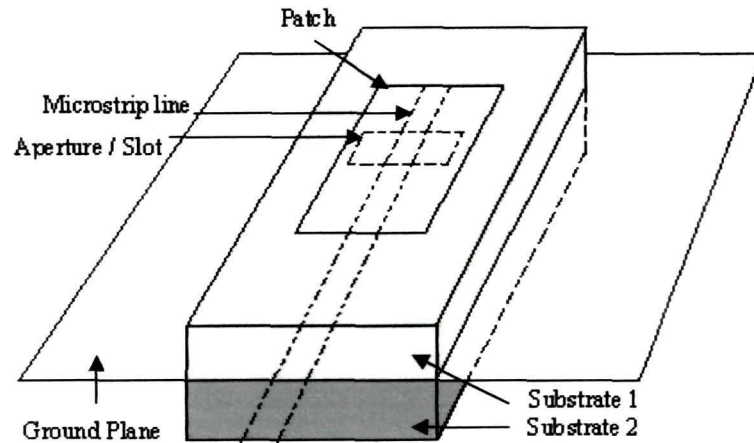


Figure 2.4 Aperture coupled feed microstrip patch antenna.

The aperture coupled feed technique has many attractive features [9, 91-95], one is it provides stronger coupling than a similar triplet or suspended stripline system because of higher concentration of fields above the feed line where the aperture is positioned. Further more, a relatively high-permittivity substrate can be used if required for the feed system, without compromising the radiating properties of

the lower-permittivity substrate carrying the microstrip patches. In this technique, the slot on the common ground plane is free to radiate bidirectionally. By using multilayer substrate, it can be made unidirectional radiation, but may result in strongly coupled surface wave modes which degraded in the antenna efficiency [96]. The cavity backed aperture coupled technique is used to improve the efficiency of antenna [97] as well as solves the above mentioned problem.

2.3.4 Proximity Coupling

In this feeding technique, the coupling of the patch and the feed line is obtained by placing the patch and the feed at different substrate levels. A thin layer of high dielectric constant substrate is used to reduce the radiation from the feed lines, whereas a thick layer of low dielectric constant substrate is used in the upper layer to increase the radiation of the patch [8,86]. The length of the feeding stub and the width-to-line ratio of the path can be used to control the match.

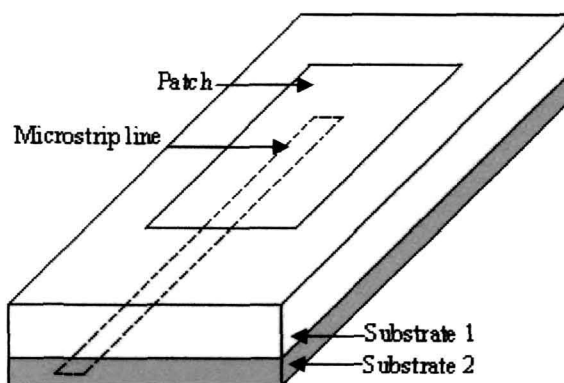


Figure.2.5 Proximity couple feed microstrip patch antenna

Using the proximity coupling, the frequency band width of a patch resonator could be significantly widened [98,99]. The special feature is that, the feed line is no longer located to an open surface and there is no need to solder different conductors, unlike co-axial feed. But a structure with two dielectric layers, however, is more complex to analyze, because the simple models developed for single layers cannot be used. The resulting structure becomes more complex to build, with two dielectric layers instead of one. Again one cannot easily connect components within the feeding circuit as it is buried inside substrate.

2.4 Wideband Probe-Fed Microstrip Patch Antenna

The microstrip antennas are having narrow impedance bandwidth, typically a few percent. The impedance bandwidth of microstrip antennas is usually much smaller than the pattern band width [100]. Hence focus is given on input impedance rather than radiation pattern in the discussion of bandwidth enhancement technique. Some generic types of band width extension technique are: increasing antenna volume by incorporating parasitic elements, stacked substrates, use of foam dielectrics; creation of multiple resonances in input response by addition of external passive networks or internal structure; and incorporation of dissipative loading by adding lossy materials or resistors [8]. Pozar [101] divided these various bandwidth enhancement technique in to three broad approaches: impedance matching; the use of multiple resonance; and the use of lossy materials. In this overview; the band width enhancement techniques are categorised into different approaches in terms of

normally used antenna structures. These are impedance matching network; edge coupled probes; stacked coupled probes; shaped probes; capacitive coupled and slot coupled. The lossy antennas are not included here because generally lossy materials are not frequently used as it limits the radiation frequencies of the antenna.

2.4.1 Impedance Matching Networks

An impedance matching network is used to improve the impedance band width of a probe feed microstrip patch antenna. In this process, without altering the antenna element, a reactive matching network is used, to compensate for the rapid frequency variations of input impedances. With this method, compared to thin substrate, a thick substrate will add some extra bandwidth. An impedance matching network is typically implemented in microstrip antenna from below the ground plane of the antenna element. The figure 2.6 shows the geometry of a microstrip patch antenna with a impedance matching network.

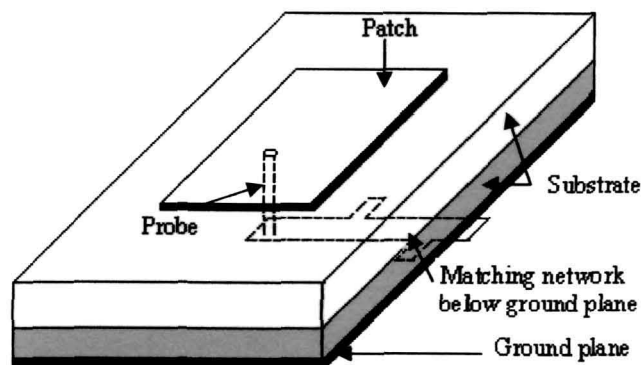


Figure 2.6 Geometry of a microstrip patch antenna with a impedance matching network.

The impedance matching network method was implemented by Pues and Capelle [14] by modeling the antenna as simple resonant circuit. Their method is unique in that it doesn't alter the radiating element itself, while a reactive matching network is used to compensate for the rapid frequency variations of the input impedance. The validity of the technique is based on the relative frequency insensitivity of the radiation pattern and gain characteristics as compared to the resonant behaviour of the input impedance. In their approach for the design of the matching network, the input impedance of a microstrip antenna should be by either a simple series resonant or a simple parallel resonant RLC circuit in the vicinity of fundamental resonant frequency. Once the RLC equivalent circuit of the antenna is obtained, a procedure similar to the design of a band pass filter[15] is used to synthesis the matching network of the microstrip patch antenna. With this approach they have achieved a increased in band width by a factor of 3.2 or 9.1 percent. Hongming An etal [16] introduced the simplified real frequency technique(SRFT) to design the loss less matching networks of microstrip antennas in order to increase bandwidth. The most significant feature of this is the numerical technique is that it does not require any analytical description of the antenna and generator, the measured or simulated impedance data are processed directly. Further more neither on a priori choice of a matching network topology nor an analytic form of the system transfer function needed. With this approach, they have managed to increase the band width for one antenna from 5.7% to 11.06% at the level of VSWR = 1.5, and for another antenna element, the band width increased from 9.4% to 16.82% for the VSWR<2. Recently, Haaj et al[30] reported an impedance bandwidth of 6.9% for a VSWR of

1.5:1 with a parallel resonant circuit.

The advantage of using the matching network is that the radiation characteristics of the antenna element remain unchanged because the antenna element do not get altered as the matching network can be placed behind the antenna's ground plane[8,86]. The radiation from the matching network is also minimum. The main drawback of this methods are, the matching networks are used to excite the individual elements in an antenna array and more than one substrate layer is required to support the antenna element and the matching network for single element antennas[8,9,86].

2.4.2 Edge-Coupled Patches (Multi Mode Operation)

The basic idea that has been used to widen the frequency band width is that to increase the band width of resonant circuits, in particular when designing band pass filters, is to couple several resonators with very closely spaced resonances. In this approach – several radiating structures are closely coupled to each other but resonating slightly different frequencies. Only one of the elements is driven directly. The other patches are coupled through proximity effects. In an Edge coupled microstrip antenna the parasitic patches can be coupled to either to the radiating edges, the non-radiating edges or to both pair of edges. This approach has been investigated by wood [102] and then Kumar and Gupta [103-105]. Using this approach R.Garg and V.S.Reddy[106] achieved an impedance band width of 23% at VSWR=2. Figure 2.7 shows an example of such an edge coupled microstrip antenna.

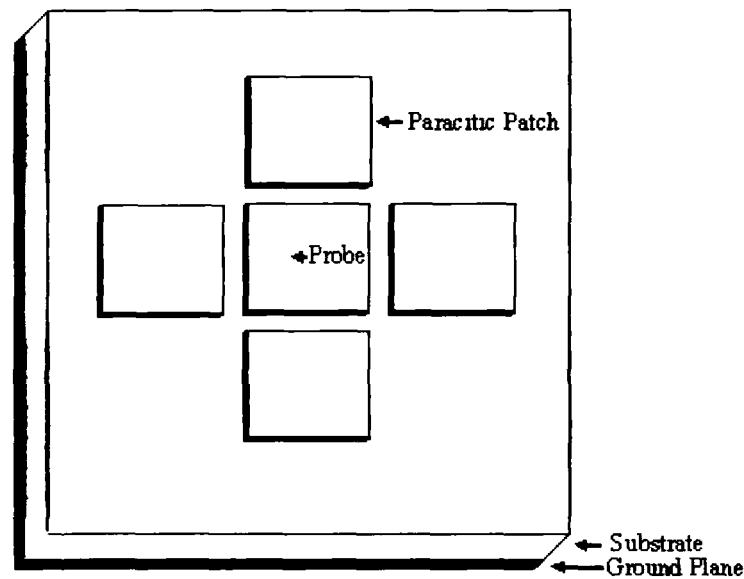


Figure 2.7 Edge coupled microstrip antenna.

The edge coupled patches can be fabricated on a single layer substrate. This coplanar nature of the structure is the advantage of the Edge coupled patch antenna. The use of additional parasitic patches increases the size of the antenna element which is one of the major drawback. Another drawback is that as the different patches radiate with different amplitudes, the radiation patterns change significantly over the operating frequencies[8].

2.4.3 Stacked Patches

In another approach, two or more electromagnetically coupled patches are placed on top of one another or stacked [86]. This is also a multimode operation technique. In stacked patch structure, the surroundings of the two patches are slightly

different; the resonant frequencies of the two patches are slightly offset, which increases the frequency bandwidth. The figure 2.8 shows a Stacked patch microstrip antenna.

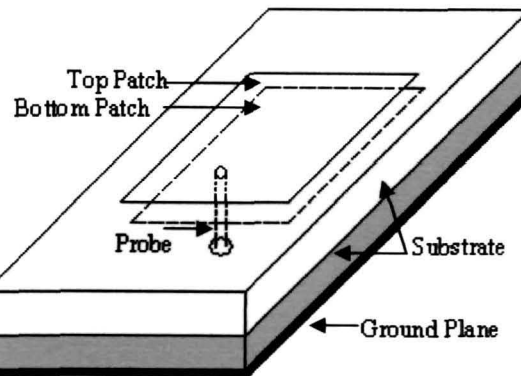


Figure.2.8 Stacked patch microstrip patch antenna.

Different size are also be stacked for the two patches, either to increase the bandwidth further or to realize an antenna operating at two different frequencies[107-110]. The frequency band width of a microstrip patch antenna is also enhanced by the increase thickness of the double layer structure, with concomitant risk of surface wave excitation. It is possible to stack more patches, but the performance may not be much better than with only two patches [9,101]. Using this technique, Waterhouse [107] achieved a 25% impedance band width for rectangular patches, Kokotoff et al [111] reported a 22% impedance bandwidth for annular ring patches and Mitchell et al [112] achieved a 33% impedance bandwidth for circular patches.

The advantages of stack patch technique are, it does not increase the

surface area of the element[8,86], it can be used in array configurations without creating grating lobes, its radiation patterns and phase centre also remains relatively constant over the operating frequency band and has the large number of parameters that can be used to optimization. At the same time it has the draw back that it require more than one substrate layer to support the patch and because of larger design parameter the optimization becomes more complex.

2.4.4 Capacitive Coupled Patches

The probe fed microstrip antenna on thick substrate show inductive nature in the input impedances. To avoid this inductive nature, capacitive coupling technique is used. In this technique, a small probe fed patch is situated below the resonant patch [113,114]. The gap between them acts as a series capacitor. Figure 2.9 shows a capacitive coupling patch.

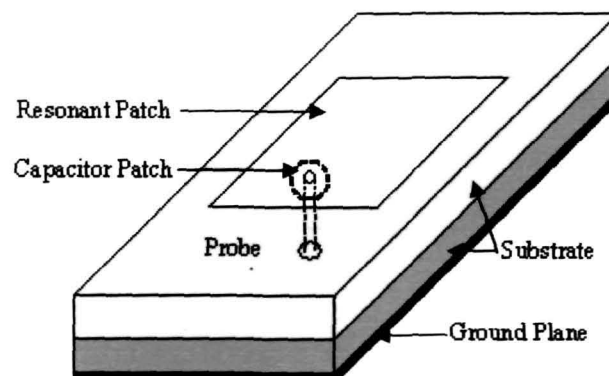


Figure 2.9 Capacitive coupled microstrip patch antenna.

By combining stacked patch and capacitive-coupled probe feed technique, Z.F.Liu et al [115] achieved a 25% impedance band width for a VSWR of 2:1 and M.A.Gonzalez et al [116] reported a impedance band width of 35.3% for a VSWR of 2:1. Recently G.Mayhew-Ridgers et al [117] reported of achieving of impedance band width of 25% at VSWR of 2:1.

For a patch where the capacitor patch is located below the resonant patch has advantages that, this approach do not increase the surface area of the element and the cross polarization levels in the H-plane are lower than the approach where the capacitor patch is located within the surface of the resonant patch. The approach of capacitor patch below the resonant patch has the disadvantages that, it require additional substrate layer to support the configuration and prone to alignment errors which create complexity in fabrication.

2.4.5 Slot Coupled Patches

The slot loaded microstrip patch antenna (figure 2.10) leads to increase in antenna impedance band width and a smaller size of the antenna elements. These slots force the surface currents to meander, thus, artificially increasing the antenna antenna's electrical length without modifying its global dimensions. This effect of increase in the length of current path can be modeled as an additional series inductance. The annular slots within the surface of the patch element may also acts as a series capacitor. It is well known fact that the inductance or capacitance is key factor to widen the impedance band width of microstrip patch antenna elements[8].

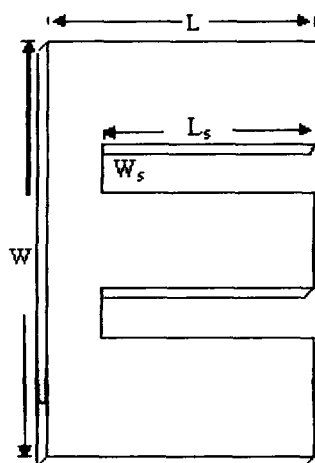


Figure 2.10 Slot coupled microstrip patch antenna.

In a circular resonant patch, using an annular slot around a small circular probe fed capacitor patch in the surface of the resonant patch, P.S.Hall[118] reported a 13.2% impedance band width at 10db return loss. S.K.Palit and A.Hamadi [119] achieved up to a 39% impedance band width with H-Shaped microstrip patch antenna. T.Huynh and K.F.Lee [120] reported a U-slot antenna with which can achieve an impedance band width exceed 30%. In slot loaded E-shaped microstrip patch antenna, F. Yang, X.-X. Zhang, X. Ye and Y. Rahmat-Samii[121] an impedance band width of 30.3%, Kin-Lu Wong and Wen-Hsiu Hsu [122] reported an impedance band width of 24%, while Wen-Hsiu Hsu and Kin-Lu Wong[123] reported of achieving of impedance band width exceed 25%. In a slot loaded circular microstrip antenna, J.H.Lu[124] reported an increase in impedance band width more than 2.3 times that of conventional circular microstrip patch antenna. Recently, Ricky Chair et al[125], reported of achieving an impedance band width of 28.6% with U-slot and half E-shaped microstrip patch antenna.

The slot loaded microstrip patch antennas reduces the size of the antenna element. Microstrip patch antennas with this technique produce greater current concentration on the antennas and therefore, increase the ohmic losses and decrease the gain of the antenna. Again proper insertion of slot in accurate position on the patch and slot size optimization is a difficult task and is very much frequency sensitive.

2.5 Modeling Techniques of Microstrip Patch Antennas

2.5.1 Introduction

The most popular methods that can be used to model and analyse the probe fed microstrip patch antennas fall into one of two broad categories: (i) approximate methods and (ii) full wave methods. The approximate methods include the transmission line model[6,7,8,10], Cavity model[6,8,33,38] and segmentation model[8]. The approximate models are easy to implement for single element antenna, it gives good physical insight with very small solution time, but has the limitation of less accurate. It becomes more complex for modeling coupling between elements, with these methods. The most popular full wave methods that can be used to model probe-fed microstrip patch antennas are the method of moment(MoM), the finite element method(FEM), and the finite-difference time-domain(FDTD) method. These are the three major paradigms of full wave electromagnetic modeling

techniques[30,126-129]. All these methods discretize the problem region and transform the field equations into a system of linear equations. Again these methods can be characterized into two groups, e.g. differential and integral. Differential method such as Finite Element Method(FEM) and Finite-Difference Time-Domain(FDTD) requires discretization of the entire problem region . Integral method such as Method of Moments (MoM) only require discretization over the conductor surface. The unknown electromagnetic property used in Moments Method(MoM) is the current density, and the electric field for the FEM and FDTD (also the magnetic field for FDTD method). The discretization process results in the electromagnetic property of interest being approximated by a set of smaller elements, but of which the complex amplitudes are initially unknown. The amplitudes are determined by applying the full-wave method of choice to the agglomeration of elements. Usually, the approximation becomes more accurate as the number of elements is increased. The features of full wave solutions may be include as follow[5]:

- i. **Accuracy:** Full wave analysis techniques generally provide the most accurate results for input impedance, mutual coupling, radar cross-section, etc.
- ii. **Completeness:** Full-wave solutions include the effects of surface waves, space wave radiation, and external coupling.
- iii. **Versatility:** Full-wave solution can be implemented for arbitrary microstrip elements and arrays, various types of feeding techniques, multilayer geometries, and for anisotropic substrates.

- iv. **Computational complexity:** Full-wave solutions are numerically intensive, and require careful programming in order to be computationally efficient.

There is an abundant literature on the theoretical analysis of probe-fed microstrip patch antennas. Hence, only brief reviews of the most popular methods which are used in the present study i.e. the transmission line method, the cavity method and the Method of Moments is included in this section.

2.5.2 Transmission Line Model

The transmission line model is the easiest of all but it yields the least accurate results and it lacks the versatility. This model represents the microstrip antenna by two slots of width W and height h , separated by a low impedance transmission line of length L . The microstrip is a non-homogeneous line of two dielectrics; typically the substrate and air. Due to the finite length and width of the microstrip patch antenna, the fields along the edges of the patch under goes fringing as shown in the figure 2.11. The amount of fringing is a function of the dimensions of the patch and the height of the substrate. The fringing influences the resonant frequency of the microstrip patch antenna, so it must be taken in to account in to the microstrip patch antennas calculation.

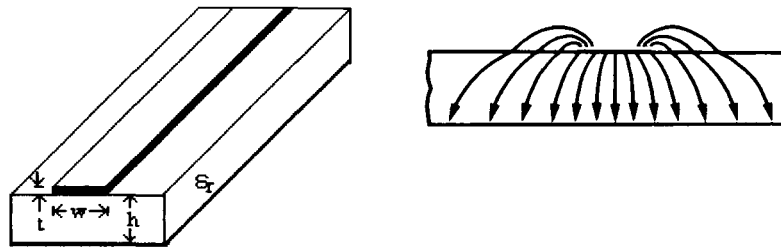


Figure 2.11 Microstrip line and its electric field lines.

As seen from figure 2.11, most of the electric field lines reside in the substrate and parts of some lines exist in air. Hence the fringing makes the microstrip line look wider electrically compared to its physical dimensions. As a result, this transmission line cannot support pure transverse electric-magnetic (TEM) mode of transmission, since, the phase velocities would be different in the air and the substrate. Instead, the dominant mode of propagation would be the quasi-TEM mode. Hence, an effective dielectric constant ϵ_{reff} must be obtained in order to account for the fringing and the wave propagation in the line. For air dielectric substrate the effective dielectric constant ϵ_{reff} has the range of $1 \ll \epsilon_{\text{reff}} \ll \epsilon_r$ and the value of ϵ_{reff} will be closer to the value of the actual dielectric constant ϵ_r of the substrate. The effective dielectric constant ϵ_{reff} is a function of frequency. At high frequency of operation, most of the electric field lines concentrate in the substrate hence the effective dielectric constant approaches the value of the dielectric constant of the substrate. The expression for ϵ_{reff} is given by Balanis [130] as:

$$\epsilon_{eff} = \frac{\epsilon_r + 1}{2} + \frac{\epsilon_r - 1}{2} \left[1 + 12 \frac{h}{W} \right]^{-\frac{1}{2}} \quad (2.1)$$

- Where,
- ϵ_{reff} = Effective dielectric constant.
 - ϵ_r = Dielectric constant of substrate.
 - h = Height of dielectric substrate.
 - W = Width of the patch.

Figure 2.12 shows a rectangular microstrip patch antenna of length L , width W , resting on a substrate of height h considering that the length is along the X direction, width is along Y direction and the height is along Z direction.

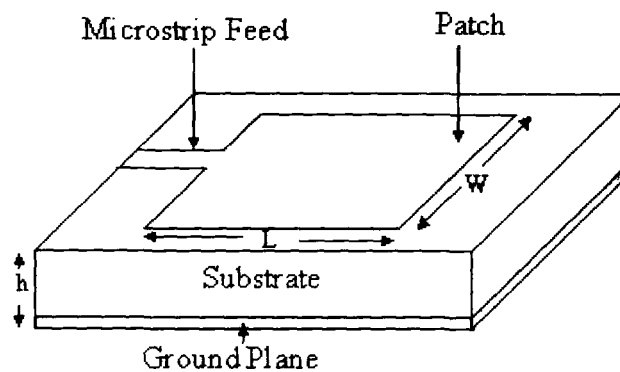


Figure 2.12 Microstrip patch antenna

For a microstrip patch antenna to be operated in the fundamental TM_{10} mode, the length of the patch must be slightly less than $\lambda/2$ where λ is the wavelength in the dielectric medium and is equal to $\lambda_0/\sqrt{\epsilon_{reff}}$ where, λ_0 is the free space wavelength. The TM_{10} mode implies that the field varies one $\lambda/2$ cycle along the length, and there is no

variation along the width of the patch. In the figure 2.13, shown below, the microstrip patch antenna is represented by the two slots, separated by a transmission line of length L and open circuited at both the ends. Along the width of the patch, the voltage is maximum and current is minimum due to open ends. The fields at the edges can be resolved into normal and tangential components with respect to the ground plane.

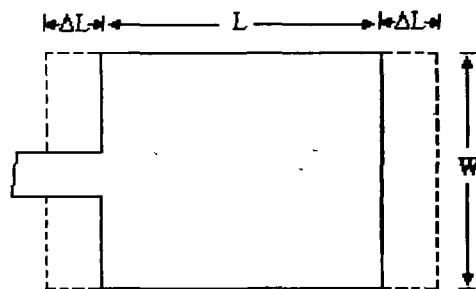


Figure 2.13 Physical and effective lengths of rectangular microstrip antenna.

From figure 2.14, it is seen that the normal component of the electric field at the two edges along the width are in opposite directions and thus, out of phase, since the path is $\lambda/2$ long and hence, they cancel each other in the broadside direction.

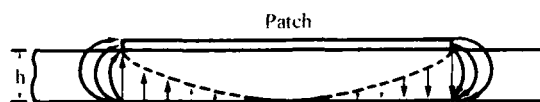


Figure 2.14 Side View of microstrip patch with electric field component.

The tangential components in phase are means that the resulting fields combine to give maximum radiated field normal to the surface of the structure. Hence the edges along the width can be represented as two radiating slots, which are $\lambda/2$ apart and excited in phase and radiating in the half space above the ground plane. The fringing

fields along the width can be modeled as radiating slots and electrically patch of the microstrip antenna looks greater than its physical dimension. The dimensions of the patch along its length have now been extended on each end by a distance ΔL , which is a function of the effective dielectric constant ϵ_{reff} and the width-to-height ratio (W/h). To calculate the normalized extension of the length, the most popular and practical relation is given empirically by Hammerstad [131] as:

$$\Delta L = 0.412h \frac{(\epsilon_{\text{reff}} + 0.3)\left(\frac{w}{h} + 0.264\right)}{(\epsilon_{\text{reff}} - 0.258)\left(\frac{w}{h} + 0.8\right)} \quad (2.2)$$

The effective length of the patch L_{eff} now becomes:

$$L_{\text{eff}} = L + 2\Delta L \quad (2.3)$$

For a given resonance frequency f_r , the length is given by [6] as:

$$L = \frac{c}{2f_r \sqrt{\epsilon_{\text{reff}}}} - 2\Delta L \quad (2.4)$$

Hence
$$L_{\text{eff}} = \frac{c}{2f_r \sqrt{\epsilon_{\text{reff}}}} \quad (2.5)$$

The resonance frequency of a rectangular microstrip patch antenna for any TM_{mn} mode is given by James and Hall [8] as:

$$f_0 = \frac{c}{2\sqrt{\epsilon_{\text{reff}}}} \left[\left(\frac{m}{L} \right)^2 + \left(\frac{n}{W} \right)^2 \right]^{\frac{1}{2}} \quad (2.6)$$

Where m and n are mode along L and W respectively.

For an efficient radiator, the practical width W is given by Bahl and Bhartia [6] as:

$$w = \frac{c}{2f_r} \sqrt{\frac{2}{\epsilon_r + 1}} \quad (2.7)$$

The transmission line model is successfully implemented by Pues and Van de Capelle[132]. With this method it is difficult to model the coupling between antenna elements, although it has been done successfully by A.G.Derneryd and E.H.Van Lil and A.R.Van de Capelle[133,134].

2.5.3 Cavity Model

The simplest analytical method to use in microstrip patch antenna is transmission line model. But transmission line model have numerous disadvantages like, it is useful only for patch antenna of rectangular shape, it ignores field variations along the radiating edge and is not adaptable to inclusion of the field. The cavity model for microstrip patch antennas[37,38] offers considerable improvement over the transmission line model.

The cavity model for the microstrip antennas is based on the following observations for thin substrates ($h \ll \lambda$)[38].

- i) The closed proximity between the microstrip antenna and the ground plane suggest that E has only the Z-component and H has only the xy-components in the region bound by the microstrip and the ground plane.
- ii) The field in the aforementioned region is independent of the z-coordinate for all frequencies of interest.
- iii) The electric current in the microstrip must have no component normal to the edge at any point on the edge, implying a negligible tangential component of H along the edge.

With this, in the cavity model, the interior region of the dielectric substrate is modeled as a cavity bounded by a magnetic wall along the edge and by electric walls on the top and bottom.

As the microstrip patch is energized, a charge distribution is seen on the upper and lower surfaces of the patch and at the bottom of the ground plane as shown in the figure 2.15.

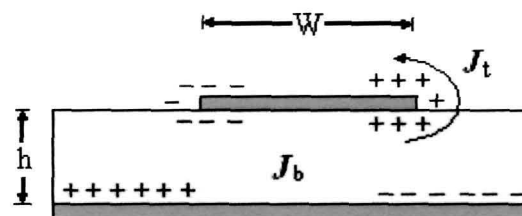


Figure 2.15 Charge distribution and current density creation on the microstrip patch.

This charge distribution is controlled by two mechanisms: an attractive mechanism and a repulsive mechanism as discussed by Richards [135]. The attractive mechanism is between the opposite charge on the bottom side of the patch, and the ground plane. This attraction tends to keep the patch charge concentration intact at the bottom of the patch. The repulsive mechanism is between the like charges on the bottom surface of the patch. This tends to push some of the charge around the edge of the patch on to its top surface. As a result of this charge movement, currents flow at the top and the bottom surface of the patch. The cavity model assumes that the height to width ratio (i.e. height of substrate and the width of the patch) is very small and as a result of this the attractive mechanism dominates and causes most of the charge concentration and the current to be below the patch surface. Much less current would flow on the top surface of the patch and as the height to width ratio further decreases, the current on the top surface of the patch would be almost equal to zero, which would not allow the creation of any tangential magnetic field component to the patch edges. Hence, the four sidewalls could be modeled as perfectly magnetic conducting surfaces. This implies that the magnetic fields and the dielectric field distribution beneath the patch would not be disturbed. However, in practice, a finite width to height ratio would be there and this would not make the tangential magnetic fields to be completely zero, but they being very small, the side walls could be approximated to the perfectly magnetic conducting [7].

The impedance function for the microstrip antenna has complex poles. The imaginary parts of these poles account for the power lost by radiation and by dielectric and conduction losses. The microstrip antenna is modeled to make it more

resemble with cavity by addition of loss to the cavity dielectric by appropriately adjusting the loss tangent of the cavity dielectric. Though impedance function for the ideal cavity has only real poles, now in microstrip antenna modeling the imaginary parts of the poles of the cavity filled with the lossy dielectric will no longer be zero. A lossy cavity would now represent an antenna and for the cavity with perfectly conducting electric and magnetic walls the loss is taken into account by the effective loss tangent δ_{eff} . At any frequency f near a resonance, the quality factor is given by [135]

$$Q = \frac{2\pi f (\text{average total stored energy})}{(\text{average power dissipated})} = \frac{1}{\delta_{\text{eff}}} \quad (2.8)$$

$$\text{Hence, } \delta_{\text{eff}} = \frac{1}{Q_T} \quad (2.9)$$

Q_T is the total antenna quality factor and has been expressed by [136]

$$\frac{1}{Q_T} = \frac{1}{Q_d} + \frac{1}{Q_c} + \frac{1}{Q_r} \quad (2.10)$$

Q_d represent the quality factor of the dielectric and is given as:

$$Q_d = \frac{\omega_r w_T}{P_d} = \frac{1}{\tan \delta} \quad (2.11)$$

Where, ω_r is the angular resonant frequency.

W_T is the total energy stored in the patch at resonance.

P_d is the dielectric loss.

$\tan\delta$ is the loss tangent of the dielectric.

Q_c represents the quality factor of the conductor and is given as:

$$Q_c = \frac{\omega_r W_T}{P_c} = \frac{h}{\Delta} \quad (2.12)$$

Where, P_c is the conductor loss.

Δ is the skin depth of the conductor.

h is the height of the substrate.

Q_r represents the quality factor for radiation and is given as :

$$Q_r = \frac{\omega_r W_T}{P_r} \quad (2.13)$$

Where P_r is the power radiated from the patch.

Substituting equations (2.11), (2.12) and (2.13) in equation (2.10), we get

$$\delta_{eff} = \tan \delta + \frac{\Delta}{h} + \frac{P_r}{\omega_r W_T} \quad (2.14)$$

Thus, equation (2.14) describes the total effective loss tangent for the microstrip patch antenna.

Once “Q” is known, the antenna can be analyzed as if it is a lossy cavity. This is significant since the most commonly used patch antenna shapes corresponds to cavities having a separable geometry amenable to simple analytical treatment. This is the basic idea used in the cavity model approximation.

2.5.4 Full Wave Method – Moment Method

The most popular method, that provides the full wave analysis for the microstrip patch antenna, is the moment method. In mathematical literature, Moment Method is known as Weighted residuals and can be applied to the solution of both differential and integral equations. The method owes its name to the process of taking moments by multiplying the function with an appropriate weighting function and integrating. On microstrip antenna analysis with this method, the surface currents are used to model the microstrip patch and the volume polarization currents are used to model the fields in the dielectric slab. It has been shown by Newman and Tulyathan (30) how an integral equation is obtained for these unknown currents and using the method of moments, these electric field integral equations are converted into matrix equations which can then be solved by various techniques of algebra to provide the result. In electromagnetic theory, the method became popular after the pioneering work done by R.F.Harrington in 1967. Since than it has been one of the most popular methods for solving the electromagnetic boundary value problem. A brief overview of the moment method described by Harrington (137) is given below:

The basic form of the equation to be solved by the method of moment is:

$$F(g) = h \quad (2.15)$$

Where, F is a known linear operator, g is an unknown function, and h is the source or excitation function. The aim here is to find g , when F and h are known. The unknown function g can be expanded as a linear combination of N terms to give:

$$g = \sum_{n=1}^N \alpha_n g_n = \alpha_1 g_1 + \alpha_2 g_2 + \dots + \alpha_n g_n \quad (2.16)$$

Where, α_n are unknown constants and g_n are known functions usually called a basis functions or expansion functions.

If the number of terms in equation (2.16) is infinite, we shall obtain an exact solution. But for computational purposes, the number of terms is finite and we obtain an approximate solution.

Substituting equation (2.16) in (2.15) and using the linear property of the operator F , we can rewrite (2.15) as:

$$\sum_{n=1}^N \alpha_n F(g_n) = h \quad (2.17)$$

The basis function g_n must be selected in such a way that each $F(g_n)$ in the above equation can be calculated. The unknown constant α_n cannot be determined

directly because there are N unknowns, but only one equation. One method of finding these constant is the method of weighted residuals. In this method, a set of trial solution is established with one or more variable parameters. The residuals are a measure of the difference between the trial solution and the true solution. The variable parameters are selected in a way which guarantees a best fit of the trial functions based on the minimization of the residuals. This is done by defining a set of weighting (or testing) functions $\{W_m\} = W_1, W_2, \dots, W_N$ in the domain of the operator F . Taking the inner product of equation (2.17) with each weighting functions W_m , $m = 1, 2, 3, \dots, N$, this lead to:

$$\sum_{n=1}^N a_n \langle w_m, F(g_n) \rangle = \langle w_m, h \rangle \quad (2.18)$$

Where $m = 1, 2, \dots, N$.

Writing in matrix form the set of equations (2.18) may be written as :

$$[F_{mm}][\alpha_n] = [h_m] \quad (2.19)$$

Where,

$$[F_{mm}] = \begin{bmatrix} \langle w_1, F(g_1) \rangle & \langle w_1, F(g_2) \rangle & \dots & \langle w_1, F(g_N) \rangle \\ \langle w_2, F(g_1) \rangle & \langle w_2, F(g_2) \rangle & \dots & \langle w_2, F(g_N) \rangle \\ \vdots & \vdots & \ddots & \vdots \\ \langle w_N, F(g_1) \rangle & \langle w_N, F(g_2) \rangle & \dots & \langle w_N, F(g_N) \rangle \end{bmatrix} \quad (2.20)$$

$$[\alpha_n] = \begin{bmatrix} \alpha_1 \\ \alpha_2 \\ \alpha_3 \\ \vdots \\ \alpha_N \end{bmatrix} \quad (2.21)$$

$$[h_m] = \begin{bmatrix} \langle w_1, h \rangle \\ \langle w_2, h \rangle \\ \langle w_3, h \rangle \\ \vdots \\ \langle w_N, h \rangle \end{bmatrix} \quad (2.22)$$

The unknown constants can now be found using algebraic techniques such as LU decomposition or Gaussian elimination. It must be remembered that the weighting functions must be selected appropriately so that elements of $\{W_n\}$ are not only linearly independent but they also minimize the computations required to evaluate the inner product. One such choice of the weighting functions may be to let the weighting and the basic function be the same, that is, $W_n = g_n$. This is called as the Galerkin's method as described by Kantorovich and Akilov [138].

From the antenna theory point of view, we can write the electric field integral equation as:

$$E = f_e(J) \quad (2.23)$$

Where, E is the known incident electric field.

J is the unknown induced current.

f_e is the linear operator.

The first step in the moment method solution process would be to expand J as a finite sum of basis function given as:

$$J = \sum_{i=1}^M J_i b_i \quad (2.24)$$

Where b_i is the i^{th} basic function and J_i is an unknown coefficient.

The second step involves the defining of a set of M linearly independent weighting functions, w_j . Taking the inner product on both sides and substituting equation (2.24) in equation (2.23) we get :

$$\langle w_j, E \rangle = \sum_{i=1}^M \langle w_j, f_e(J_i, b_i) \rangle \quad (2.25)$$

Where $j = 1, 2, \dots, M$.

Writing in matrix form as:

$$[Z_{ij}] [J] = [E_j] \quad (2.26)$$

Where $Z_{ij} = \langle w_j, f_e(b_i) \rangle$

$E_j = \langle w_j, H \rangle$

J is the current vector containing the unknown quantities.

The vector E contains the known incident field quantities and the terms of the Z matrix are functions of geometry. The unknown coefficients of the induced current are the terms of the J vector. Using any of the algebraic schemes mentioned earlier, these equations can be solved to give the current and then the other parameters such as the scattered electric and magnetic fields can be calculated directly from the induced currents. Thus, the moment method has been briefly explained for use in antenna problems. The software used in this thesis, Zeland Inc's IE3D[139] is a moment method simulator.

CHAPTER 3

**A BRIEF REVIEW OF ARTIFICIAL
NEURAL NETWORKS**

3.1 Introduction

The potential of modeling of large complex systems is a most fascinating aspect of Artificial Neural Networks(ANN), which have attracted the attention of scientists and technologists from a number of disciplines[140]. Artificial Neural systems function as parallel distributed computing networks[141-147]. There are a large number of neural models. Type of application, determines the type of neural networks to be selected. In order to perform a particular task, a neural network must be trained. They learn new associations, new patterns, and new functional dependencies. One of the distinct strengths of neural networks is their ability to generalize well when it sensibly interpolates input pattern that are new to the network. The parallel distribution structure and generalization capability make neural network to solve complex problems[146]. Neural networks have a built in capability to adapt their synaptic weights with changes in the surrounding environment. A neural network trained to operate in a specific environment can be easily retrained to deal with minor changes in the operating environmental conditions[147-229].

3.2 Biological Motivation of Neural Network

The concept of Artificial Neural Network is based on the human brain which can perform sophisticated and intelligent computations in very fast manner. An artificial Neural Network is a machine that is designed to model the way in which the brain performs a particular task or function of interest; the network is usually implemented by simulated software on a digital computer.

An Artificial Neural Network can be defined as “a system composed of many simple processing units operating in parallel whose function is determined by network structure, connection strength, and processing performed at computing elements or nodes”.

Biological neurons are the basic building block of human brain. The brain consists of huge number of neurons(of the order of 10^{10}) and interconnecting synapses between them(of the order of 60×10^{12}). The neurons perform pattern recognition, perception and motor control. Neuron, as shown in the figure 3.1(a), consists of synapses, dendrites, cell body and axon. The synapse converts a pre-synaptic electrical signal into a chemical signal and then back into a post-synaptic electric signal. The post-synaptic signals are aggregated and transferred along the dendrites to the neuron cell body. If the cumulative inputs received raises the electrical potential of the cell body then the neuron fires by propagating the action potential down the axon to excite or inhibit other neurons. The frequency of firing of a neuron is proportional to the total synaptic weights.

3.3 Model of a Neuron

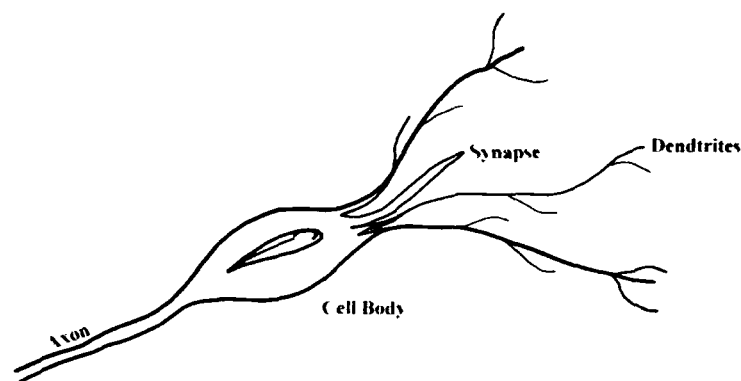


Figure 3.1 (a) Structure of biological neuron.

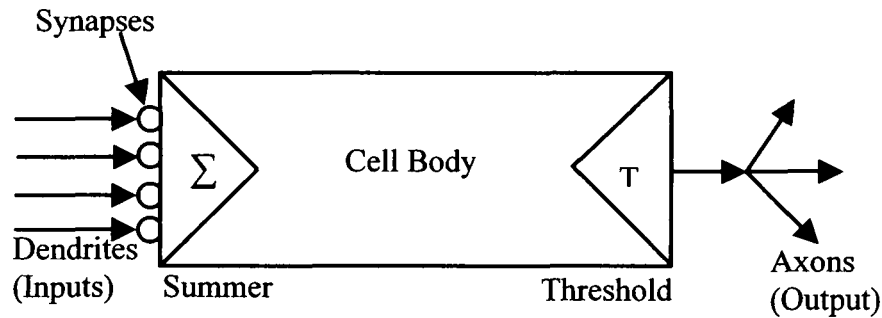


Figure 3.1 (b) Model of biological neuron.

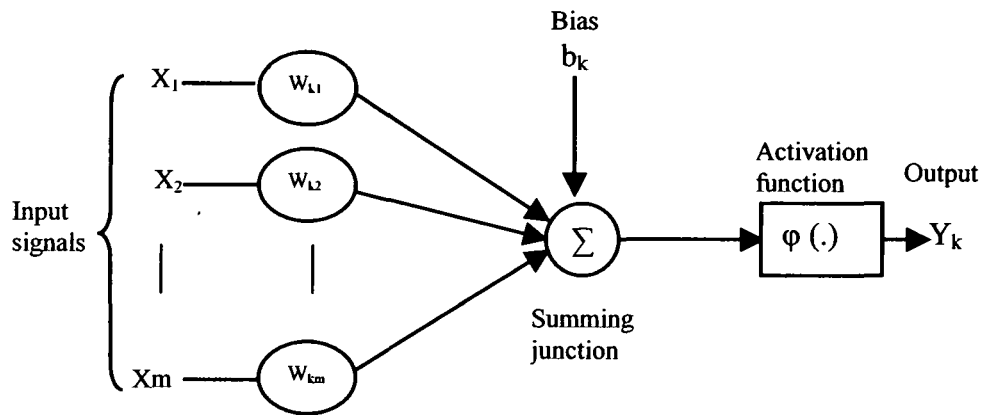


Figure 3.1 (c) Model of Artificial Neuron.

The biological neuron can be represented as a simple model as shown in figure 3.1(b). The analogous model shown in figure 3.1(c) is called artificial neuron. It is this model which forms the basis of artificial neural network. All the information processing operation of neural network occurs at the neuron. The four basic elements of a neuron are synapses or connecting weights, summing junction, activation function, and bias. A set of synapses or connecting weights, each of which are characterised by a weight or strength of its own. Specifically, a signal x , at the

input of synapse j connected to neuron k is multiplied by the synaptic weight w_{kj} . The synaptic weight of an artificial neuron may lie in a range that includes negative as well as positive values. At the summing junction, the input signals weighted by the respective synapses of the neuron, get added up. The activation function or squashing function limits the amplitude of output of neuron. The normalized amplitude range of the output of a neuron lies between 0 and 1 or -1 and 1. The bias, with fixed input $+1$, has the effect of increasing or decreasing the net input of the activation function, depending on whether it is positive or negative, respectively.

The output of a neuron k can be written as,

$$y_k = \phi(v_k) \quad (3.1)$$

Where,

$$v_k = \sum_{j=1}^m w_{kj} x + b_k \quad (3.2)$$

x_1, x_2, \dots, x_m are input signals, $w_{k1}, w_{k2}, \dots, w_{km}$ are the synaptic weights of neuron k , b_k is the bias, $\phi(\cdot)$ is the activation function and y_k is the output signal of neuron.

3.4 Activation Function and Characteristics

The activation function defines the output of a neuron in terms of induced local field v . Various types of activation functions are used in neural networks[230]. Broadly, the activation function can be put into three categories.

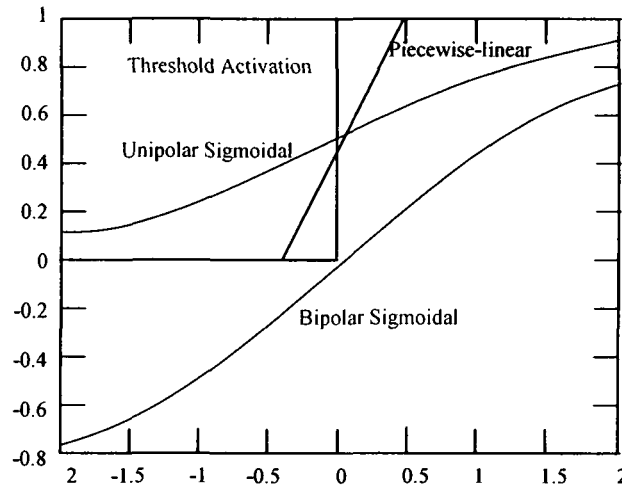


Figure 3.2 Activation functions.

Threshold Function

In this model, the output of a neuron takes on the value of 1 if the induced local field of that neuron is nonnegative and 0 otherwise as shown in figure 3.2.

i.e. in mathematical form,

$$\varphi(v) = \begin{cases} 1 & \text{if } v \geq 0 \\ 0 & \text{if } v < 0 \end{cases} \quad (3.3)$$

Piecewise-Linear Function

The piecewise-linear function can be described as shown in figure 3.2. It can be represented as:

$$\varphi(v) = \begin{cases} 1, & v \geq +\frac{1}{2} \\ v, & +\frac{1}{2} > v > -\frac{1}{2} \\ 0, & v \leq -\frac{1}{2} \end{cases} \quad (3.4)$$

The two special forms of the piecewise-linear functions are:

- ✦ A linear combiner arises if the linear region of operation is maintained without running into saturation.
- ✦ The piecewise-linear function reduces to a threshold function if the amplification factor of the linear region is made infinitely large.

Sigmoid Activation Function

The sigmoid is most common form of activation function in construction of neural network. Mathematically,

$$\varphi(v) = \frac{1}{1 + \exp(-\lambda v)} \quad (3.5)$$

$$\varphi(v) = \frac{2}{1 + \exp(-\lambda v)} - 1 \quad (3.6)$$

Where, λ is called activation constant. It is the slope controlling parameter of the sigmoid. Figure 3.2 shows the input-output shape of various activation functions. The range of unipolar sigmoid, expressed in equation 3.5, lies between 0 and 1. Whereas the sigmoid, expressed in equation 3.6, is bipolar. Its range lies between -1 and 1 .

An alternative form of the sigmoid function is the hyperbolic tangent. It is represented as,

$$\varphi(v) = \tanh(v) \quad (3.7)$$

The choice of activation function for a neural network may influence the learning speed. Neural networks with sigmoid activation functions are capable of approximating unknown mappings arbitrary well[231]

3.5 Learning Rules

Like human brain, neural networks follow a similar pattern of decision making. As done by the human being, who learns from its environment, neural networks also need to be trained. While training, care has to be taken to distinguish the learning from memorization. In fact, training of neural network is done on a case-to-case basis. In some cases, the memorization may be important than the learning.

Training a neural network in input-output mapping, involves modification of the synaptic weights by applying a set of training samples called patterns. Each pattern consists of input signal and corresponding desired response. The synaptic weights are modified to minimise the difference between the desired

response and the actual response of the network produced by the input signal in accordance with an appropriate statistical criterion. The training of the network is repeated for many examples in the set until the network reaches a steady state, where there are no further significant changes in the synaptic weights. Thus, the network learns from the examples by constructing an input-output mapping for the problem at hand.

Neural Networks does not have a unique learning algorithm, as one would expect. There is a saga of neural networks, each of which offers advantage of its own. The selection of a particular network depends on the type of application. Depending upon the type of neural network, there is a learning rule. To name a few, following are the learning rules, (i)Hebbian learning rule, (ii)Perceptron learning rule, (iii)Delta learning rule, (iv)Widrow-Hoff learning rule, (v)Correlation learning rule, (vi)Winner-Take-All learning rule and (vii)Outstar learning rule.

However, as shown in figure 3.3, following general learning procedure is adopted for training in neural network[232]. The weight vector increases in proportion to the product of inputs x and learning signal 'r'. The learning signal 'r' is in general a function of w_i , x and the testing signal d_i and can be expressed as,

$$r = r(w(t), x, d_i) \quad (3.8)$$

Where, $w_i = [w_{i1}, w_{i2}, w_{i3}, \dots, w_{ij}, w_{in}]^T$ is the weights connecting i th neuron.

w_{in} stands for the bias weight. The input x_n of input vector x is the fixed input of bias with a value of -1 . The increment of the weight vector i w produced by the learning step at time t according to the general learning rule is,

$$\Delta w_i(t) = cr[w_i(t), x(t), d_i(t)]x(t) \quad (3.9)$$

where, c is a positive number called the learning constant that determines the rate of learning. The weight vector adapted at time t becomes at the next instant, or learning step and is expressed as,

$$w_i^{k+1} = w_i^k(t) + cr[w_i^k, x^k, d_i^k]x^k \quad (3.10)$$

The learning in equation 3.9 is in the form of a sequence of discrete-time weight modifications. However, continuous-time learning can be expressed as,

$$\frac{dw_i(t)}{dt} = crx(t) \quad (3.11)$$

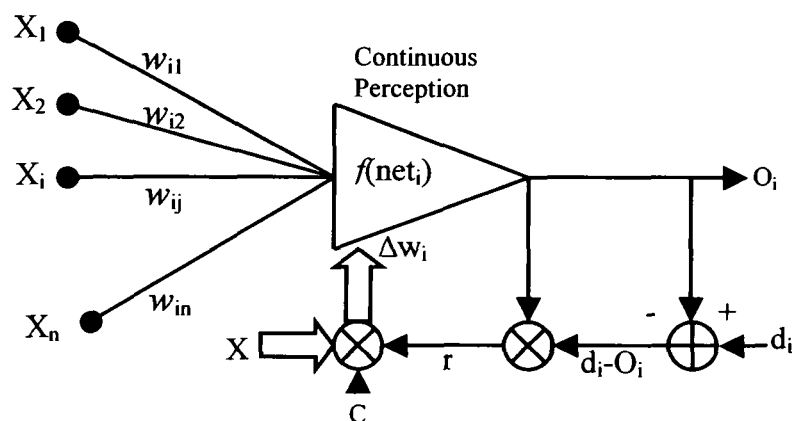


Figure 3.3 Generalised learning rule

3.6 Multilayer Neural Network

The most important attribute of multilayer feed forward network, as shown in figure 3.4, is that it can learn a mapping of any complexity. The network learning is based on repeated presentations of the training samples. A three layer neural network, in principle, is sufficient to model a problem[233,235]. The nodes in the input layer supply input vector to the second layer or first hidden layer. The output of second layer or first hidden layer flows to the second hidden layer, and so on for the rest of the network. The set of output signals of the neurons in the output layer or final layer constitutes the response of the network for the input pattern applied in the input layer. Figure 3.4 shows three layers i.e one input layer, one hidden layer and one output layer, feed forward neural network.

From the point of view of active phase, ANNs can be classified as feedforward(static) and feed back(dynamic) systems. Based on their learning phase, it can be classified into supervised and unsupervised systems. Feedforward supervised networks are typically used for function approximation tasks. Linear recursive leastmean-square(LMS) networks, Backpropagation networks and radial basis networks belong to this category. Feedforward unsupervised networks are used to extract important properties of the input data and map input data into representation domain. Hebbian networks and competitive network belong to this category. Feedback networks are used to learn temporal features of the input data and their internal state evolve with time. Feedforward and feedback supervised neural networks mostly used in CAD application of microwave and antenna

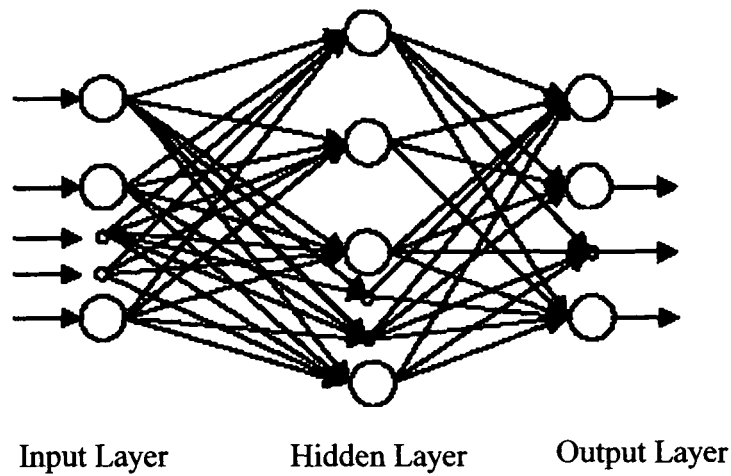


Figure 3.4 Multilayer neural network structure

3.7 Implementation Procedures and Issues Involved in Neural Network Training

Initially, a neural network is ignorant about the system (e.g slot loaded Microstrip antenna). In order to represent the system, the neural network has to be trained with its behaviour i.e a set of input-output patterns. The key steps involved in modeling a system with neural network comprises data generation/collection, data scaling, choice of neural network and its structure and finally training. Input Layer Hidden Layer Output Layer.

The preliminary step in neural model development for a particular problem is identification of model inputs on which the output depends on. Once the inputs and outputs are identified data need to be generated. The source of data may be either measured results or results obtained from simulators like FEM, FDTD or MoM

or may be from some theoretical model. In general, data generation means, collection of a set of output vector for a input vector. The total number of patterns to be collected for a given problem is chosen such that the developed model suitably represents the original problem. The choice of data generator depends on the application, availability of data generator and accuracy concerned. Data collected from measurements is always regarded as the best choice.

While presenting input-output patterns to a neural network the values of the patterns need to be suitably scaled between 0 to 1 or -1 to 1 depending upon a unipolar or bipolar activation function respectively used. The necessity arises due to the fact that the activation function transforms the input signals to the above stated range. It is worth noting that the data scaling restricts application of neural network trained for a particular problem to a specific range of input and output parameters only. Commonly a linear scaling or a log scaling is used for data scaling. An intelligent choice of scaling can enlarge the range of operation. In general, the input-output scaling makes the problem better conditioned for training.

The accuracy of neural network based model may very dramatically depend on many features, including the network topology and learning technique. For a learning in error backpropagation algorithm, the choice of initial synaptic weights for the learning network may significantly affect the learning convergence[235-237]. The best network chosen is often not the best. A common practice is to carve out a small set of data from test data set and use it for cross validation after training. Sometimes, a neural network becomes a unstable predictor. A small change in data set may yield a different configuration and consequently different performance on unseen

data[238,239].

Hidden units allow a network to learn nonlinear functions and allow the network to represent combinations of input features. Given too many hidden units, a neural network will simply memorize the input patterns. Given few hidden units, the network may not be able to represent all of the necessary generalization.

The learning rate limits the weight changes for each iteration. Ideally, the learning rate should be small but then learning becomes very slow. If the learning rate is too high then the system can suffer from severe oscillations. Over training leads a network into memorization. It means the network has been trained to exactly respond to only one type of input.

3.8 Background of Development of ANN Code

3.8.1 Introduction

The invention of error backpropagation algorithm for training multilayer artificial neural networks gives new pace in the research of artificial neural networks. Rumelhart et al [240] represented a clear and concise description of the backpropagation algorithm. It is a systematic method of training multilayer artificial neural networks with sigmoids as activation function. As the name suggests, neuron activation propagates forward and error calculated at the output layer are backpropagated to the hidden layers and weights are modified according to these changes. Although a Backpropagation can be applied to networks with any number of layers, it has been shown that one hidden layer suffices to approximate any function

with finitely many discontinuities to arbitrary precision, provided the activation functions of the hidden units are non-linear[241-244].

Coding of the algorithms in the present thesis work are done using a mixed C/C++[246] in Linux platform using Anjuta GUI. This chapter presents the mathematical details of backpropagation and tunnel based backpropagation algorithm using gradient descent learning rule.

3.8.2 Backpropagation Algorithm

The generalized Backpropagation algorithm can be best explained with a three layer neural network(one input layer, one hidden layer and one output layer).

Let the activation function(which is differentiable) of the total input, given by

$$y_k^p = \varphi(s_k^p) \quad (3.12)$$

$$\text{Where, } s_k^p = \sum w_{jk} y_j^p + \theta_k \quad (3.13)$$

$$\Delta_p w_{jk} = -\eta \frac{\delta E^p}{\delta w_{jk}} \quad (3.14)$$

The error measure, E^p is defined as the total quadratic error for pattern p at output units

$$\text{Thus, } E^p = \frac{1}{2} \sum_{o=1}^{N_o} (d_o^p - y_o^p)^2 \quad (3.15)$$

Where d_o^p is the desired output for units o when pattern p is clamped.

Further, $E = \sum_p E^p$ as the summed squared error.

One can write,

$$\frac{\delta E^p}{\delta w_{jk}} = \frac{\delta E^p}{\delta s_{jk}^p} \frac{\delta s_{jk}^p}{\delta w_{jk}} \quad (3.16)$$

Using equation 3.13, the second term of equation 3.16 can be expressed as,

$$\frac{\delta E^p}{\delta s_{jk}^p} = y_j^p \quad (3.17)$$

The error signal δ_k^p produced by k^{th} neuron is defined as

$$\delta_k^p = -\frac{\delta E^p}{\delta s_{jk}^p} \quad (3.18)$$

There for equation 3.16 can be rewritten as

$$\frac{\delta E^p}{\delta w_{jk}} = \delta_k^p y_j^p \quad (3.19)$$

So equation 3.16 is modified to

$$\Delta_p w_{jk} = \eta \delta_k^p y_j^p \quad (3.20)$$

Expression 3.20 represents the general formula for weight adjustments for a single layer network in delta training/learning. It can be noted that $\Delta_p w_{jk}$ in equation 3.20 does not depend on the form of activation function. It also follows from

3.20 that the adjustment of weight w_{jk} is proportional to the input activation y_j , and to the error signal value δ_{ok} at k^{th} neuron's output.

To compute δ_k^p we apply the chain rule to write this partial derivative as the product of two factors, one factor reflecting the change in error as function of the output unit and one reflecting the change in the output as a function of change in the input,

$$\text{Thus, } \delta_k^p = -\frac{\delta E^p}{\delta s_{jk}^p} = -\frac{\delta E^p}{\delta y_k^p} \frac{\delta y_k^p}{\delta s_k} \quad (3.21)$$

The second term can be computed as

$$\frac{\delta y_k^p}{\delta s_k} = \varphi'(s_k^p) \quad (3.22)$$

Which is simple derivative of the squashing function φ for the k^{th} unit evaluated at the net input s_k^p .

To compute the first factor of equation 3.21, we consider two cases. First, assume that k is an output unit $k=o$ of the network. In this case, it follows from the definition of E^p that

$$\frac{\delta E^p}{\delta y_o^p} = -(d_o^p - y_o^p) \quad (3.23)$$

Substituting equation 3.23 and 3.22 in equation 3.21, we get

$$\delta_o^p = (d_o^p - y_o^p) \phi'(s_o^p) \quad (3.24)$$

for any output unit o .

Secondly, if k is not an output unit but a hidden unit $k=h$, one does not readily know the contribution of the unit to the output error of the network. However, the error measure can be written as a function of the net inputs from hidden to output layer.

$E^p = E^p(s_1^p, s_2^p, s_3^p, \dots, s_j^p, \dots)$ and we use the chain rule to write,

$$\begin{aligned} \frac{\delta E^p}{\delta y_h^p} &= \sum_{o=1}^{N_o} \frac{\delta E^p}{\delta s_o^p} \frac{\delta s_o^p}{\delta y_h^p} \\ &= \sum_{o=1}^{N_o} \frac{\delta E^p}{\delta s_o^p} \frac{\delta}{\delta y_h^p} \sum_{j=1}^{N_o} w_{ko} y_j^p \\ &= \sum_{o=1}^{N_o} \frac{\delta E^p}{\delta s_o^p} w_{ho} = - \sum_{o=1}^{N_o} \delta_o^p w_{ho} \end{aligned} \quad (3.25)$$

Substituting this in equation 3.21 yields

$$\delta_h^p = \phi'(s_h^p) \sum_{o=1}^{N_o} \delta_o^p w_{ho} \quad (3.26)$$

Equation 3.24 and 3.26 give a recursive procedure for computing the δ 's for all units in the network, which are then used to compute the weight changes according to equation 3.20. This procedure constitutes the generalized delta rule for feed forward network of non-linear units.

Working with Backpropagation Algorithm

The application of the generalized delta rule thus, involves two phases: During the first phase, the input \mathbf{X} is presented and propagated forward through the network to compute the output values y_o^p for each output unit. This output is compared with its desired value d_o , resulting in an error signal δ_o^p for each output unit. The second phase, involves a backward pass through the network during which the error signal is passed to each unit in the network and appropriate weight changes are calculated.

Weight Adjustments with Sigmoid Activation Function

The Backpropagation algorithm can be summarised in following three equations:

- ✦ The weight of a connection is adjusted by an amount proportional to the product of an error signal δ_k on the unit k receiving the input and the output of the unit j sending this signal along the connection:

$$\Delta_p w_{jk} = \eta \delta_k^p y_j^p \quad (3.27)$$

✦ If the unit is an output unit, the error signal is given by

$$\delta_o^p = (d_o^p - y_o^p) \varphi'(s_o^p) \quad (3.28)$$

Taking the activation function ' φ ' as the 'sigmoid' function.

$$y^p = \varphi(s^p) = \frac{1}{1 + e^{-sp}} \quad (3.29)$$

In this case the derivative is equal to

$$\begin{aligned} \varphi'(s^p) &= \frac{\delta}{\delta s^p} \frac{1}{1 + e^{-sp}} \\ &= \frac{1}{(1 + e^{-sp})^2} (-e^{-sp}) \\ &= \frac{1}{(1 + e^{-sp})^2} \frac{(-e^{-sp})}{(1 + e^{-sp})} \\ &= y^p (1 - y^p) \end{aligned} \quad (3.30)$$

Such that the error signal for an output unit can be written as:

$$\delta_o^p = (d_o^p - y_o^p) y^p (1 - y^p) \quad (3.31)$$

✦ The error signal for a hidden unit is determined recursively in terms of error signals of the units to which it directly connects and the weights of those connections.

For the sigmoid activation function:

$$\begin{aligned}
\delta_o^p &= \varphi'(s_h^p) \sum_{o=1}^{N_o} \delta_o^p w_{ho} \\
&= y_h^p (1 - y_h^p) \sum_{o=1}^{N_o} \delta_o^p w_{ho}
\end{aligned} \tag{3.32}$$

In a Backpropagation algorithm, when a learning pattern is clamped, the activation values are propagated to the output units, and the actual network outputs is compared with the desired output values, we usually end up with an error in each of the output units. This error, e_o (say) for a particular output unit o . We have to bring e_o to zero. One strives to change the connections in the neural network in such a way that, next time around, the error e_o will be zero for this particular pattern. From the delta rule, in order to reduce an error, we have to adapt its incoming weights according to,

$$\Delta w_{ho} = (d_o - y_o) y_h \tag{3.33}$$

But, when we apply this rule, the weights from input to hidden units are never changed, and we do not have the full representation power of the feed-forward network as promised by the universal approximation theorem. In order to adapt the weights from input to hidden units, we again want to apply the delta rule. In this case, however, we do not have a value for δ for the hidden units. This is solved by the chain rule, which does the following:

Distribute the error of an output unit o to all the hidden units that it is connected to, weighted by this connection. Differently put, a hidden unit h receives a delta from each output unit o equal to the delta of the output unit weighted with (=multiplied by) the weight of the connection between those units. In

symbols: $\delta_h = \sum \delta_o w_{ho}$. The activation function of the hidden unit; 'φ' has to be applied to the delta, before the backpropagation process can continue.

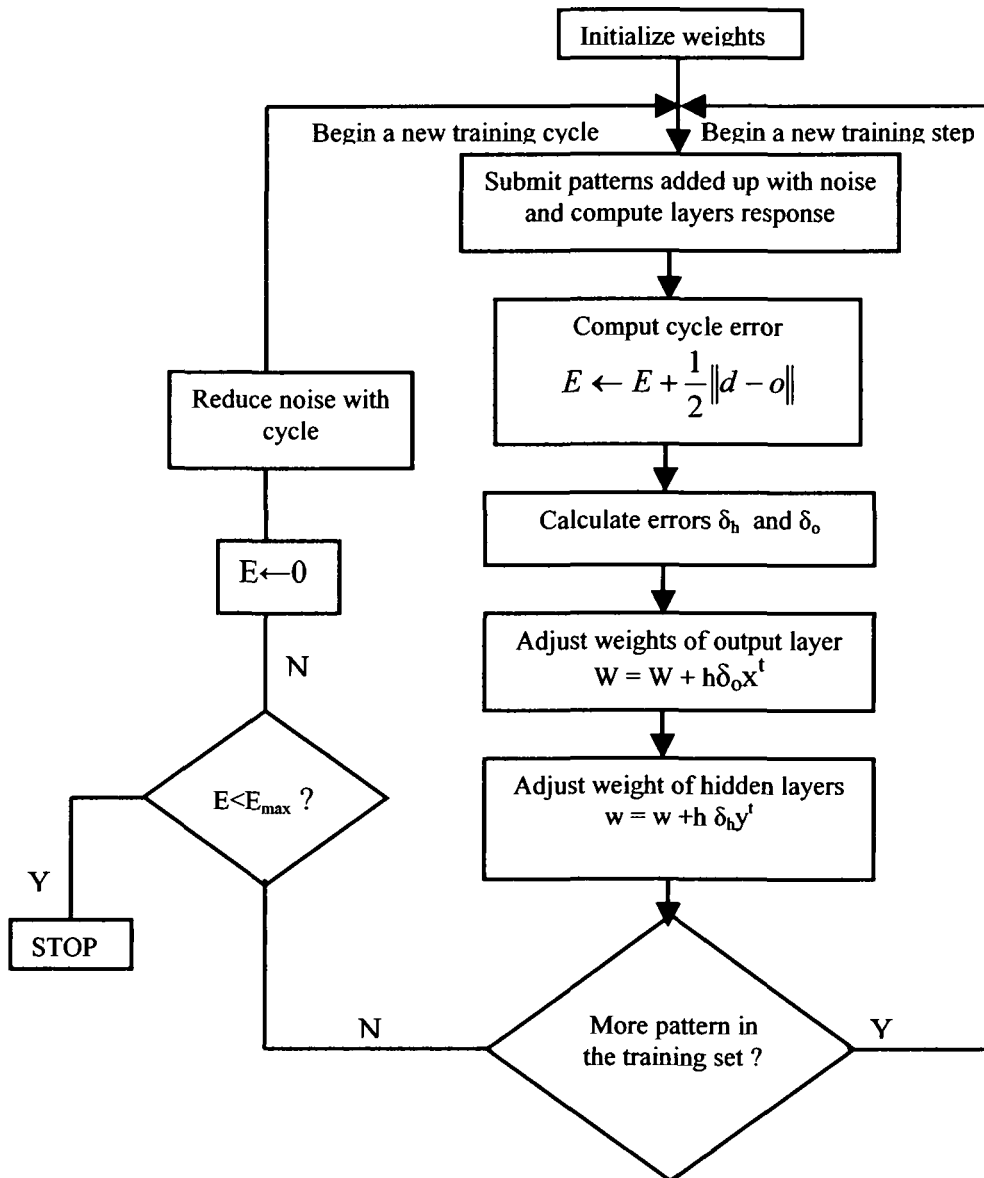


Figure 3.5 Flow Chart of Backpropagation algorithm

Momentum Method

The learning procedure requires that the change in weight is proportional to $\frac{\delta E^p}{\delta w}$. True gradient descent requires that infinitesimal incremental/decremental steps. Practically, the learning rate is chosen as large as possible, to conserve time, without leading to oscillation. One way to avoid oscillation at large learning constant ' η ', is to make the change in weight dependent on the past weight change by adding a momentum term, given by,

$$\Delta w_{jk}(t+1) = \eta \delta_k^p y_j^p + \alpha \Delta w_{jk}(t) \quad (3.34)$$

where ' t ' indexes the presentation number and ' α ' is moment factor which determines the effect of the previous weight change. Typically ' α ' is chosen between 0.1 and 0.8. When momentum term is not used, it takes a long time before the minimum has been reached with a low learning rate, whereas for high learning rates the minimum is never reached because of the oscillations.

Learning Constant

The effectiveness and convergence of the error Backpropagation learning algorithm depend significantly on the value of the learning constant η . In general, however, the optimum value of η depends on the problem being solved. There is no single learning constant suitable for different training cases. When broad minima yield small gradient values, then a large value of η will result in a more

rapid convergence. However, for problems with steep and narrow minima, a small value of η should be chosen to avoid overshooting the solution. Learning constant ' η ' should be chosen experimentally for each problem. It is seen that only small learning constants guarantee a true gradient descent. The price of this guarantee is an increased total number of learning steps that need to be made to reach the satisfactory solution. Though the choice of the learning constant depends strongly on the class of the learning problem and on the network architecture. The values ranging from 10^{-3} to 10 as reported in literature have been successfully applied for many computational Backpropagation experiments.

Noise Factor

Adding noise factor helps in breaking out of local minima. It enhances generalization ability of the network [245]. Another reason for using noise is to prevent memorization by the network. Since, one effectively presents a different input pattern with each cycle, so it becomes hard for the network to memorize patterns. A random number is added to each input component of the input vector as it is applied to the network. This is scaled by an overall noise factor which has a 0 to 1 range. The noise factor is gradually decreased to zero with the increase in the number of iteration.

Steepness of the Activation Function

The neuron's continuous activation function $\phi(\text{net}, \lambda)$ is characterized by its steepness factor λ . Also, the derivative of $\phi'(\text{net})$ of the activation function

serves as a multiplying factor in building components of the error signals. Thus, both choice and shape of the activation function would strongly affect the speed of network learning.

3.3 Tunnel Based Backpropagation Algorithm

Due to gradient nature and arbitrary choice of learning constant, the backpropagation algorithm can become oscillatory. Then, it gets stuck in local minima in many instances. Maximum effort of a backpropagation algorithm is spent to overcome the local minima. A tunneling technique is incorporated with the backpropagation algorithm to tunnel out of the local minima. It was first proposed for discrete problem by Choudhry et al [246].

An initial point is chosen in the weight space at random and then it is slightly perturbed. The new point is tested for either gradient descent or tunneling phase in the following manner.

Let the random point chosen on the weight space be denoted by W , where $W \in R^n$, where n denotes the dimension of the search space. The new point is represented by $W + \epsilon$, where ϵ is a small quantity ($\ll 1$). Depending on the relative value of mean square error (mse), which is the mean of the squared error given by 3.15, at W and $W + \epsilon$; i.e if $mse_{w+\epsilon} \leq mse_w$ then learning in gradient descent is initiated, else tunneling takes place in the weight space. If a gradient descent phase is initiated then it finds a point for the gradient descent. After this, the algorithm automatically enters either of the two phases alternately and weights are updated

according to the modification rule of the respective phase. The learning procedure continues till the global optimal weights are obtained with minimum mean square error(mse).

Phase-I Backpropagation Phase

This phase is according to explained in section 3.8.2.

Phase-II Tunneling Technique

The dynamic tunneling technique is an implementation of Hook-Jeev pattern search method[247], reproduced as below,

Let, ${}_{eq}u$ is an equilibrium point of the system.

$$\frac{du}{dt} = g(u) \quad (3.35)$$

is termed as attractor or repeller if no eigen value of the matrix A

$$A = \frac{\partial u_{uq}}{\partial t} \quad (3.36)$$

has a positive real part. Typically, dynamical system such as (3.35) obey Lipschitz condition

$$\left| \frac{\partial u_{uq}}{\partial t} \right| < \infty \quad (3.37)$$

which guarantees the existence of a unique solution for each initial condition u_0 . Usually such systems has infinite relaxation time to an attractor and escape time from a repeller. Based on the violation of Lipschitz condition at equilibrium points, which induces singular solution such that each solution approaches an attractor, or escapes from a repeller in finite time.

Consider a system given by

$$\frac{du}{dt} = -u^{\frac{1}{3}} \quad (3.38)$$

The system represented by (3.38) has an equilibrium point at $u = 0$, since

$$\left| \frac{du}{dt} \right| = \left| -\frac{1}{3u^{-\frac{2}{3}}} \right| \rightarrow \infty, \quad \text{as } u \rightarrow 0 \quad (3.39)$$

The equilibrium point of the above mentioned system is termed as attracting equilibrium point, since from any initial condition $u_0 \neq 0$, the dynamical system in (3.38) reaches the equilibrium point $u = 0$ in a finite time t_1 given by

$$t_1 = -\int u^{-\frac{1}{3}} du = \frac{3}{2u_0^{\frac{2}{3}}} \quad (3.40)$$

Similarly, the dynamic system

$$\frac{du}{dt} = -u^{-\frac{1}{3}} \quad (3.41)$$

has a repelling unstable equilibrium point at $u = 0$ which violates the Lipschitz condition. Any initial condition, which is infinitesimally close to the repelling point $u = 0$ will escape the repeller, to reach point u_0 in a finite time given by

$$t_1 = \int u^{-\frac{1}{3}} du = \frac{3}{2u^{\frac{2}{3}}} \quad (3.42)$$

The concept of dynamic tunneling algorithm is based on the violation of Lipschitz condition at equilibrium point, which is governed by the fact that any particle placed at small perturbation from the point of equilibrium will move away from the current point to another within a finite of time.

The tunneling is implemented by solving the differential equation given by

$$dw_{j,k}^l / dt = \rho(w_{j,k}^l - w_{j,k}^{l*})^{\frac{1}{3}} \quad (3.43)$$

Here, ρ represents the strength of learning, $w_{j,k}^{l*}$ represents the last local minimum for $w_{j,k}^l$. It is obvious from 3.35 that the local minimum point W^* is also the point of equilibrium of the tunneling system. The value of $w_{j,k}^l$ is $w_{j,k}^{l*} + \varepsilon_{j,k}^l$, where $\varepsilon_{j,k}^l \ll 1$ and 3.43 is integrated for a fixed amount of time (t), with a small time-step (Δt). After every time step, mse_w is computed with the new value of $w_{j,k}^l$ keeping remaining components of W same as $w_{j,k}^{l*}$. Tunneling comes to halt when $mse_w \ll mse_{llm}$, where llm indicates last local minimum (the condition for descent), and initiates the next gradient descent. If this condition of descent is not

satisfied then this process is repeated with all the Components of $w_{j,k}^{i*}$ until the above condition of descent is satisfied, then the last local minimum is the global minimum point.

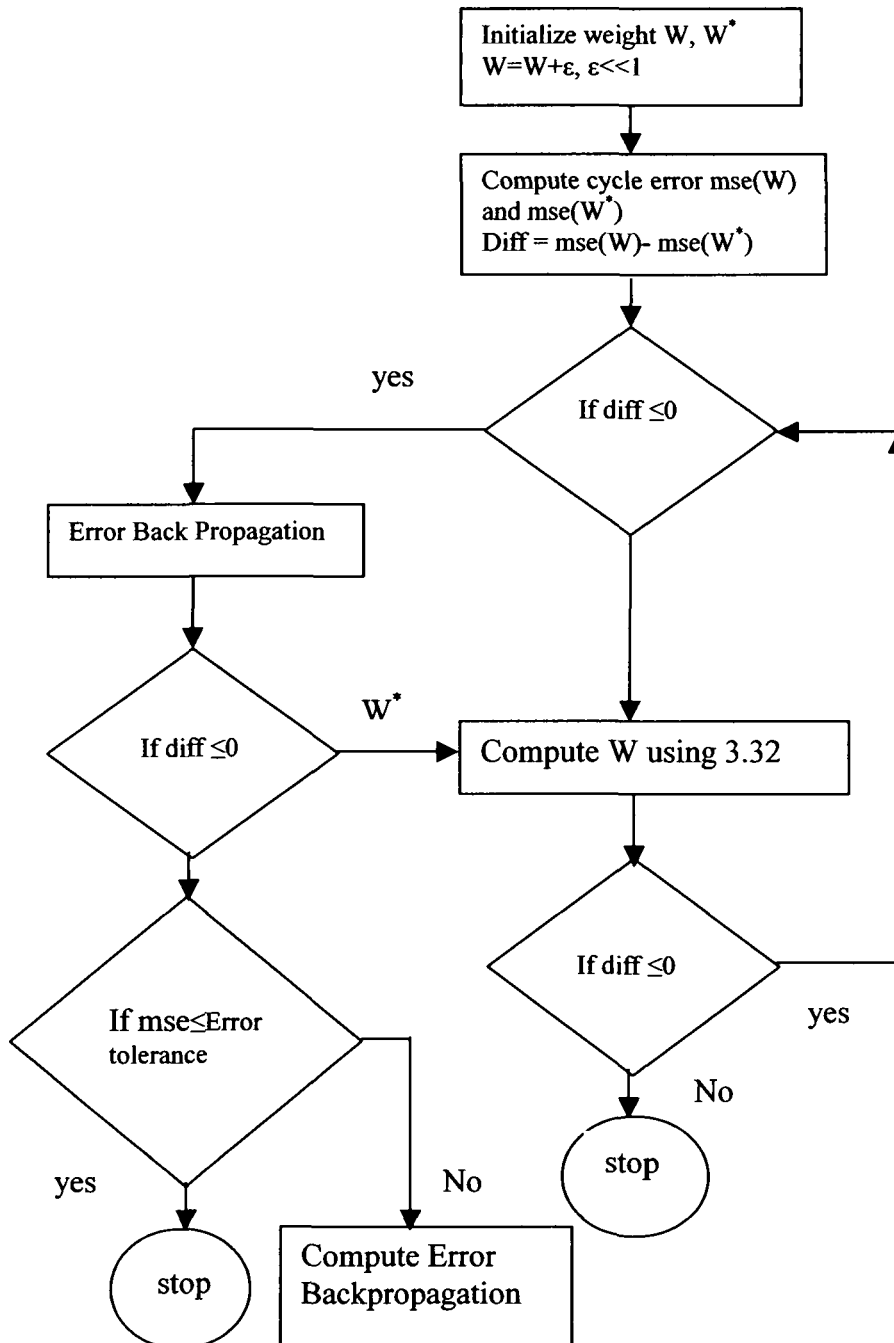


Figure 3.6 Flow chart of tunnel based backpropagation algorithm.

CHAPTER 4

**HORN SHAPED MICROSTRIP
PATCH ANTENNA**

4.1. Introduction

The rapid developments in wireless communication, single patch, wide-band antennas have attracted researchers' attention [248-250]. For a probe feed patch antenna with a single radiating patch, it is very difficult to achieve an impedance band width greater than 10%. In the last decades, many papers have been published on the band width widening techniques of microstrip antennas. However, these designs have the disadvantages of having increasing lateral size, complex design for fabrication and increasing thickness. Here in this chapter, a new design of microstrip antenna has been presented on thin substrate to give wide-band (32%) without any design complexities. For this new design, the basic plan size of the rectangular microstrip antenna is calculated by using the Transmission Line Method. The designed Horn shaped antennas parameters are calculated using IE3D, a Method of Moment based software[139]. The measurements were performed in Microwave Antenna Laboratory, at North Eastern Regional Institute of Science and Technology (NERIST), India.

In section 4.2., the design specification and the antenna structure is presented. The computational and measurement results for dielectric constant of 2.2 and air are given in section 4.3 and in section 4.4 respectively.

4.2 Design Specification and Antenna Structure

To design the horn shaped microstrip patch antenna, the basic parameters i.e. length and width of a rectangular microstrip patch antenna are

Calculated using simplified equation of Transmission Line Method [7] as given below.

The three basic parameters for the calculation of the rectangular shape are the dielectric constant (ϵ_r), Height of the dielectric constant (h) and the expected resonance frequency (f_0). For the design, the dielectric material is Taconic (dielectric constant (ϵ_r) 2.2). The height of the substrate are 02mm and 3.175mm respectively. The range of frequency of operation is 5-10GHz with centre frequency at 8.5GHz.

(i) Calculation of Width (W)

The width of the microstrip antenna is given by equation 2.7 as:

$$W = \frac{c}{2f_r \sqrt{\frac{\epsilon_r + 1}{2}}} \quad (4.1)$$

Substituting $c = 3 \times 10^8$ m/s, $\epsilon_r = 2.2$, and $f_r = 8.5$ GHz, We get

$$W = 13.9512 \text{ mm.}$$

(ii) Calculation of Effective Dielectric Constant (ϵ_{eff})

The effective dielectric constant is calculated by using the equation 2.1 as:

$$\epsilon_{eff} = \frac{(\epsilon_r + 1)}{2} + \frac{(\epsilon_r - 1)}{2} \left[1 + 12 \frac{h}{W} \right]^{-\frac{1}{2}} \quad (4.2)$$

Substituting $\epsilon_r = 2.2$, $W = 13.9512$ mm and height $h = 2$ mm, we get,

$$\epsilon_{eff} = 1.963378$$

(iii) Calculation of the Length of the Antenna

Equation 2.5 gives the effective length of the antenna is

$$L_{eff} = \frac{c}{2f_r \sqrt{\epsilon_{eff}}} \quad (4.3)$$

Substituting ϵ_{eff} , c and f_0 we get,

$$L_{eff} = 12.5929\text{mm}$$

From equation 2.2 we get,

$$\Delta L = 0.412h \frac{(\epsilon_{eff} + 0.3)\left(\frac{w}{h} + 0.264\right)}{(\epsilon_{eff} - 0.258)\left(\frac{w}{h} + 0.8\right)} \quad (4.4)$$

Substituting the values of $\epsilon_{eff} = 1.963378$, $W = 13.9512$ mm and $h = 2$ mm, we get

$$\Delta L = 1.01817\text{mm}$$

The actual length is given by equation-

$$L = L_{eff} - 2 \Delta L \quad (4.5)$$

Substituting the values $L_{eff} = 12.5929\text{mm}$ and $\Delta L = 1.01817\text{mm}$, we get,

$$L = 10.5566\text{mm}.$$

(iv) Horn Shaped Microstrip Patch Antenna

The calculated values of the basic rectangular microstrip antenna is $L = 10.5566\text{mm}$ and $W = 13.9512\text{ mm}$ & height 02mm . For the proposed design, the value of L and W are rounded to $L = 10\text{mm}$ and $W = 14\text{mm}$. On this basic rectangular microstrip antenna, two triangular notches are incorporated as shown in figure 4.1. The triangle size is defined by the two sides as L_s and W_s . The values of L_s and W_s are optimized on trial & error method. The most acceptable values are $L_s=06\text{mm}$ and $W_s=06\text{mm}$.

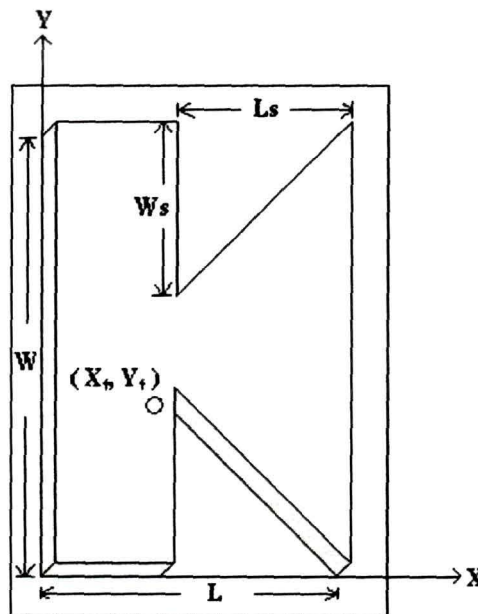


Figure 4.1 Horn Shaped microstrip patch antenna ($L=10\text{mm}$, $W=14\text{mm}$, $L_s=6\text{mm}$, $W_s=6\text{mm}$, $X_f=3.2$, $Y_f= 5.2$).

(v) Determination of Feed Point(X_f, Y_f)

A co-axial feed of radius = 0.6mm is used in this antenna. The feed point is required to be located at the point on the patch, where the input impedance is 50ohm for the resonant frequency. Hence, trial and error method is used to locate the feed point. The feed point is selected where return loss is less than -15dB.

(vi) Calculation of the Ground Plane (L_g and W_g)

An infinite ground plane is considered in case of transmission line method. For practical consideration, it is essential to have a finite ground plane. It has been shown [9] that similar results for finite and infinite ground plane can be obtained if the size of the ground plane is greater than the patch dimension by approximately six times the substrate thickness all around the periphery. Hence, the minimum value of ground plane dimensions is calculated as,

$$L_g = 6h + L = 6(2) + 10 = 22\text{mm.} \quad (4.6)$$

$$W_g = 6h + W = 6(2) + 14 = 26\text{mm.} \quad (4.7)$$

4.3 Computational and Measured Results

To achieve wide band width, this antenna is designed based on the ideas that, in micro-strip antenna, some part of the radiating surface or ground plane can be removed without any significant changes of antenna performance in terms of radiation patterns as the current distribution remains intact [30,251]. It is known that the frequency of a patch antenna also can be increased or decreased by capacitive or

inductive load. The slot length (L_s), width (W_s) and feed position are important parameters in controlling the bandwidth. The length of the current path is increased due to the notch, which leads to additional inductance in series [252]. Thus, the antenna changes from a single LC resonant circuit to dual resonant circuit and the two resonant circuits couple together and gives wide bandwidth.

Measured and calculated results are shown in figure 4.2 for the Horn shaped antenna on Taconic substrate of thickness 2mm and dielectric constant of 2.2. From the figure it can be observed that the antenna has two resonant frequencies: one at 6.7GHz and another at 7 GHz. The frequency band with -10dB return loss covers the frequency range of 6.53 to 7.24 GHz. It has a band width of 10.32% with a thin (2mm) substrate of dielectric constant (ϵ_r) 2.2.

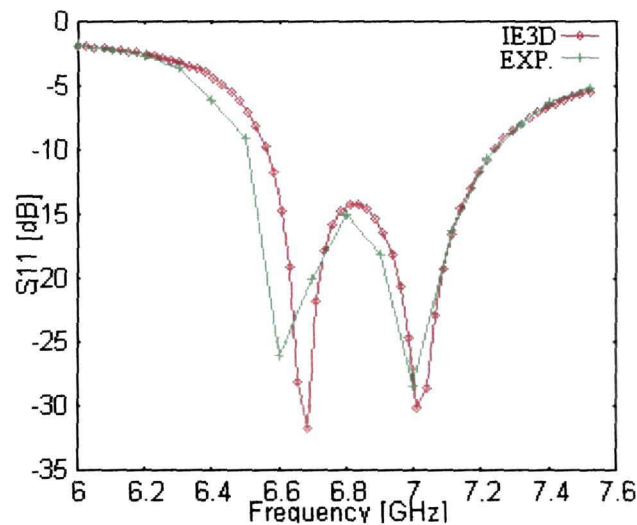


Figure 4.2 Measured and calculated return loss of horn-shaped microstrip patch antenna with 2mm thick substrate.

The Horn shaped antenna is studied for substrate thickness of 3.175 of dielectric constant 2.2. The antenna parameters are listed below (in millimeters):

$$(L, W, h) = (10, 14, 3.175),$$

$$(X_f, Y_f) = (3.2, 5.2),$$

$$(L_s, W_s) = (06, 06).$$

As depicted in Figure 4.3, the antenna frequency band with -10dB return loss covers the frequency range of 6.00 to 8.25 GHz. An impedance band of 32% is achieved for this antenna. From Figure 4.3, it is clear that the antenna has two resonant frequencies one at 6.1GHz and the other at 7.3GHz. This is in agreement with the coupling of two resonant circuits to give wide bandwidth. It also shows the increase of band width with the increase of substrate height.

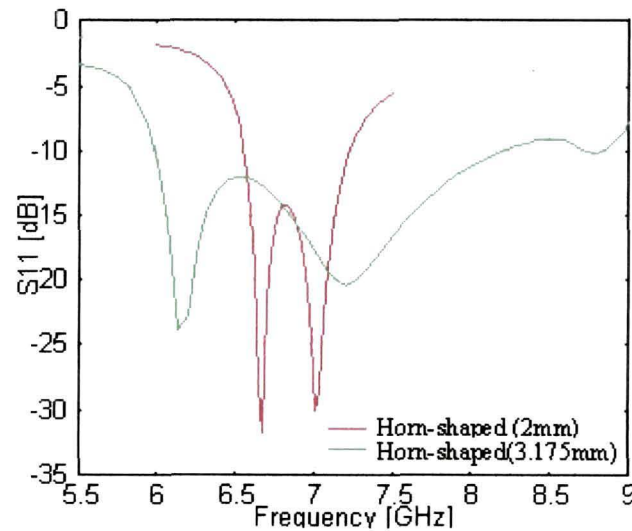


Figure 4.3 Return loss of horn-shaped microstrip patch antenna with 2mm and 3.175mm thickness.

For the Horn shaped antenna, it is observed that the notch size i.e. parameter L_s and W_s are important parameter to control the resonant frequencies and bandwidth of the antenna. Figure 4.4 gives the variation of bandwidth with the change in L_s . At $L_s = 7\text{mm}$, the impedance bandwidth increases but the antenna efficiency decreases for higher frequency components. Figure 4.5 illustrates the dependency of bandwidth on W_s .

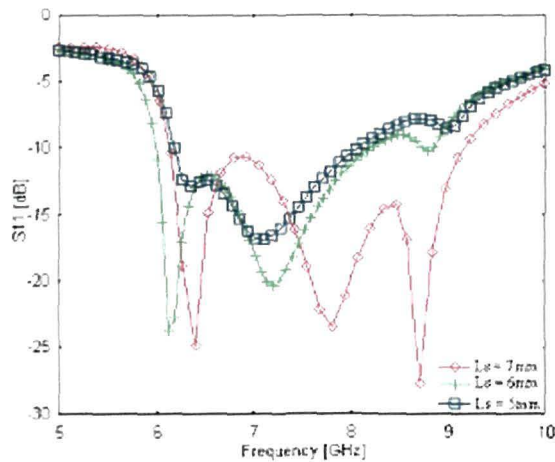


Figure 4.4 Calculated S_{11} of horn-shaped microstrip patch antennas with different notch length (L_s).

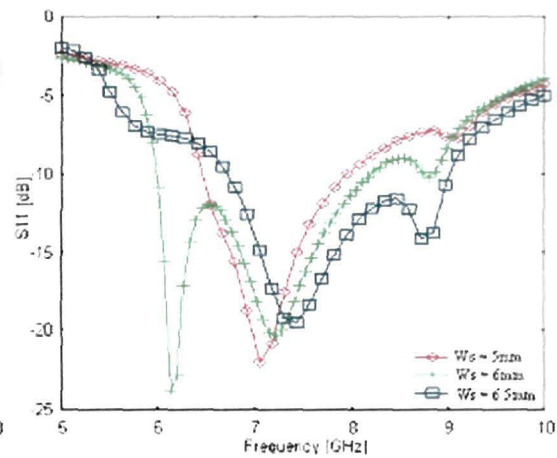


Figure 4.5 Calculated S_{11} of horn-shaped microstrip patch antenna with different notch widths (W_s).

The current distributions are calculated using method of moments. To see the pattern bandwidth, these antennas are simulated at different frequencies to study the radiation patterns both in azimuth and elevation planes. Figure 4.6(a) and Figure 4.6(b) respectively represent the azimuth radiation pattern and elevation radiation patterns of Horn-shaped microstrip patch antenna of 2mm thick substrate. The frequencies 6.532GHz to 7.241GHz are seen within 3dB for both azimuth and elevation pattern of the antenna. The 3dB pattern bandwidth is calculated to be 0.709 GHz. The azimuth patterns and elevation patterns of Horn-shaped microstrip patch antennas of 3.175mm thick substrate are plotted in Figure 4.7(a) and Figure- 4.7(b) respectively. The frequencies from 6.10266GHz to 7.72152 GHz are seen to be within 3dB for both azimuth and elevation pattern of the antenna.

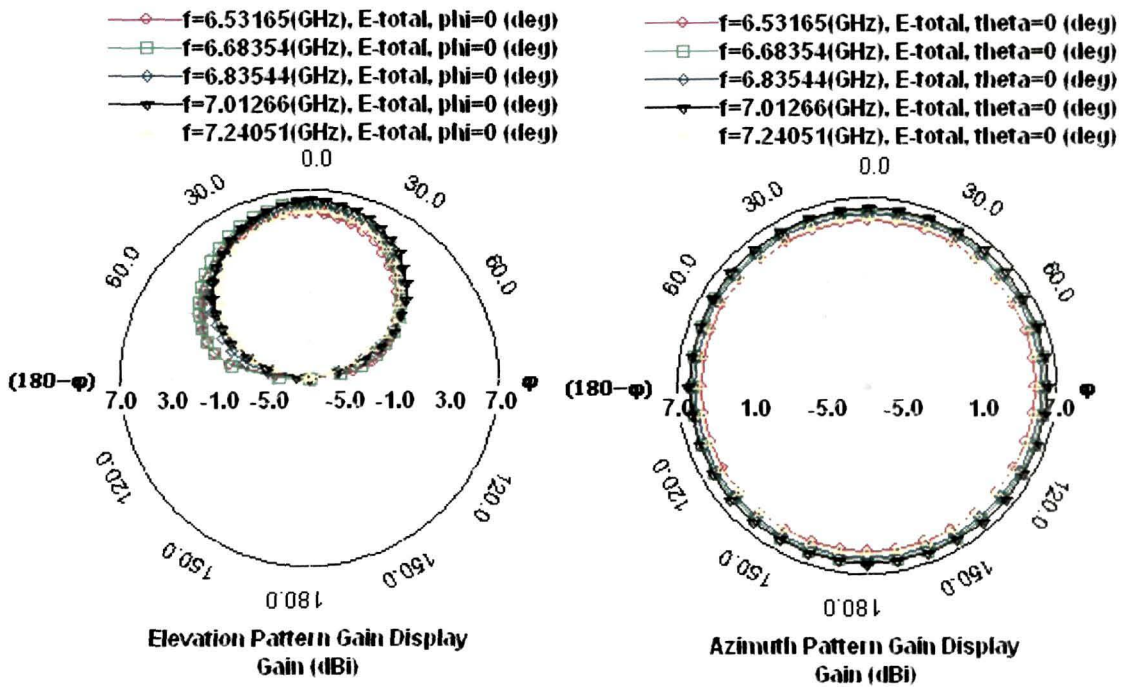


Figure 4. 6(a) Azimuth pattern of horn-shaped microstrip antenna of 2mm thick substrate.

Figure 4.6(b) Elevation pattern of horn-shaped microstrip antenna of 2mm thick substrate.

It is clear from the Figure 4.7(a) and figure 4.7(b) respectively that the 3dB pattern bandwidth is 1.83 GHz. The linear gain of the Horn-shaped microstrip antenna of 2mm thick substrate is calculated to be 6.32 dBi while that for 3.175mm thick substrate is 5.6521 dBi. The large bandwidth has been achieved with a substrate of thickness 3.175mm compared to that of 10 mm thickness of E-shaped microstrip antenna [121].

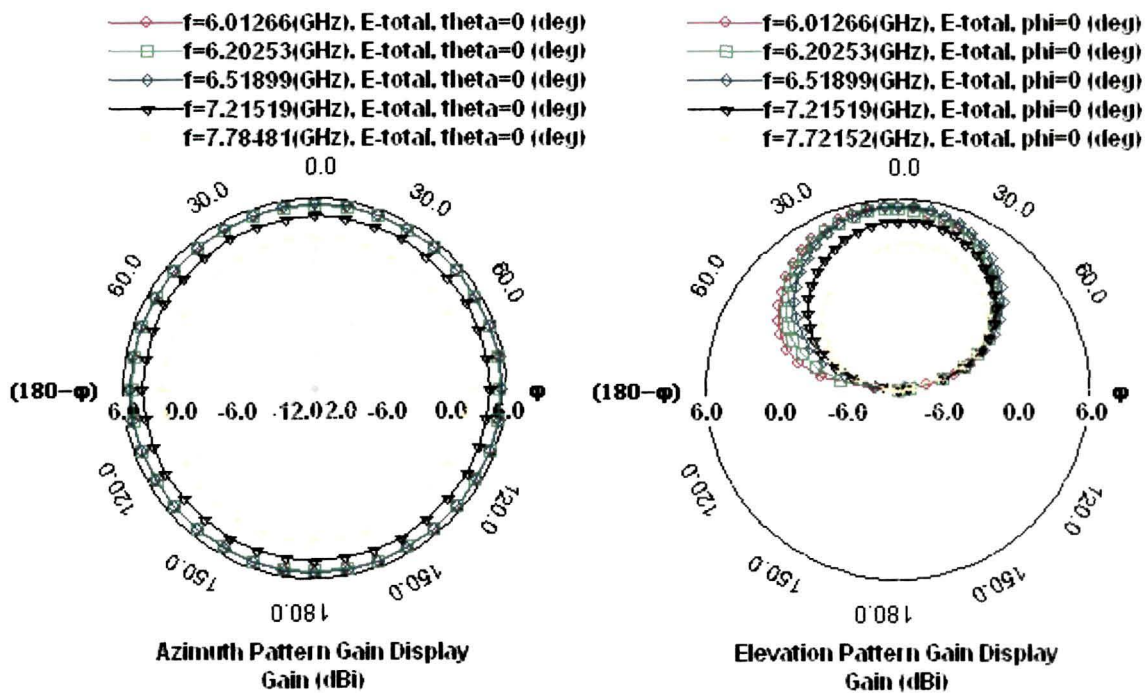


Figure 4.7(a) Azimuth pattern of horn-shaped antenna of 3.175mm thick substrate.

Figure 4.7(b) Elevation pattern of horn-shaped antenna of 3.175mm thick substrate.

4.4. Horn Shaped Patch antenna for Air Dielectric

The Horn Shaped microstrip patch antenna parameters are calculated for air dielectric of thickness of 2mm and 3mm respectively. The calculated return loss of 2mm thick antenna is given in figure 4.8 and in figure 4.9, the comparative plot of return loss of 2mm & 3mm thick antenna for air dielectric is given. The antenna parameters are given below (in millimeters):

$$(L, W, h) = (10, 14, 3.175),$$

$$(X_f, Y_f) = (3.2, 5.7)$$

$$(L_s, W_s) = (06, 06).$$

As depicted in Figure 4.8, the antenna resonates at two frequencies i.e. at 8.2GHz and at 9.5GHz. The 9.5 GHz is due to the normal rectangular shape and the lower resonant frequency is due to the notched. The length of the current path is increased due to the notch, which leads to additional inductance in series. The antenna frequency band with -10dB return loss covers the frequency range of 9.25 GHz to 9.98 GHz. An impedance band width of 7.6% is achieved for this antenna.

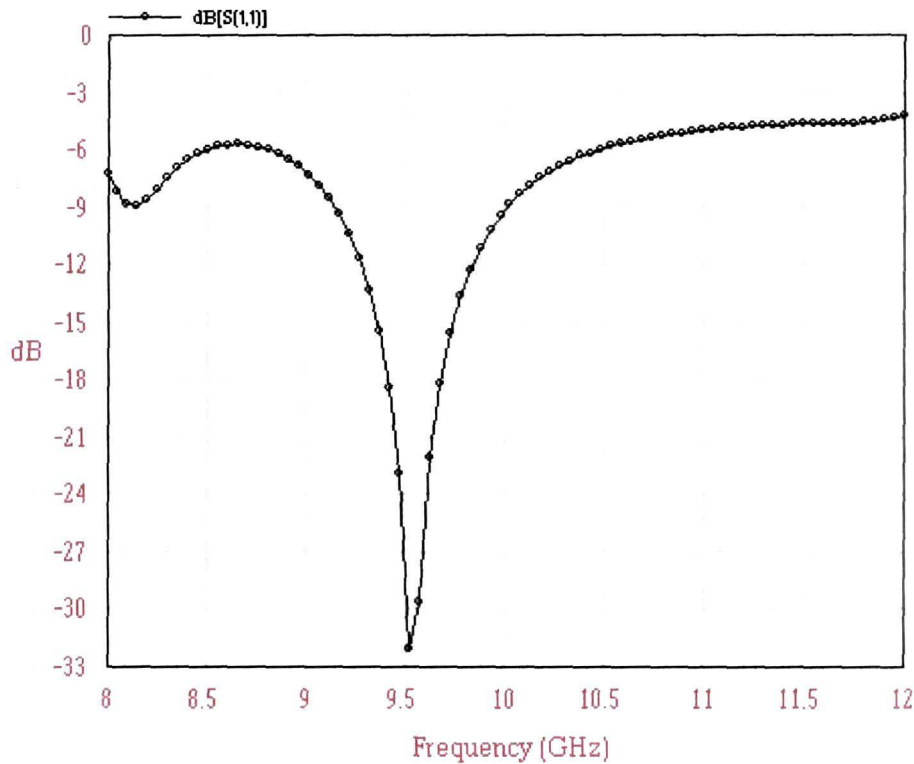


Figure 4.8 Calculated return loss of horn-shaped microstrip patch antenna with 2mm thick air substrate.

The calculated results of the antenna for 2mm & 3mm thick air substrate are shown in figure 4.9. From the figure it can be observed that the antenna with 3mm thick air substrate also has clearly two resonant frequencies: 8.6 GHz and 9.9 GHz. It agrees well with the explanation given above. The frequency band with -10dB return loss covers the frequency range of 8.35GHz to 10.71 GHz. It has a bandwidth of 24.8% with a thin (3mm) air substrate.

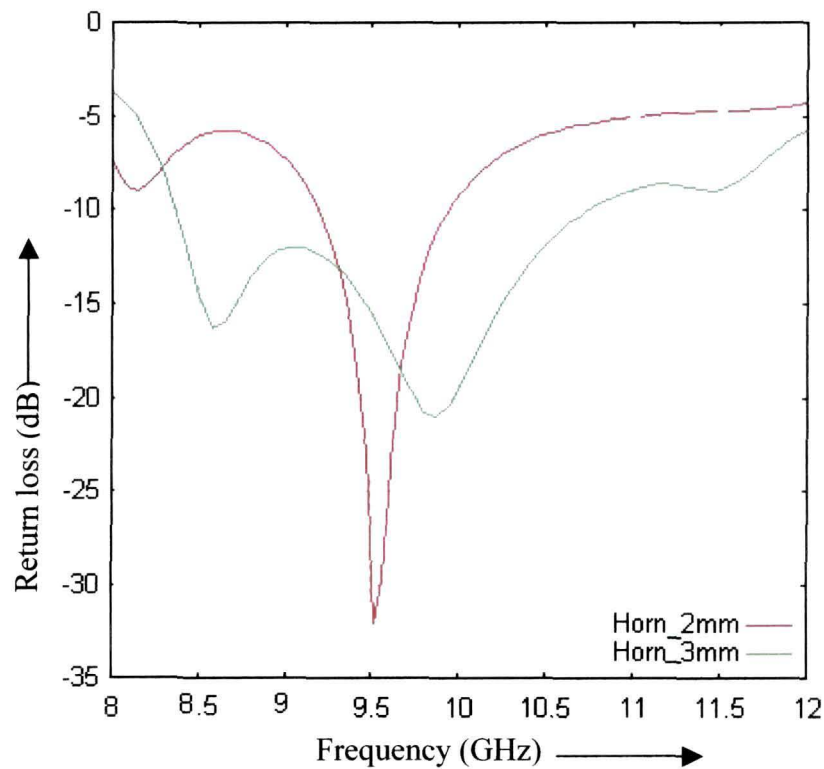


Figure 4.9 Calculated return loss of horn-shaped microstrip patch antenna with 2mm and 3mm thick air substrate.

The elevation patterns and azimuth patterns of Horn-shaped microstrip patch antennas of 2mm thick air substrate are plotted in Figure 4.10 and Figure 4.11 respectively. The 3dB pattern band width is of 7.4%.

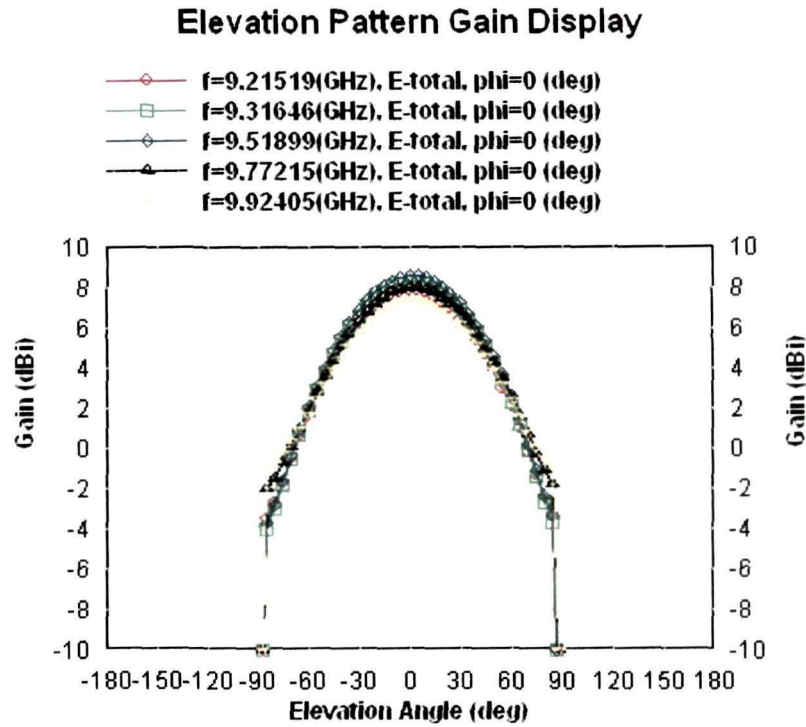


Figure 4.10 Elevation pattern of horn-shaped microstrip antenna of 2mm thick air substrate.

In the figure 4.12 and figure 4.13, the elevation patterns and azimuth patterns of Horn-shaped microstrip patch antennas of 3mm thick air substrate are shown respectively. The frequencies from 8.35 GHz to 10.71 GHz are seen within the beam width 3dB for both azimuth and elevation pattern of the antenna. It is clear from the Figure 4.12 and figure 4.13 respectively that the 3dB pattern bandwidth is 2.36GHz. The linear gain of the Horn-shaped microstrip antenna of 2mm thick air substrate is calculated to be 8.74 dBi with antenna efficiency of 97.1% while that for 3mm thick air substrate is 8.10 dBi with antenna efficiency of 95%.

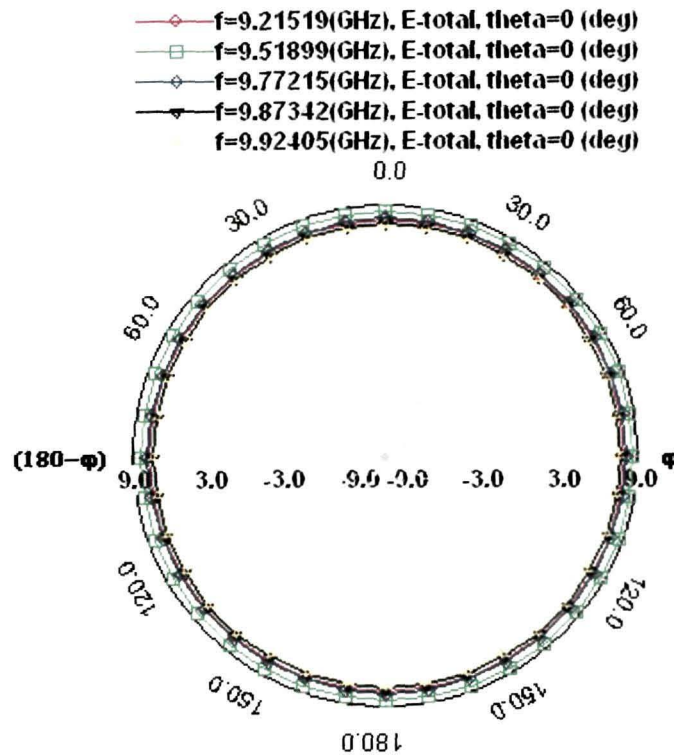


Figure 4.11 Azimuth pattern of horn-shaped microstrip antenna of 2mm thick air substrate.

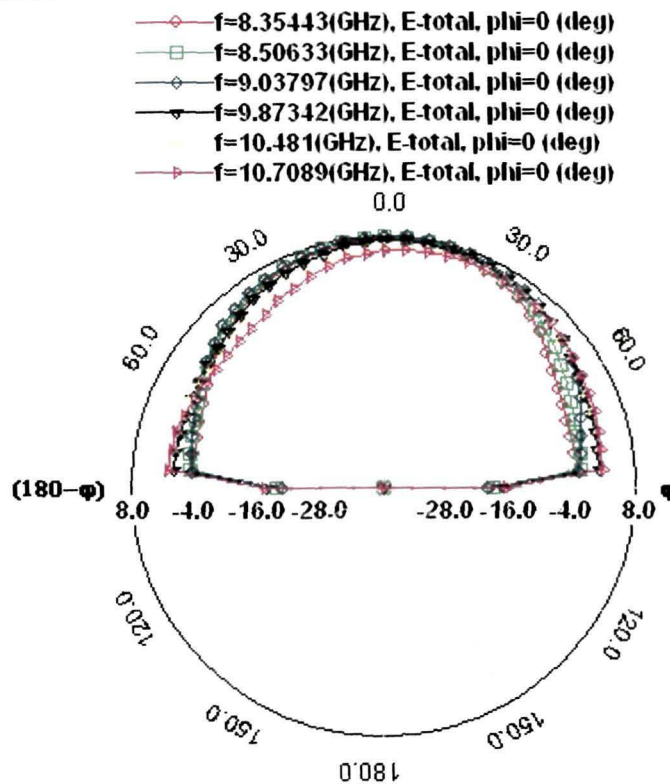


Figure 4.12 Elevation pattern of horn-shaped microstrip antenna of 3mm thick air substrate.

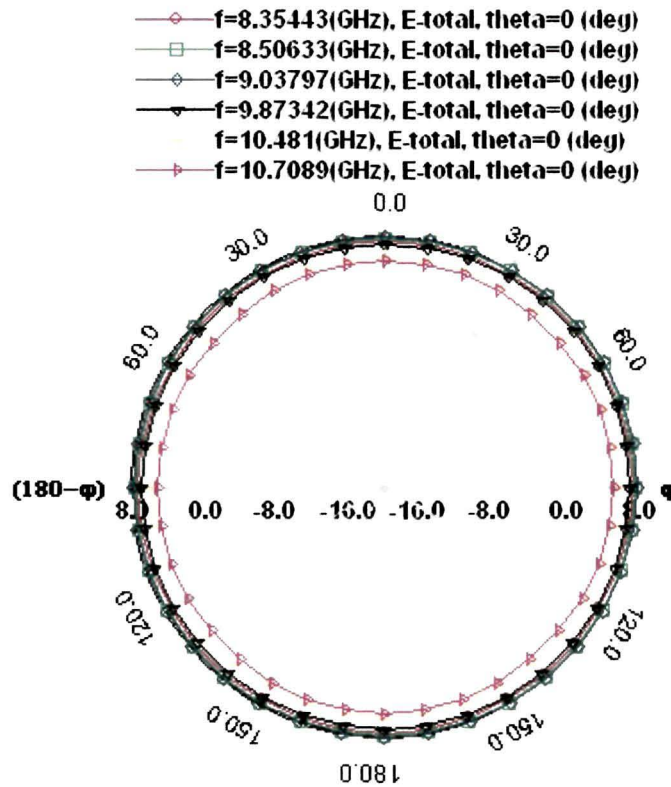


Figure 4.13 Azimuth pattern of horn-shaped microstrip antenna of 3mm thick air substrate.

4.5 Conclusion

This chapter presented a detailed of practical design of Horn Shaped patch antenna on thin substrate and its impedance and radiation characteristics. Simplicity and reduction in size are the special features of this antenna. Compared to the conventional wideband microstrip patch antenna, achievement of wideband with a substrate thickness of 2 mm or 3.175 mm is the focus of attention. Large impedance bandwidth and pattern bandwidth have been achieved without using parasitic coupling or stack structure. The good agreement with

experimental results validates the design. High gain with large bandwidth is a special feature of this antenna. Variation of L_s and W_s to control the bandwidth gives flexibility to control the bandwidth for varied applications. Looking into the recent requirements of micro spacecraft, the horn shaped microstrip patch antenna seems to be a potential radiator.

CHAPTER 5

**INVERTED-L, PARASITIC
COUPLED INVERTED-L SHAPED
AND T-SHAPED MICROSTRIP
PATCH ANTENNA**

5.1 Introduction

Microstrip antennas in various forms and geometries have been extensively used in many applications [253,254,286-288]. In recent past, significant works have been reported on small size, broad band width and suitable polarization of microstrip patch antenna for wireless communication systems. To enlarge the inherent narrow band width of microstrip patch antenna, large numbers of techniques have been proposed [1-25]. Uses of thick substrate, stacking etc., are the acceptable techniques in broad band design [1-25]. In this chapter, coax fed-inverted-L shaped microstrip patch antenna, a parasitically coupled inverted-L microstrip patch antenna and parasitic coupled T-shaped antenna that are designed are presented. Inverted-L microstrip patch antenna gives impedance band width of 30.62% which has been increased to 35.1% by parasitic coupling. The bandwidth has been achieved with a substrate thickness of 2mm. Radiation patterns and gains are also studied and presented. The T-shaped antenna gives dual band resonant frequencies on a thin substrate. The two resonant frequencies are within the 3dB band width which shows wide band width. For this new design, the basic plane size of the rectangular microstrip patch antenna is calculated by using the Transmission Line Method. The designed antennas parameters are calculated by using IE3D [139]. The measurements were performed in Microwave Antenna Laboratory, of North Eastern Regional Institute of Science and Technology (NERIST), India.

The antenna design specifications and the antenna structure of the inverted-L shaped microstrip patch antenna and parasitically coupled inverted-L

microstrip patch antenna are presented in section 5.2. In the section 5.3, the computational and measurement results of the inverted-L shaped microstrip patch antenna and parasitically coupled inverted-L shaped microstrip patch antenna are presented. The section 5.4, represents the design specifications and the antenna structure of T-shaped microstrip patch antenna. The computational and measurement result of the T-shaped microstrip patch antenna is presented in the section 5.5.

5.2 Design Specification and Antenna Structure of Inverted-L Microstrip Patch Antenna and Parasitic Coupled Inverted L-shaped Microstrip Antenna

For design of the inverted-L microstrip patch antenna, the basic rectangular shapes parameters i.e. length and width are calculated using simplified equation of Transmission Line method [7] as already discussed in the chapter-4. The calculated values are length $L = 10\text{mm}$ and width $W = 10\text{mm}$ for the substrate height of 2mm, dielectric constant of 2.2 and the resonant frequency of 9GHz. On this basic rectangular structure a square notch is inserted on one corner of the rectangle and thus, the antenna got the shape of inverted-L. Hence, the name inverted-L microstrip patch antenna. Figure 5.1 depicts the geometry of the inverted-L microstrip patch antenna, which is fed at a point ($X_f=3.8$, $Y_f=3.2$). The minimum value of the ground plan size is calculated to be $L_g = 22\text{mm}$ and $W_g = 22\text{mm}$ using the concept given in chapter-4.2.(VI). The value of L_1 and W_1 are important parameters in controlling the resonant

frequency of the antenna. In this antenna, the value of $L_1=4.5\text{mm}$ and $W_1=4.5$ are the optimize values. The feed point is highly dependent on L_1 and W_1 . It is seen that the probe dimension affects impedance. The practical radius of central conductor of an available SMA connector is 0.6mm. In the present problem, we have presented our result with this value.

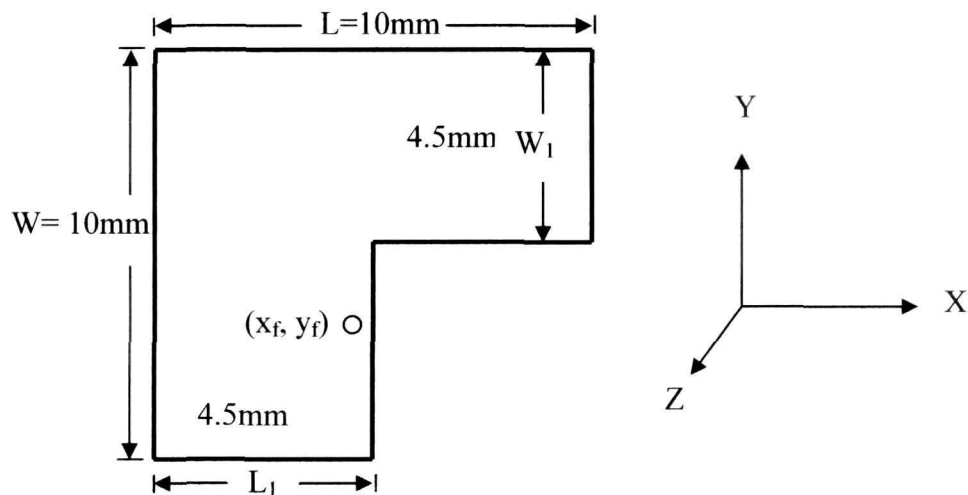


Figure 5.1 Inverted L-shaped microstrip patch antenna ($L=10\text{mm}$, $W=10\text{mm}$, $L_1=4.5\text{mm}$, $W_1=4.5\text{mm}$).

5.3 Computational and Measured Results of Inverted-L Microstrip Patch Antenna and Parasitic Coupled Inverted-L Shaped Microstrip Patch Antenna

The measured and calculated results are shown in figure 5.2 of the inverted-L microstrip patch antenna for Taconic substrate of thickness 2mm and dielectric constant of 2.2. From the figure it can be observed that the antenna has clearly two resonant frequencies: 10 GHz and 11.6GHz. These two resonance frequencies get

coupled to give wide band width[121]. The frequency band with -10dB return loss covers the frequency range of 9.38GHz to 12.73GHz i.e. impedance band width of 30.6%. The large band width has been achieved on a substrate thickness of 2mm (thin substrate) without any stacking or parasitic elements[256].

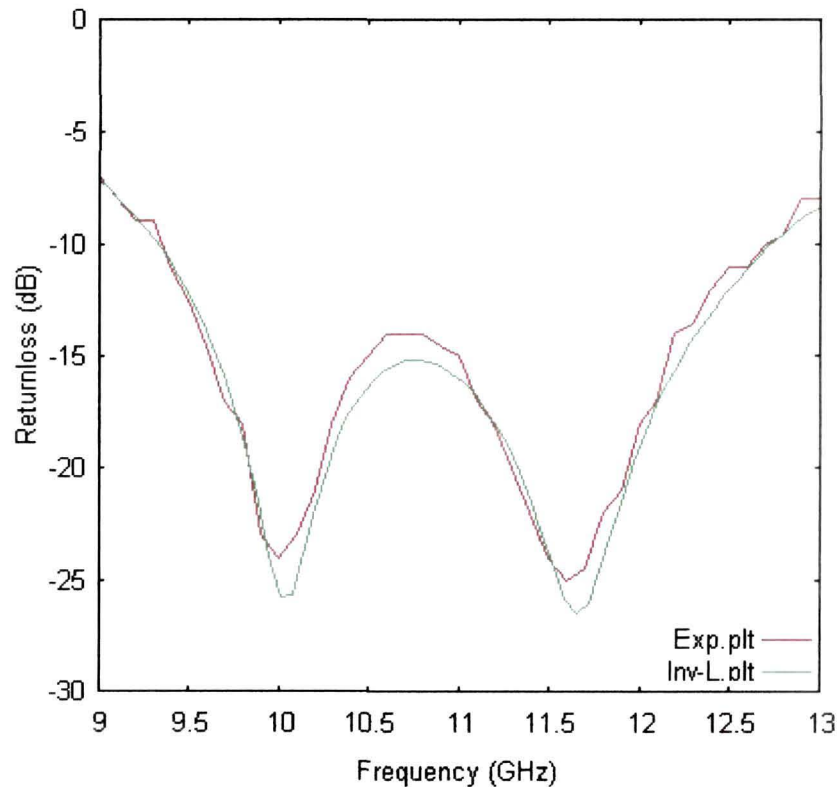


Figure 5.2 Measured and calculated return loss of inverted-L microstrip patch antenna with 2mm thick substrate.

Again seeing the current distribution of the inverted-L microstrip patch, a parasitic strip is placed on the side of the notched edge. The selection of parasitic element is based on the idea, to compensate the reactance component to generate further wide band width. The width of the parasitic strip and spacing from the main patch are selected based on the current distribution on the patch. The figure 5.3 shows the parasitically coupled inverted-L microstrip patch antenna. Figure 5.4(a) and

Figure 5.4(b) show the VSWR plots of inverted-L microstrip patch antenna and parasitically coupled inverted-L microstrip patch antenna respectively. As seen from figures, for the parasitically coupled inverted-L microstrip patch antenna the impedance band width (VSWR<2.0) covers the frequency range of 8.89GHz to 12.68GHz i.e. the inverted L-microstrip patch antenna offers impedance bandwidth of 3.35GHz while parasitically coupled inverted-L microstrip patch antenna offers 3.79GHz. Thus, the impedance band width is increased by 0.44GHz due to the addition of the parasitic element with the inverted-L microstrip patch antenna[256].

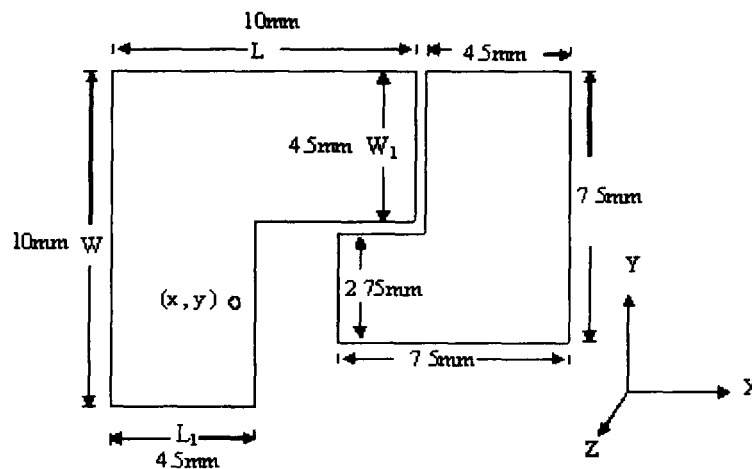


Figure 5.3 Parasitic coupled inverted-L shaped microstrip patch antenna.

To see the pattern bandwidth, these antennas are simulated at different frequencies to study the radiation patterns both in azimuth and elevation planes.

Figure 5.5(a) and Figure 5.5(b) represent the azimuth radiation pattern and elevation radiation patterns of inverted-L microstrip patch antenna.

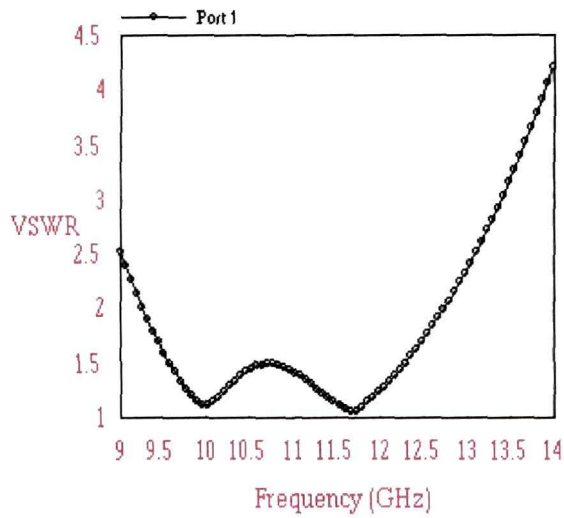


Figure 5.4(a) VSWR plot of inverted-L shaped microstrip patch antenna.

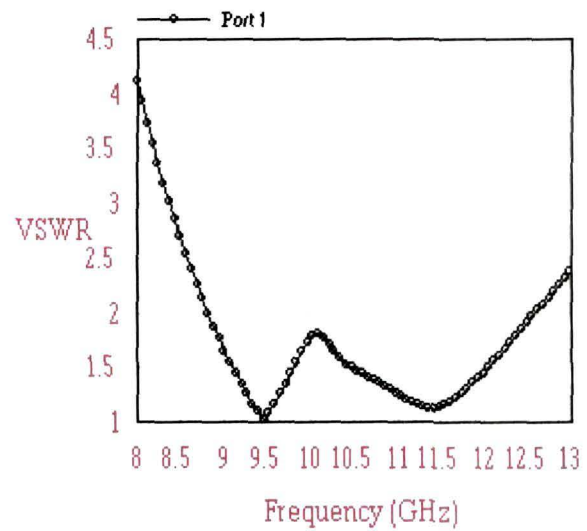


Figure 5.4(b) VSWR plot of parasitically coupled inverted-L shaped microstrip patch antenna.

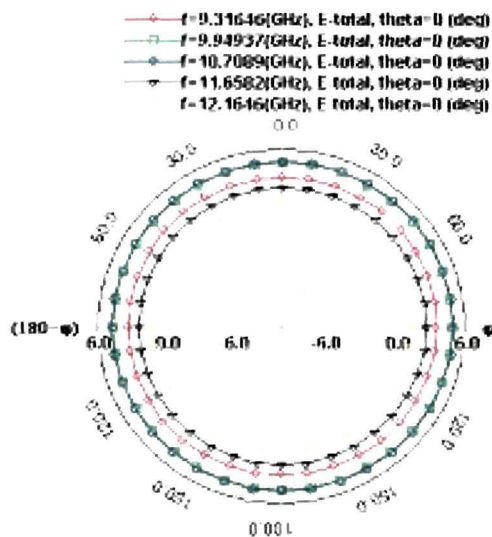


Figure 5.5(a) Azimuth pattern of inverted-L shaped microstrip patch antenna.

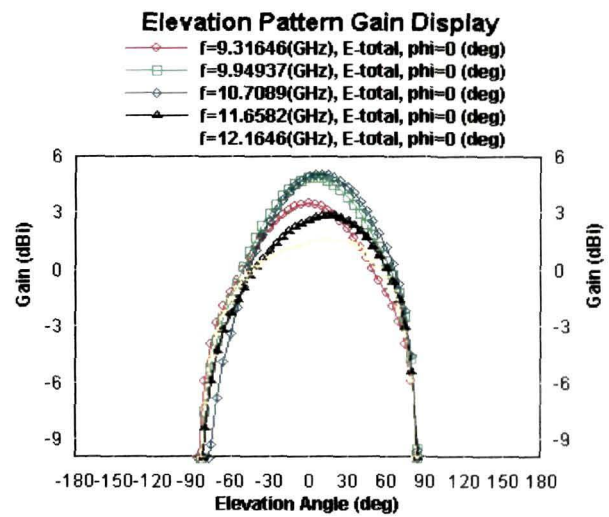


Figure 5.5(b) Elevation pattern of inverted-L shaped microstrip patch antenna.

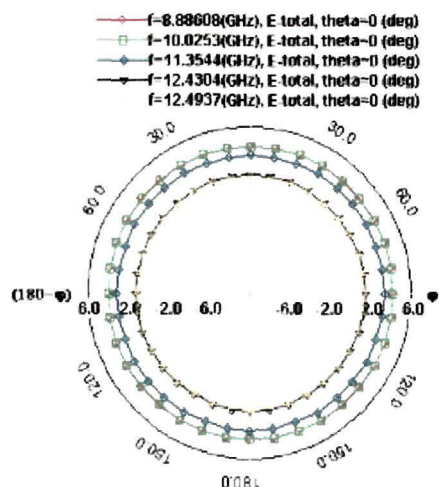


Figure 5.6(a) Azimuth pattern of parasitically coupled inverted-L shaped microstrip patch antenna.

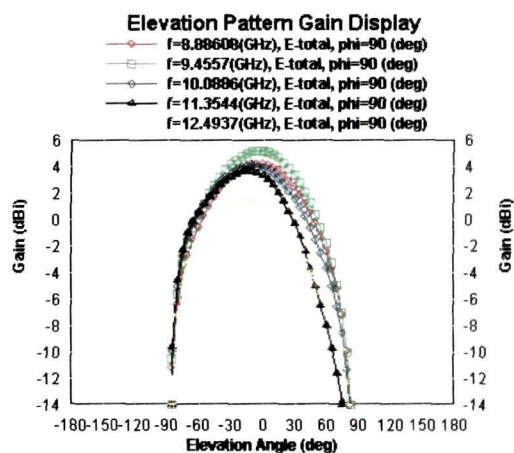


Figure 5.6(b) Elevation pattern of parasitically coupled inverted-L shaped microstrip patch antenna.

5.4 Design Specifications and Antenna Structure of T-shaped Microstrip Patch Antenna

This inverted-L shaped microstrip patch antenna was further studied by decreasing the value of L_1 and W_1 . The antenna parameters are Length (L) of each arm is of 11mm, width (W) is of 01mm and feed position is at $X_f = 13.5\text{mm}$ and $Y_f = 0.5\text{mm}$ respectively. The dielectric constant of the substrate material is 2.2. To increase the band width of the antenna, a parasitic element is placed to compensate the reactive component of the antenna [8] as shown in figure 5.7. The length (L) of the parasitic element is 11mm, width(W) is 01mm and is placed at a gap (b) of 02mm. Now the antenna looks like a T, hence, the name is T-shaped microstrip path antenna.

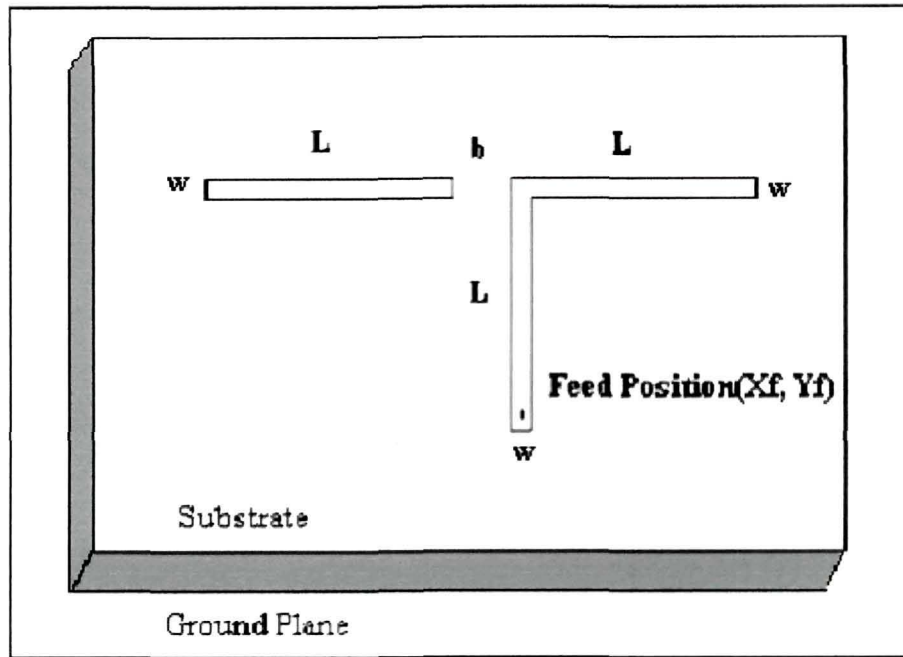


Figure 5.7 T-Shaped microstrip patch antenna($L=11\text{mm}$, $W=01\text{mm}$, $b=02\text{mm}$, $X_f=13.5\text{mm}$, $Y_f=0.5\text{mm}$).

5.5 Computational and Measured Results of T-shaped Microstrip Patch Antenna

The T-shaped antenna is simulated for substrate thickness of 0.7874mm and dielectric constant of 2.2 and the return loss plot is shown in figure 5.8. The antenna is fabricated on a Taconic substrate of 0.7874mm thick and dielectric constant of 2.2 . Measured and calculated results are shown in figure 5.9.

From the figure 5.8, it can be observed that the antenna has clearly two distinct resonant frequencies: 19.73GHz and 24.05GHz . The frequency bandwidth with -10dB return loss covers the frequency range of 19.32GHz to 20.20GHz for the first resonance frequency and 23.58GHz to 24.32GHz for the second resonance

frequency. Around 5% impedance band width has been achieved for each resonant frequency on a substrate thickness of 0.784mm (thin substrate).

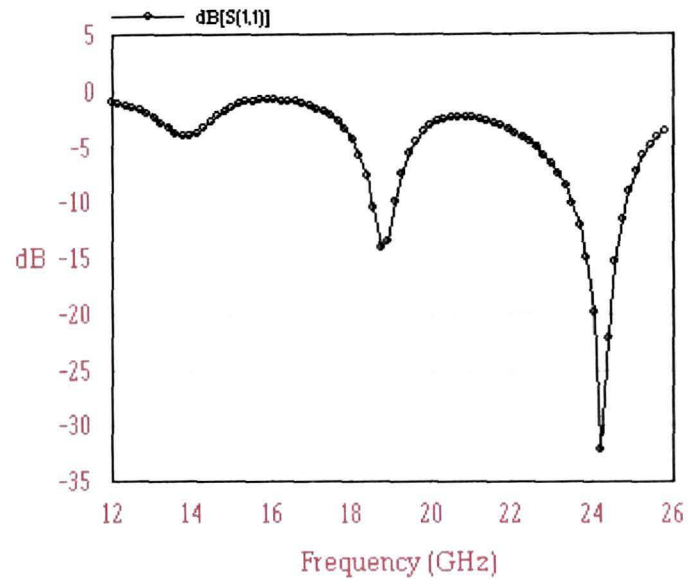


Figure 5.8 Return loss of T-shaped antenna.

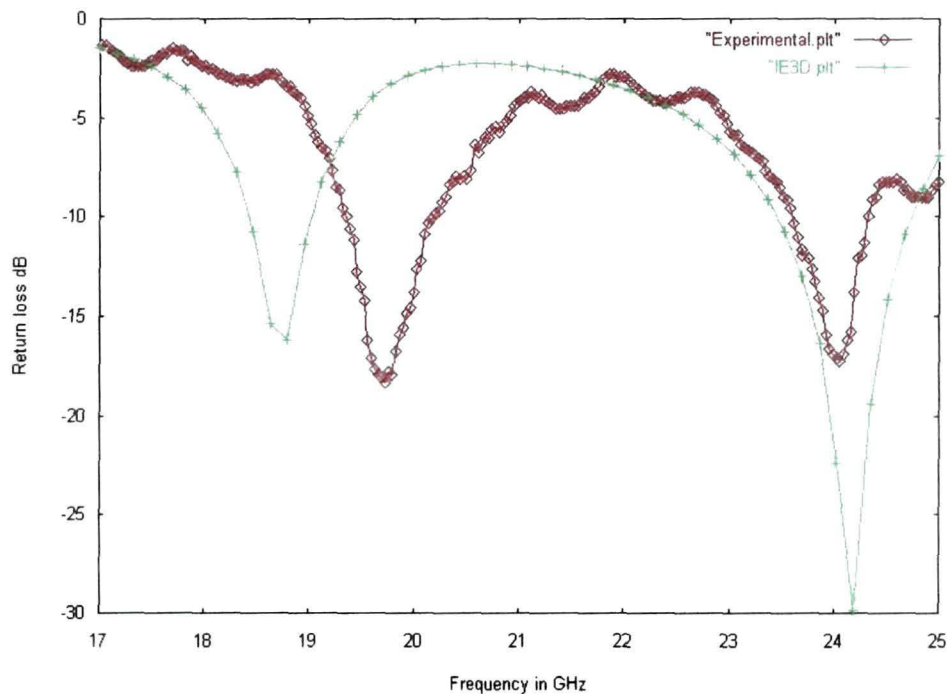


Figure 5.9 Measured and calculated return loss plot of T-shaped microstrip patch antenna.

This antenna is simulated for the two resonant frequencies to study the radiation patterns both in azimuth and elevation planes. Figure 5.10 and Figure 5.11 represent the elevation radiation pattern and azimuth radiation patterns of T-shaped microstrip patch antenna respectively. From the figure it is clear that both the frequencies i.e. 19.73GHz and 24.05GHz are well within 3dB. To see the effect of the position of the feed point, the feed position is varied along x axis and it is observed that both the resonance frequency shifted towards higher frequency value without changing the band width. The shifting of resonance frequency with the variation of position is shown in figure- 5.12.

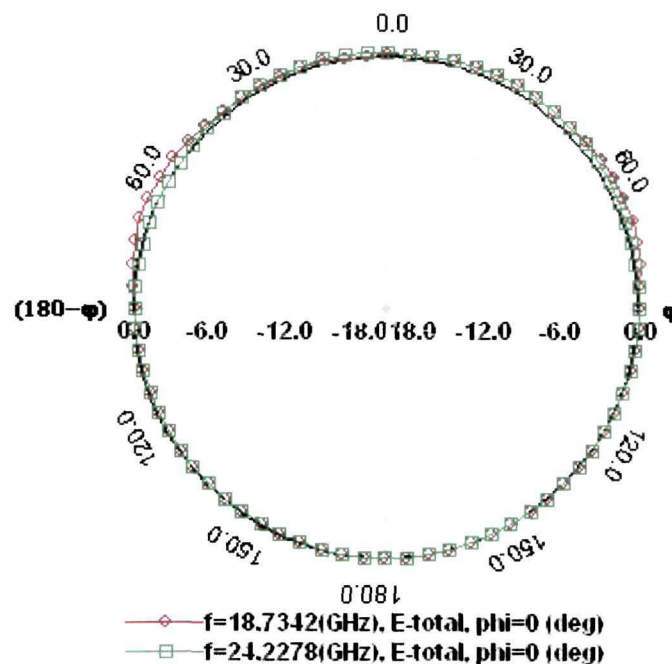


Figure 5.10 Elevation pattern of T-shaped microstrip patch antenna.

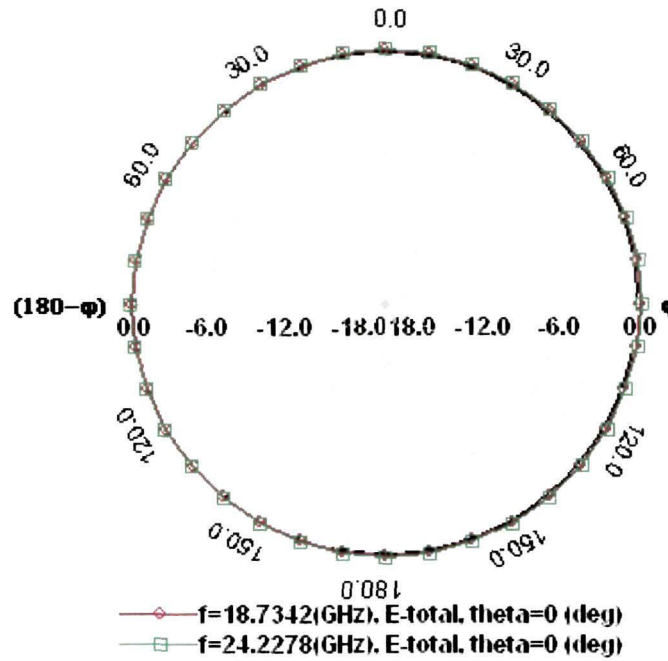


Figure 5.11 Azimuth pattern of T-shaped microstrip patch antenna.

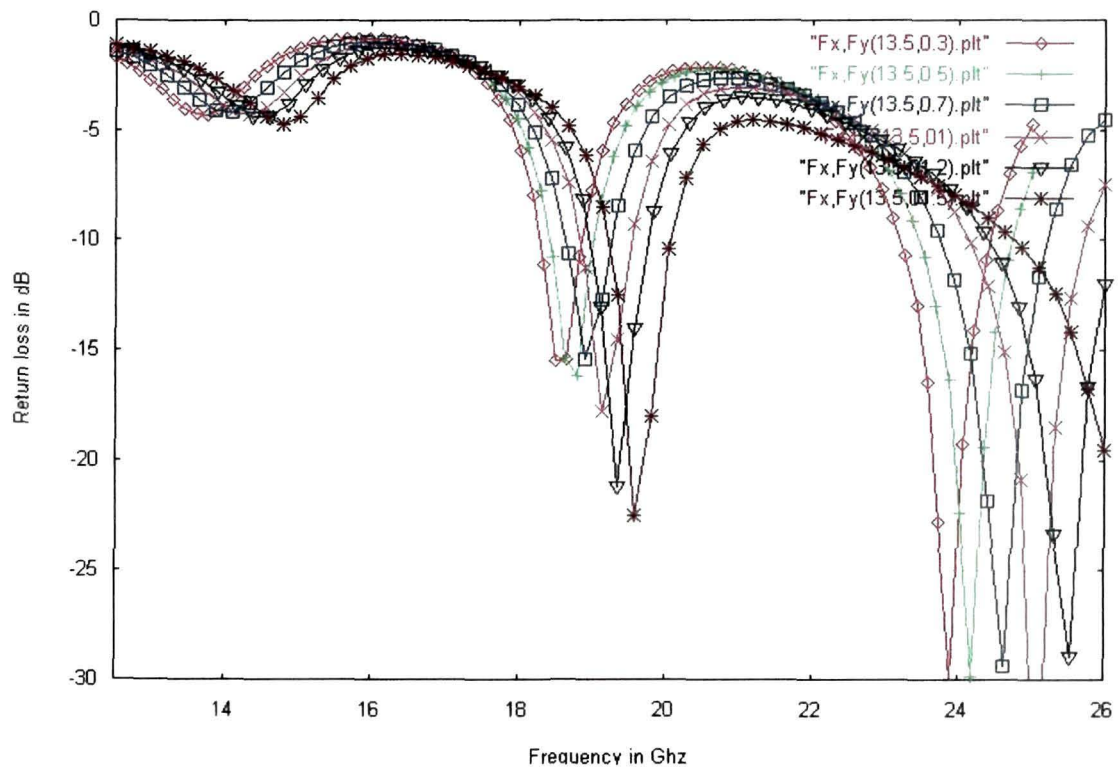


Figure 5.12 Variation of resonant frequency with the variation of feed position of T-shaped antenna.

5.6 Conclusion

In this chapter, the impedance and radiation characteristics of inverted-L microstrip patch antenna, parasitically coupled inverted-L microstrip patch antenna and T-shaped microstrip patch antenna have been presented. The impedance plots and radiation patterns of inverted-L and parasitically coupled inverted L-microstrip patch antenna show that these antennas exhibit wider bandwidth. On the other hand the T-shaped microstrip patch antennas impedance plot and the radiation patterns show clearly the dual band of frequency for operation with perfect isolation between them. Study of current distribution gives an insight to the technique of choosing shape (width) and spacing of the parasitic element and hence, to increase the efficiency and band width. Inverted-L shaped microstrip patch antenna with simple structure and large band width and the T-shaped microstrip patch antenna with simple structure and dual band frequencies seem to be potential radiators for wireless communication and biomedical applications. These antennas (inverted-L, parasitically coupled inverted-L microstrip patch antenna and T-shaped microstrip patch antenna) are potential new designs on thin substrate.

CHAPTER 6

MULTI-SLOTS HOLE COUPLED MICROSTRIP PATCH ANTENNA

6.1 Introduction

Wireless communication systems come in a variety of sizes ranging from small hand held devices to wireless local area networks. The integration of different radio modules in to the same pieces of equipment has created a need for multi-band antennas. Present trends of size reduction of wire less hand held devices and multi functionality poised as challenges for antenna designer to design multi-frequencies antenna with simple and ease of fabrication procedures. Complex geometries and complexity in the design are not in the interest of rapid growing wireless industries[70,249,250,257,258]. This chapter deals with the design of multi-slot hole-coupled microstrip patch antennas on substrate of thickness 2mm that gives multi frequencies (wide-band). The Method of Moments based software IE3D [139] is used for calculation of the parameters of the antennas. The measurements were performed at Microwave Antenna Laboratory (open space) of North Eastern Regional Institute of Science and Technology (NERIST), India.

The design specification and the antenna structure are presented in section 6.2. In the section 6.3, the computational and measurement results are discussed for antennas on substrate of thickness 2mm.

6.2 Design Specifications and Antenna Structure

In microstrip patch antenna, incorporation of double slot of equal size in opposite sides of the antenna increases the band width. And the frequency of a patch antenna can be increased or decreased by capacitive or inductive load[119].

It is also known that some parts of the radiating surface or ground plane can be removed without any significant changes of antenna performance in terms of the radiation patterns, as the current distributions remain relatively intact[121]. The multi-slots microstrip patch antenna presented in this chapter has been designed implementing the above facts to achieve multi frequency and wide bandwidth[223].

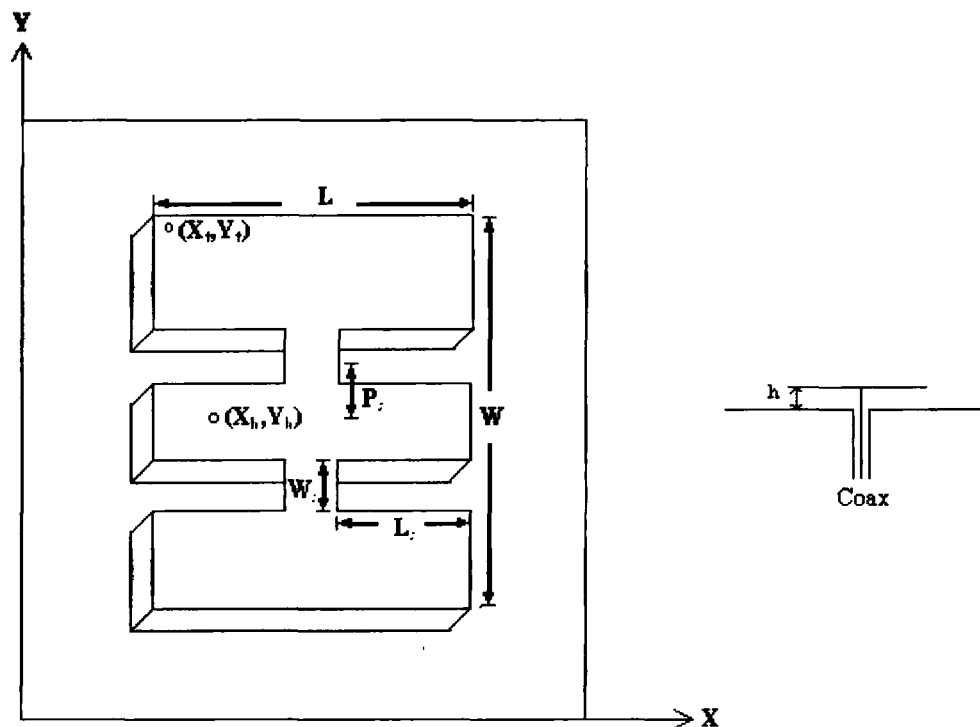


Figure 6.1 Geometry of the Multi-Slots Hole-Coupled Microstrip Antenna ($L=45$ mm, $W=71$ mm, $h=2$ mm, $L_s=17.5$ mm, $W_s=04$ mm, $X_f=0.75$ mm, $Y_f=69$ mm, $X_h=6.75$ mm., $Y_h=35.5$ mm).

The antenna has been designed on a rectangular patch of size $L=45$ mm, $W=71$ mm and substrate of thickness $h=2$ mm with $\epsilon_r=2.2$. The patch size is characterized by length, width and thickness (L , W , h). Four slots of equal size with length (L_s), width (W_s), are incorporated into this patch and are positioned on both sides of the hole position. The slot length (L_s), width (W_s) and position (P_s) are

important parameters in controlling the bandwidth. The value of L_s , W_s and P_s are calculated on trial and error basis. Due to slots, the length of the current path is increased[8], which leads to additional inductance in series. Hence, the wide band is generated as resonant circuits get coupled. The slots aggregate the currents, which give additional inductance, which is controlled by patch width (W). A hole of 0.2mm diameter has been made at location (X_h, Y_h) for impedance matching. The value of $Y_h = W/2$, X_h is chosen on trial and error method for best fit position. For impedance compensation and for better matching, the hole is made at $(X_h = 6.75 \text{ mm}, Y_h = 35.5 \text{ mm})$. In the antenna shown figure 6.1, the approach of creating a hole gives the flexibility to change the reactive component for impedance matching. The antenna is fed at one corner by a coaxial probe at position (x_f, y_f) . The position of the fed location is made on trial and error basis for better impedance matching. An infinite ground plane is considered in case of transmission line method. For practical consideration, it is essential to have a finite ground plane of the antenna. The ground plan is calculated based on the principle described in chapter-4, section-(VI). The value of ground plan is taken as $L_g = 55\text{mm}$ and $W_g = 81\text{mm}$.

6.3 Computational and Measured Results

The Calculated and Measured return loss plot of the Multi-slots-hole-coupled microstrip patch antenna on Taconic substrate of thickness 2mm and dielectric constant of 2.2 is shown in figure 6.2.

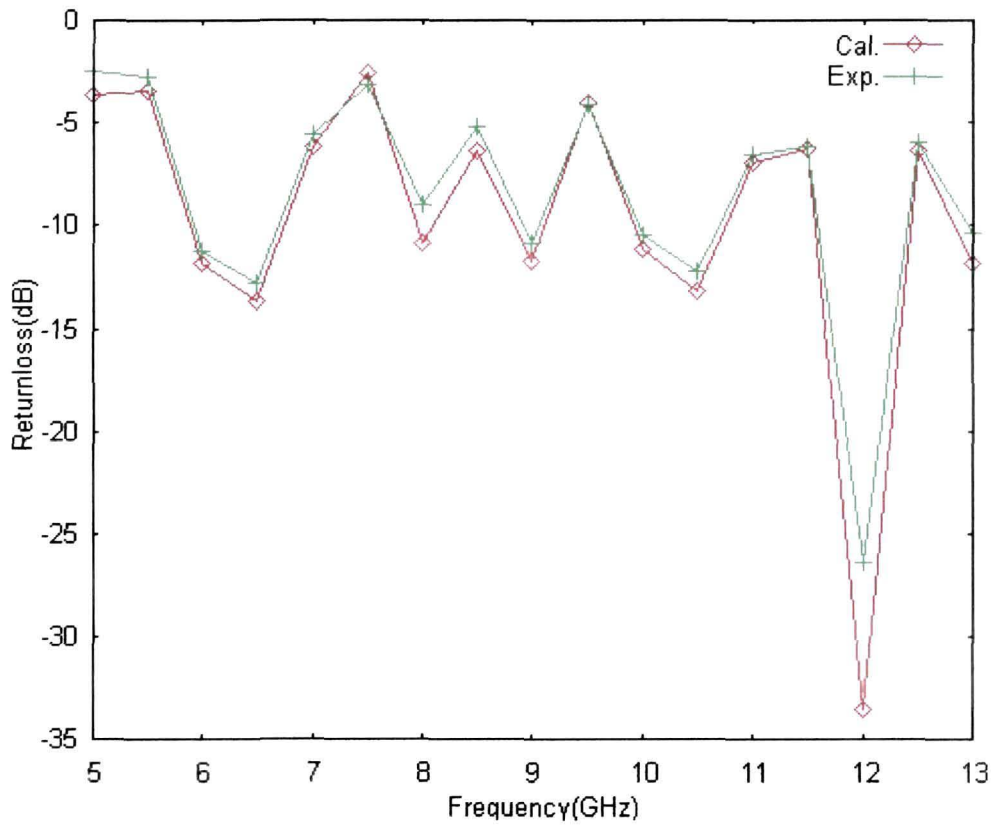


Figure 6.2 Calculated and measured return loss plot of multi-slots hole coupled microstrip patch antenna with 2mm thick substrate.

As seen from the return loss plot of the Multi-slots-hole-coupled microstrip patch antenna (figure 6.2), the antenna operates in distinct multi-frequency bands with center frequency at 6GHz, 6.5GHz, 9GHz, 10.5GHz and 12GHz. To see the pattern bandwidth, the antenna is simulated at different frequencies to study the radiation patterns both in azimuth and elevation planes. Figure 6.3 and Figure 6.4 respectively represent the azimuth radiation pattern and elevation radiation patterns of the Multi-slots-hole-coupled microstrip patch antenna on 2mm thick substrate.

The calculation of radiation patterns show that the radiation patterns of 6GHz, 6.5GHz, 10.5GHz and 12GHz are well with in the 3dB beamwidth.

Interestingly, the linear gain of 6GHz almost matches with 10.5GHz i.e. linear gain = 8dBi, where as that of 6.5GHz matches with 12GHz and linear gain =7dBi. The -10dB (S_{11}) bandwidth is nearly 800 MHz at each of these frequencies. There exists also a perfect isolation between these bands. Slot lengths, width and position of hole are varied to see the effects on return loss and VSWR. It is observed that antenna performances can be controlled by changing these parameters. The dimensions presented in this figure 6.1, are the optimum dimensions after considering all these effects to achieve the best results. Figure 6.5 shows the (S_{11}) in dB with slot length of $L_s=19.5$ mm i.e. for increased slot length and (S_{11}) in dB with slot width $W_s=3$ mm i.e. for decreased slot width. These clearly show the effect of L_s and W_s on S_{11} .

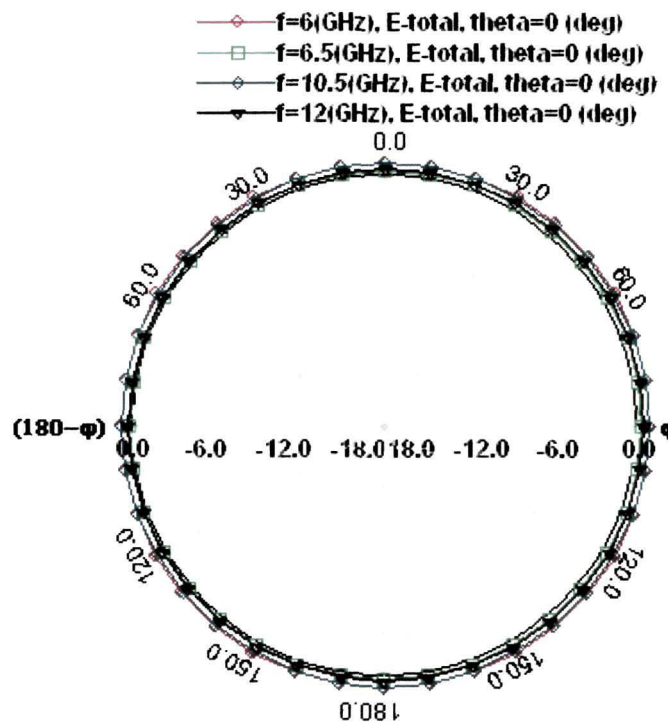


Figure 6.3 Azimuth pattern of multi-slots-hole-coupled microstrip patch antenna of 2mm thick substrate.

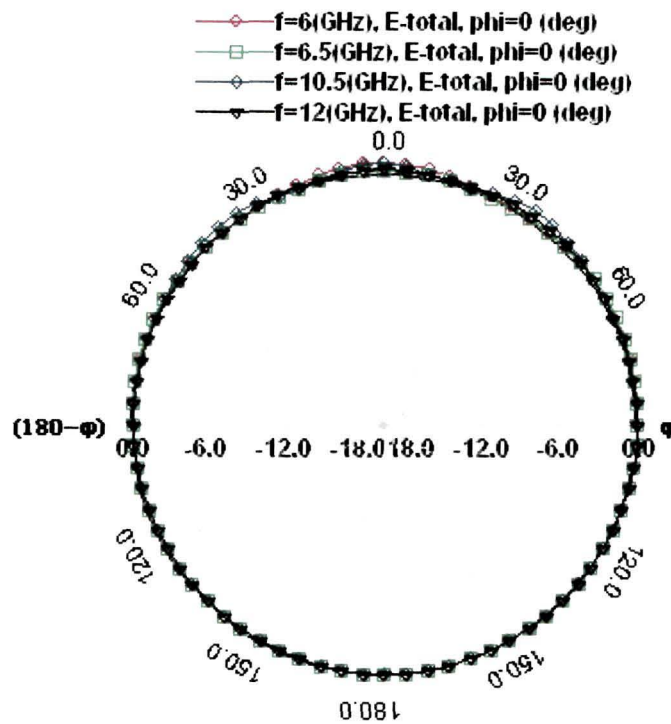


Figure 6.4 Elevation pattern of Multi-slots-hole-coupled microstrip patch antenna of 2mm thick substrate.

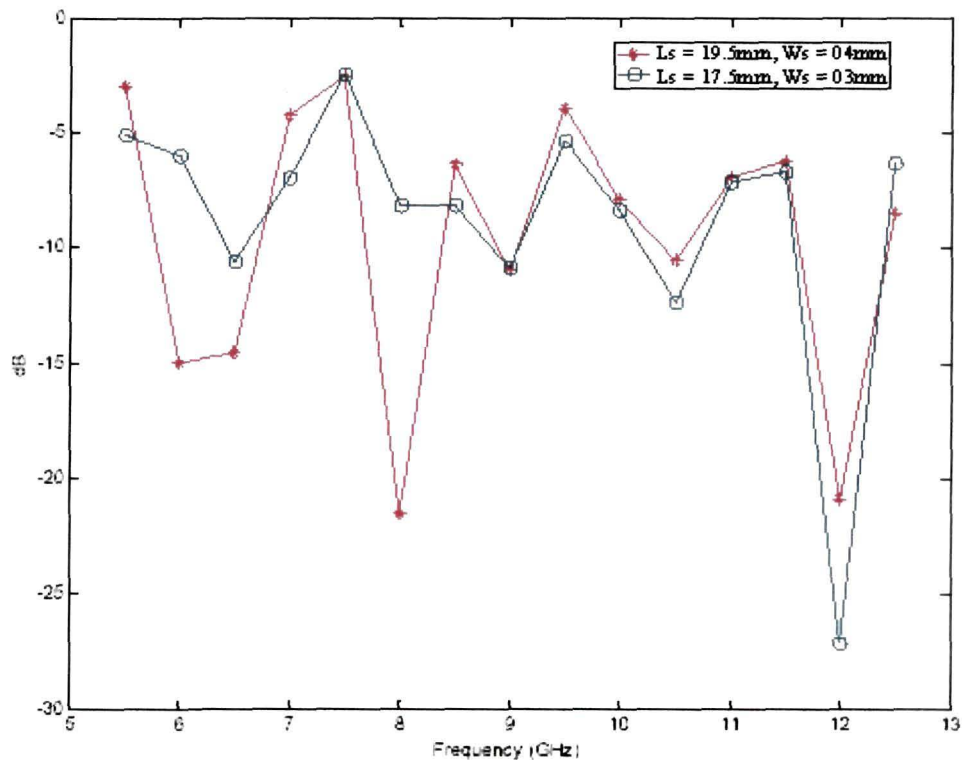


Figure 6.5 Return loss of the multi-slots hole-coupled microstrip patch antenna with varying L_s and W_s .

6.4 Conclusion

The return loss and radiation patterns of the multi-slots-hole-coupled microstrip patch antenna presented in this chapter show clearly that the antenna is a wide band, multi-frequencies antenna. It has the attractive features of simplicity and flexibility of controlling the bandwidth having high isolation between bands of frequencies. And with almost omni directional radiation patterns, the multi slots hole coupled microstrip patch antenna seems to be a good antenna for wireless communications specially for cellular telephone applications. The achievement of wide bandwidth with a substrate thickness of 2mm is a focus of attentions. Careful study of the current distribution may help to house the active components in etched region of the patch for possible system level integration of this antenna. The variation of slot parameters, hole size and positions gives the flexibility to shift the frequency and match the impedance, which is a notable feature of the referred antenna. The Multi-slots-hole-coupled microstrip patch antenna is unique in the design on a thin substrate and no result for this design is available in the literature.

CHAPTER 7

GENERALISED FORMULA FOR DETERMINATION OF RESONANCE FREQUENCY OF SLOT COUPLED MICROSTRIP ANTENNA

7.1 Introduction

Microstrip patch antennas are employed widely in fast developing technological applications ranging from satellite communication to bio-medical diagnostics [5,259,286-288]. It is known from the research and practical applications that a microstrip patch antenna can work efficiently only close to their resonant frequencies and at the same time microstrip patch antenna has the drawback of very narrow bandwidth. For this reason, the accurate evaluation of this parameter is of fundamental importance in the microstrip patch antenna design process. Now an accurate evaluation of the resonant frequency of the microstrip patch antenna requires rigorous analysis of full wave model. The Method of Moment (MoM) has been proved to be a very powerful tool for the analysis of such antennas, providing rigorous solution to the problem at hand [260-262]. In MoM, during final numerical solution, the choice of the test function and the path of integration are most critical. Thus, it involves rigorous mathematical formulation and extensive numerical procedure. Hence, this technique requires considerable computational effort and it is very time consuming. In the past few years, a number of alternative methods for the determination of resonant frequency have been developed in the technical literature [42,46,263-272]. Generally, these techniques are applicable only for regular shapes (rectangular, square, triangular, circular semi-circular) microstrip patch antenna. In this chapter, a generalized method is presented to determine the resonance frequency of slot coupled rectangular microstrip patch antenna. In section 7.2, the theoretical model of the method is analysed. The comparison of calculated resonant frequency

with present method for different shapes of slot with measured and reported result is given in section 7.3. In section 7.4, the new method with the modified equation is used to determine the two resonant frequencies of E-shaped microstrip patch antenna. The comparative results of calculated value with present method and reported results are shown.

7.2 Theoretical Model

The length, width and dielectric constant are important parameters in controlling the resonant frequency of a microstrip patch antenna. For determination of the resonance frequency of a slot loaded rectangular microstrip patch antenna (SLRMSPA), the antenna is converted into a equivalent rectangular microstrip patch antenna (ERMSPA). The frequency dependence of the model parameter is taken in to account through frequency dependence of dielectric constant (ϵ_{eff}), effective length (L_{eff}) and effective width (W_{eff}). To calculate the open-end edge extension, expression for ΔL [8] is modified empirically. Finally, the resonance frequency is calculated using expression[7]:

$$f = \frac{v_0}{2L_{eff} \sqrt{\epsilon_{eff}}} \quad (7.1)$$

Where, v_0 = velocity of light in free space.

L_{eff} = Effective length of the antenna.

ϵ_{eff} = Effective dielectric constant.

For conversion of the SLRMSPA in to the ERMSPA, the length(l) of the ERMSPA is taken equal to the width(W) of the SLRMSPA. The width(w) of the corresponding ERMSPA is calculated in such a way that the area of SLRMSPA is equal to the area of ERMSPA. The equations for calculation of widths of the ERMSPA for various SLRMSPA are given below. In the calculation L , W , L_s and W_s represents the length, width, Slot length and the Slot width of SLRMSPA respectively as shown in the figure 7.1.

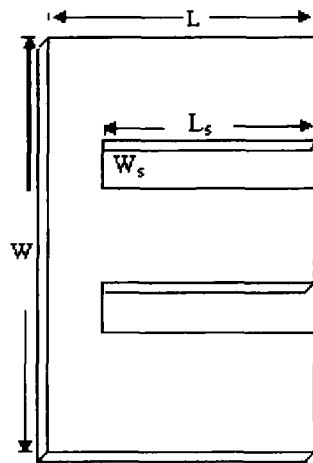


Figure 7.1 (a) E-shaped microstrip patch antenna.

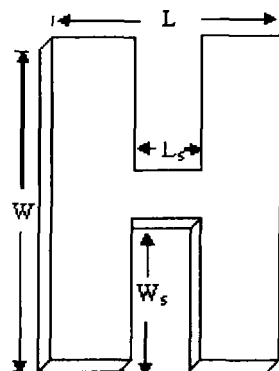


Figure 7.1 (b) H-shaped microstrip patch antenna.

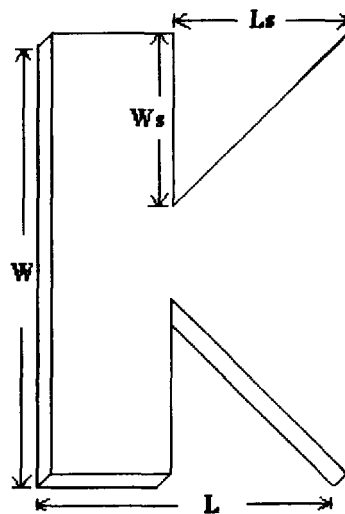


Figure 7.1 (c) Horn-shaped microstrip patch antenna.

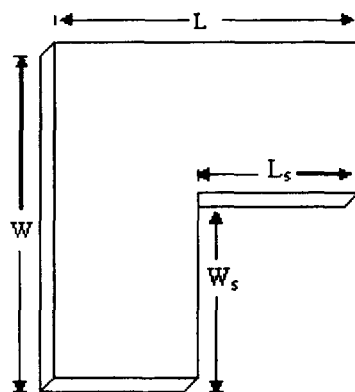


Figure 7.1 (d) L-Shaped Microstrip patch antenna.

Figure 7.1 (a), (b), (c) & (d): Different slot loaded rectangular microstrip patch antenna(SLRMSPA).

(a) The equation for calculation of width (w) of the ERMSPA for E-shaped and H-shaped antenna is represented as:

$$w = \frac{(LW - 2L_s W_s)}{L} \quad (7.2)$$

(b) The equation for calculation of width (w) of the ERMSPA for L-shaped, inverted L-shaped, and Horn-shaped antenna is represented as:

$$w = \frac{(LW - L, W_s)}{L} \quad (7.3)$$

Effective dielectric constant $\epsilon_{\text{eff}}(w)$ and $\epsilon_{\text{eff}}(l)$ are calculated after accounting for the dispersion effect [8] for the ERMSPA of length l and width w . Now for the ERMSPA with parameters h as the thickness of the substrate, ϵ_r as the dielectric constant and t as the thickness of the strip conductor, the frequency dependent formula used for the computation of effective dielectric constant $\epsilon_{\text{eff}}(w)$ is [8]:

$$\epsilon_{\text{eff}}(w) = \epsilon_r - [(\epsilon_r - \epsilon_{\text{eff}}(0)) / (1 + P)] \quad (7.4)$$

Where, $\epsilon_{\text{eff}}(0)$ is static effective dielectric constant and is given as

$$\epsilon_{\text{eff}}(0) = \frac{1}{2} \{ \epsilon_r + 1 + (\epsilon_r - 1) G \} \quad (7.5)$$

$$G = (1 + 10h/w)^{-AB} - [(\ln 4/\pi) (t(wh)^{-1/2})] \quad (7.6)$$

$$A = 1 + \frac{1}{49} \ln \left\{ \frac{(wh)^4 + w^2 / (52h)^2}{(wh)^4 + 0.432} \right\} + \frac{1}{18.7} \ln \{ 1 + [w / (18.1h)]^3 \} \quad (7.7)$$

$$B = 0.564 \exp [-0.2/ (\epsilon_r + 0.3)] \quad (7.8)$$

$$P = P_1 P_2 [(0.1844 + P_3 P_4) f_n]^{1.5763} \quad (7.9)$$

$$P_1 = 0.27488 + [0.6315 + \{0.525/ (1+0.0157 f_n^{20})\}] \\ u-0.065683 \exp(-8.7513u) \quad (7.10)$$

$$P_2 = 0.33622 [1 - \exp (- 0.03442 \epsilon_r)] \quad (7.11)$$

$$P_3 = 0.0363 \exp (-4.6u) \{1 - \exp[-(f_n/38.7)^{4.97}]\} \quad (7.12)$$

$$P_4 = 1+2.751 \{1 - \exp [-(\epsilon_r/15.916)^8]\} \quad (7.13)$$

$$f_n = 47.713 kh, \text{ where } k = 2 \pi/\lambda_0 \quad (7.14)$$

$$u = [w + (dw - w) / \epsilon_r] / h \quad (7.15)$$

$$dw = w + (t/\pi)[1 + \ln \{4 / (t/h)^{1/2} + (1/\pi)^2/(w/t + 1.1)^2\}] \quad (7.16)$$

The effective dielectric constant $\epsilon_{\text{eff}}(l)$ corresponding to length equal to l , is computed by replacing w by l in all above equations. The effective dielectric constant is calculated using [8, 269]:

$$\epsilon_{\text{eff}}(f) = [\epsilon_{\text{eff}}(W)\epsilon_{\text{eff}}(L)]^{\frac{1}{2}} \quad (7.17)$$

The effective width W_{eff} and effective length L_{eff} of the ERMSPA are calculated as follows [8]:

$$W_{\text{eff}} = w + 2\Delta l_1 \quad (7.18)$$

$$L_{\text{eff}} = l + 2\Delta l_2 \quad (7.19)$$

The Δl_1 and Δl_2 are edge extensions from side l and w of the ERMSPA, respectively and are calculated using $\mathcal{E}_{\text{eff}}(l)$ and $\mathcal{E}_{\text{eff}}(w)$ [8].

The edge extension Δl_2 for the width w of the ERMSA is determined using the following expressions [8].

$$\Delta l_2 = h \xi_1 \xi_3 \xi_5 / \xi_4 \quad (7.20)$$

Where, ξ_1 is empirically modified as,

$$\xi_1 = 0.434907 \frac{\mathcal{E}_{\text{eff}}(w)^{0.81} + 0.26(w/h)^{0.8544} + 0.236}{\mathcal{E}_{\text{eff}}(w)^{0.81} - 0.189(w/h)^{0.8544} + 20.1167} \quad (7.21)$$

and

$$\xi_2 = 1 + \frac{(w/h)^{0.371}}{2.358\epsilon_r + 1} \quad (7.22)$$

$$\xi_3 = 1 + \frac{0.5274 \arctan\{0.067(w/h)^{1.9413/\xi_2}\}}{\epsilon_{\text{eff}}(w)^{0.9236}} \quad (7.23)$$

$$\xi_4 = 1 + 0.0377 \arctan[0.067(w/h)^{1.456}] [6 - 5 \exp\{0.036(1 - \epsilon_r)\}] \quad (7.24)$$

$$\xi_5 = 1 - 0.218 \exp(-7.5 w/h) \quad (7.25)$$

Similarly, Δl_1 is calculated by replacing w by l and $\epsilon_{\text{eff}}(w)$ by $\epsilon_{\text{eff}}(l)$ in equation (7.219) to (7.25).

Finally the resonance frequency of the slot loaded antenna is calculated using equation 7.1.

7.3 Calculated and Measured Results of Slot Loaded Microstrip Patch Antenna

Calculation is carried out for E-Shaped, H-Shaped, Horn-Shaped, L-Shaped and Inverted L-Shaped antenna with the above mentioned method. Again all these antennas are simulated with IE3D[139]. The measured results, simulated results obtained with IE3D and the calculated results using present method are listed in the Table 7.1.

Table 7.1 Comparison of Resonant Frequencies

Slot Loaded Rectangular Microstrip Patch Antenna	L, W, h, L _s , W _s (mm)	ϵ_r	RF _{IE3D} (GHz)	RF _{ME} (GHz)	RF _{PM} (GHz)
E-Shaped [22]	45, 70, 10, 30, 5	1	2.43	2.2	2.11
	45, 70, 10, 35, 4	1	2.42	2.12	2.11
	50, 70, 15, 40, 6	1	2.02	1.9	2.1
H-Shaped [23]	24, 38, 1.57, 13.5, 8	2.2	2.75	2.75	2.63
Horn-Shaped [24]	10, 14, 2, 6, 6	2.2	6.7	6.6	6.9
Inverted L-Shaped [25]	10, 10, 2, 5.5, 5.5	2.2	9.9	9.8	9.8
L-Shaped [26]	45, 50, 8, 22, 20	1.07	2.8	2.7	2.8
RF _{ME} RF _{IE3D} RF _{PM}	Measured resonant frequency. Resonant frequency determined using IE3D. Resonant frequency determined using present method.				

The calculated and experimental results for the E-Shaped antennas have been taken from [121], for the H-Shaped antenna we refer [274], for the Horn-Shaped antenna the data have been taken from [275], for the Inverted L-Shaped antenna the results have been taken from [256] and for the L-Shaped antenna it is from [255].

7.4 Determination of Two Resonance Frequencies of E-Shaped Microstrip Patch Antenna

Dual resonance frequencies play important role in enhancement of bandwidth of Microstrip antenna. In E-Shaped antennas, the two resonance frequencies get coupled to give a wide band-width[121,122]. Hence determination of the two resonance frequencies is important study of the E-Shaped antenna.

To determine the two resonance frequencies, the E-Shaped antenna is converted to equivalent rectangular microstrip patch antenna (ERMSPA). The effective dielectric constant ϵ_{eff} , effective length (L_{eff}) and width (W_{eff}) of ERMSPA are calculated using the new method mentioned in section 7.3. From the calculated ERMSPA, the two resonant frequencies are determined as:

The lower resonance frequency is calculated using equation (7.1) i.e.

$$f_1 = \frac{v_0}{2L_{eff} \sqrt{\epsilon_{eff}}}$$

And the next resonance frequency is derived as:

$$f_2 = \left(\frac{0.36v_0}{W_{eff} \sqrt{\epsilon_{eff}}} \right) \quad (7.14)$$

Where, v_0 = the velocity of light in free space.

The computed results using the new method along with the reported theoretical and experimental results for E-Shaped Microstrip Patch Antenna are given in Table 7.2.

Table 7.2 Comparison of Resonant Frequencies

Antenna	L, W, h, L _s , W _s (mm)	RF _{IE3D} (GHz)		RF _{HP-HFSS} (GHz)		RF _{ME} (GHz)		RF _{PM} (GHz)	
		f ₁	f ₂	f ₁	f ₂	f ₁	f ₂	f ₁	f ₂
E-Shaped [22]	45, 70, 10, 30, 5	2.43	2.67	2.25	2.48	2.2	2.52	2.11	2.55
	45, 70, 10, 35, 4	2.42	2.79	2.2	2.54	2.12	2.66	2.11	2.54
	50, 70, 15, 40, 6	2.02	2.42	1.89	2.29	1.9	2.40	2.1	2.40
E-Shaped [27]	65,105, 14.3,47.6,3	--	--	--	--	1.49	1.75	1.41	1.75
E-Shaped with U- Shaped ground plan [28]	60, 90, 14.3, 53, 4	--	--	--	--	1.6	1.82	1.63	1.88
--	Not available								
RF _{ME}	Measured resonant frequency								
RF _{IE3D}	Resonant frequency determined using IE3D								
RF _{HP-HFSS}	Resonant frequency determined using HP-HFSS								
RF _{PM}	Resonant frequency determined using present method								

The calculated and experimental results for the E-Shaped antennas have been referred from [121, 122], and for the E-Shaped with U-Shaped ground

plane antenna have been taken from [123]. IE3D Version-7.04 [139] is used to simulate the reported antenna.

7.5 Conclusion

This chapter presented the detailed technique and theoretical formulation that was implemented for determination of resonance frequency of slot loaded rectangular microstrip patch antenna. In section 7.3, for different slot loaded rectangular microstrip patch antenna with varied values of dielectric constant and height, were compared with measured results and with IE3D software simulated values. The good agreement of the present method established the validity of the formula developed.

Again in section 7.4, for E-Shaped microstrip patch antenna, when compared with measured values, the agreement of the present method is better than that of reported HP-HFSS software simulated results and much better than that of IE3D simulated results.

The suggested method gives quite accurate result without any complicated mathematical functions or operations. Thus, this method can be useful for development of fast CAD algorithm. The advantage of this method is its simplicity and accuracy. To summarise, although part of this technique is implemented and reported before, this implementation is new in the conversion of the slot loaded rectangular microstrip patch antenna in to equivalent rectangular microstrip patch antenna and modification of edge extension calculation formula along with the modified resonance frequency formula.

CHAPTER 8

**APPLICATIONS OF ARTIFICIAL
NEURAL NETWORKS ON
DESIGNED MICROSTRIP PATCH
ANTENNA**

8.1 Introduction

Wireless communications have demand for wireless device of light weight, small size, having low energy consumption and of more practicability. The microstrip antenna is the best choice that fulfills the basic requirements of wireless communication device i.e. antenna should be relatively cheap, light weight, robust, easy to manufacture and with a minimum impact on environment. The microstrip patch antennas are of narrow band width because of which the design parameters of patch antenna must be determined with high precision. So, with in a fabrication process of such kind of antennas, Artificial Neural Networks(ANNs) based models trained with experimental/generated data of same class, previously collected, can preliminary estimate the design parameters, reducing the number of real prototypes to be constructed, saving time and resource[41-47,151,152,170,216,240,276-285]. The results obtained using, Artificial Neural Networks(ANN) techniques are close to experimental results and Electromagnetic computer (EMC) simulating tools. Therefore to design Microstrip patch antennas for wireless communication, Artificial Neural Network techniques can be embedded in computer added design(CAD) system.

8.2 Determination of Resonance Frequency and Band Width

The Resonance frequency and impedance bandwidth are the vital parameters of microstrip patch antennas. Microstrip patch antennas can work efficiently only close to their resonant frequencies. The impedance bandwidth is related to the input impedance and radiation efficiency of a microstrip patch antenna.

The Microstrip patch antenna has the drawback of very narrow bandwidth. The accurate evaluation of these parameters is of fundamental importance in the microstrip design process. The resonance frequency and impedance band width of designed Horn shaped antenna is dependent on the slot length and width of the antenna (chapter 4, figure 4.4 & 4.5). The variation of slot length(L_s) and slot width(W_s) to control the bandwidth gives flexibility to control the bandwidth for varied applications. In this section, an attempt has been made to exploit the capability of Artificial Neural Networks to calculate the resonance frequency and impedance bandwidth of the designed Horn shaped microstrip patch antenna with the variation of slot length(L_s) and slot width(W_s).

Development of Model

The back propagation algorithm, a gradient decent algorithm is used for training the network in a supervised manner. Three layers neural networks of structures have been considered for the model as shown in figure 8.1. The training parameters of the network are shown in Table 8.1 for width variation(W_s) calculation.

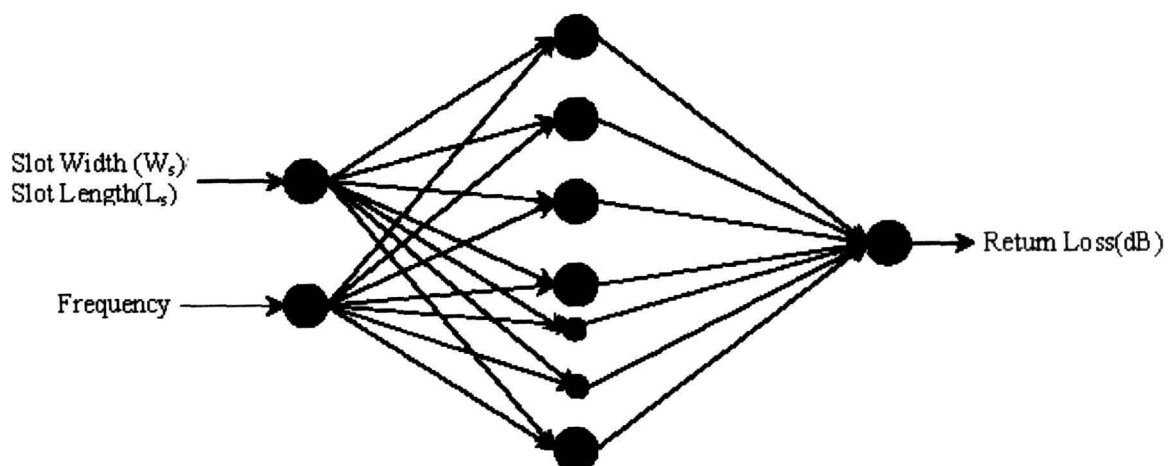


Figure 8.1 Network architecture showing slot width(W_s)/slot length(L_s) and frequency as input and return loss(dB) as output.

Table 8.1 Network Parameters(width variation)

Parameter	Value
Number of input neuron	02
Number of hidden neuron	37
Number of output neuron	01
Noise parameters	0.04
Learning Constant(parameter)	2
Momentum factor	0.04

For length variation(L_s), the network parameters for training are given in Table 8.2. Two hundred ninety five patterns are taken for training the network for width variation and are given in the Table 8.3. For length variation calculation, one hundred thirty seven of patterns are taken for training the network and are presented in the table 8.4. The figure 8.2 shows the no of iteration vs error plot.

Table 8.2: Network Parameters(Length variation)

Parameter	Value
Number of input neuron	02
Number of hidden neuron	43
Number of output neuron	01
Noise parameters	0.04
Learning Constant(parameter)	4
Momentum factor	0.002

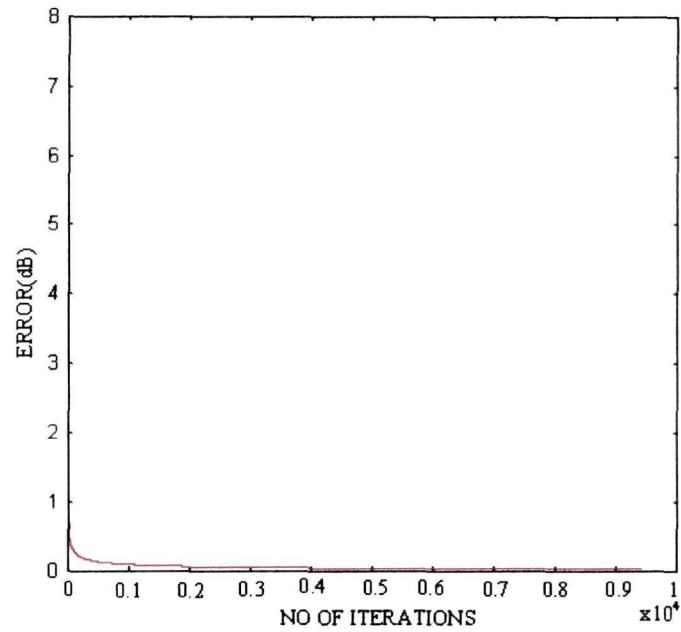


Figure 8.2 No of iterations vs Error plot.

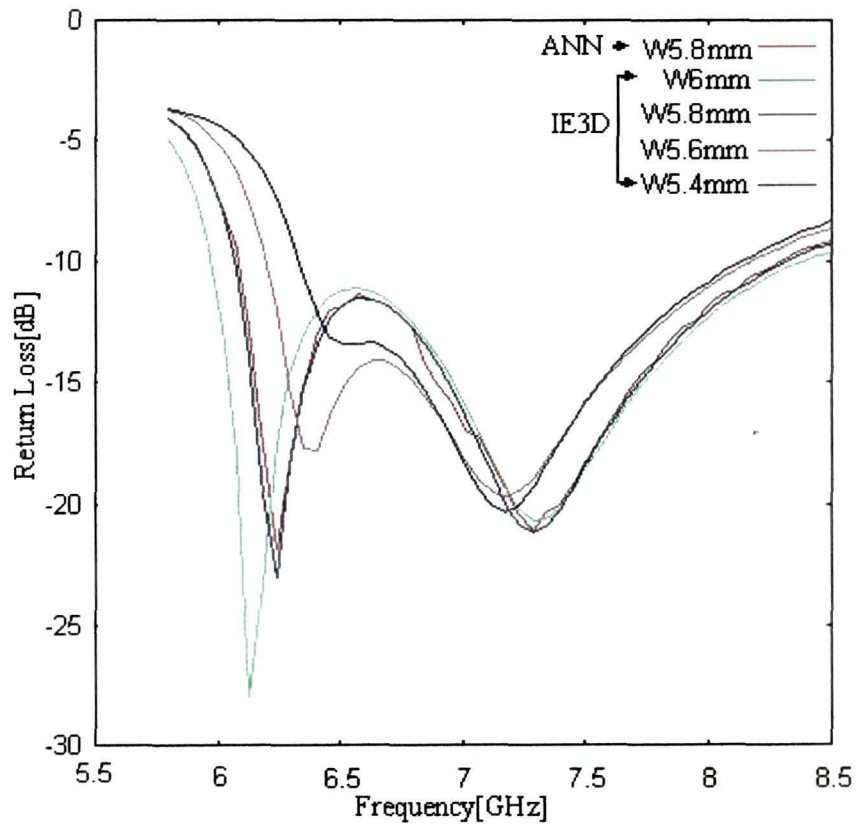


Figure 8.3 (a) Comparisons of returnloss of horn shaped antenna for slot width(W_s) variations .

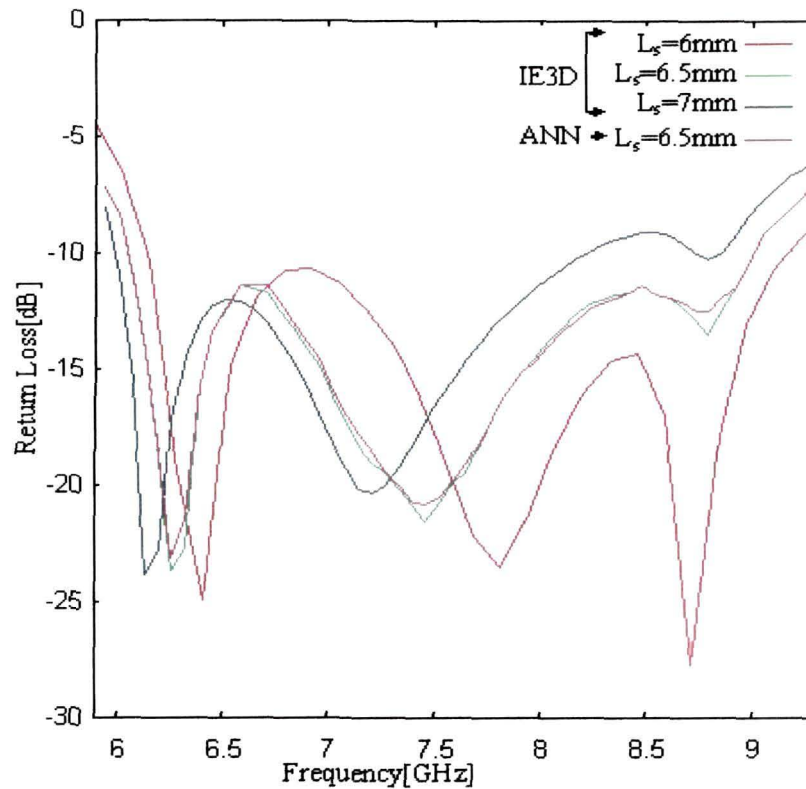


Figure 8.3 (b) Comparisons of returnloss of horn shaped antenna for slot length(L_s) variations.

8.3 Calculation of Radiation Pattern of Microstrip Antenna

The radiation pattern of a microstrip patch antenna is a mathematical representation or a graphical representation of the radiation properties of the antenna as a function of space coordinates. Therefore determination of radiation pattern of a designed antenna is most important task to define the performance of the antenna in practical applications. Artificial Neural Networks due to its greater generalization capability has been used to calculate the radiation patterns of the designed multi slot hole coupled microstrip patch antenna (chapter 6)[223]. The back propagation algorithm has been used to train the network, which learns using gradient descent method (Chapter 3 section 3.8.2). The training time has been reduced considerably by

using tunneling technique in the fast ANN algorithm (Chapter 3 section 3.8.3). A three 2x80x1 Network structure, shown in figure 8.4 is used for training the network.

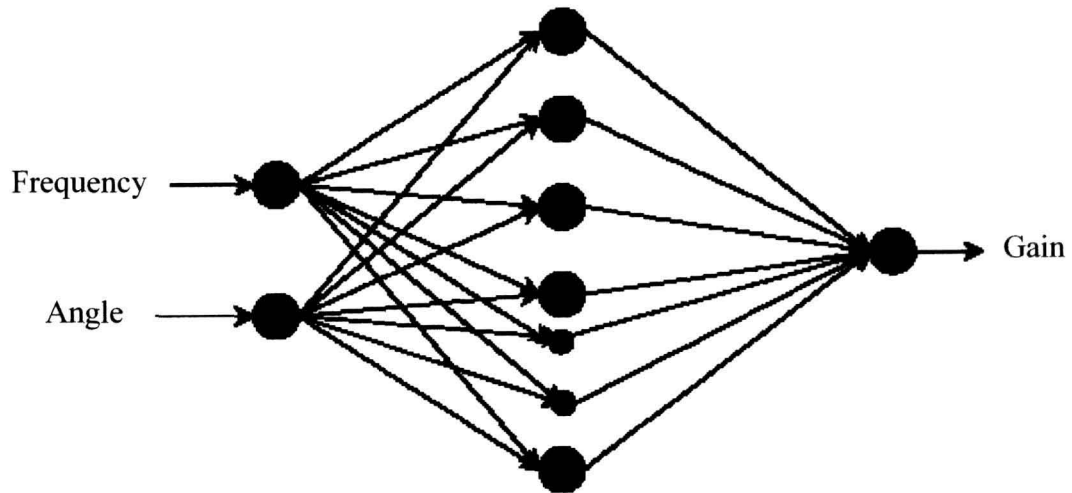


Figure 8.4 Network architecture showing frequency and angle as input and gain as output.

The other network parameters used are,

Noise Factor=0.004,

Momentum Factor=0.075,

Learning Constant=0.08,

Time Step for Integrating for the Differential Equation= 5×10^{-15} ,

Strength of Learning for Tunneling=0.08.

Thirty six patterns each at a step angle of 10 degree for frequencies 6GHz, 6.5GHz, 10.5GHz and 12 GHz are generated Using IE3D[139]. These (35x4) 144 patterns(gain in dB at angle)are used to train the network. Finally, the network is subjected to testing for (120x4) 480 patterns which are generated at a step angle of 3 degree for each of the above cited frequencies. Figure 8.5 shows the radiation at

6GHz and 10.5GHz whereas Figure 8.6 shows the radiation pattern at 6.5GHz and 12GHz respectively.

The average error(deviation from the data taken for testing) at 6GHz is 0.0408, at 6.5GHz is 0.0520241, at 10.5 GHz is 0.0745005 and that of at 12 GHz is 0.0181725. Experimental measurements are carried out to see the radiation patterns at 10.5GHz and at 12GHz. The results are in good agreement with the results of IE3D and with ANN.

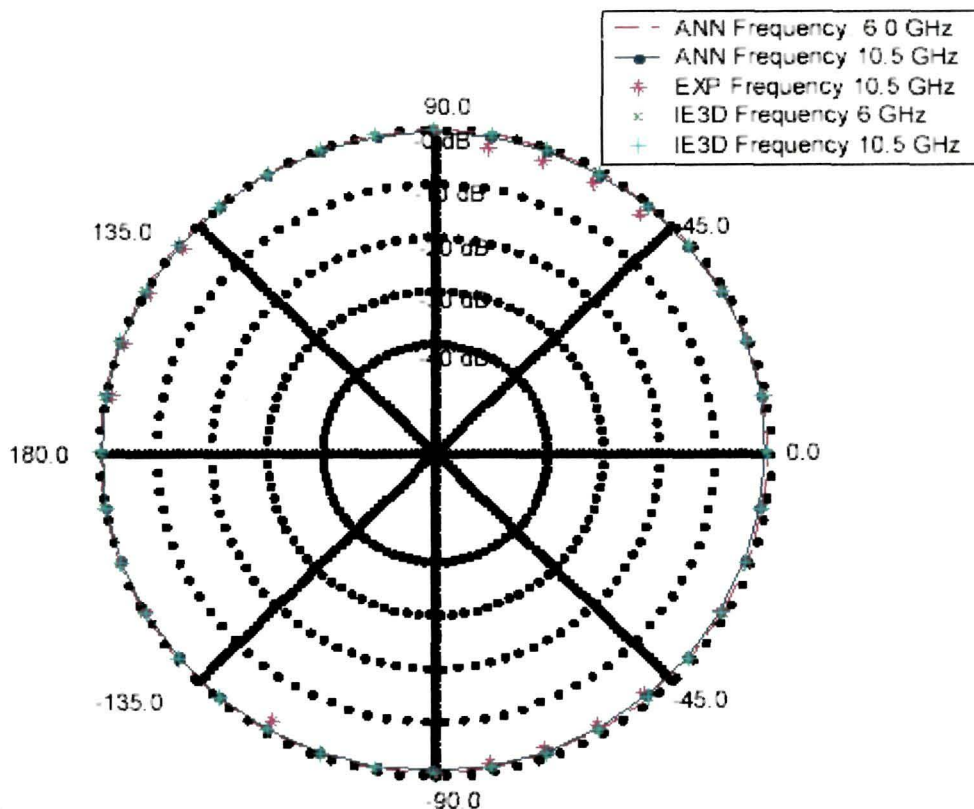


Figure 8.5 Radiation pattern for E-Total, theta=0 at 6 GHz and 10.5GHz.

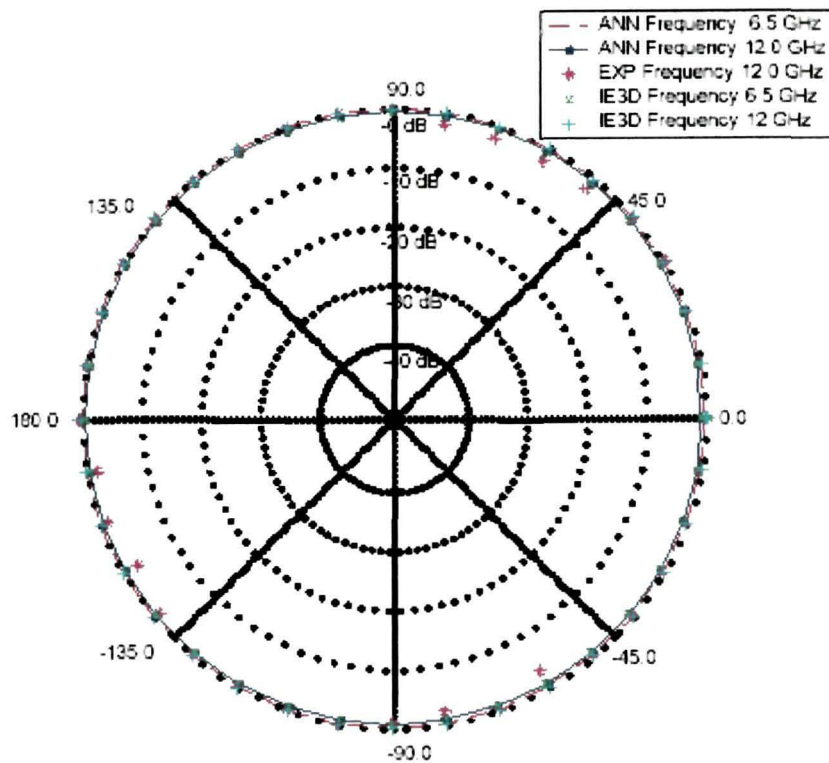


Figure 8.6 Radiation pattern for E-Total, theta=0 at 6.5GHz and 12.0GHz.

8.3 Conclusion

Application of artificial neural networks for the calculation of return loss of coax fed Horn shaped antenna for variations of slot width and slot length seems to be a simple, inexpensive, and accurate method having a very good agreement with the available results. As seen from figure 8.3 (a) &(b), ANNs results are in very good agreement with the calculated data for variation of slot width and slot length of horn shaped antenna. The simulation time using IE3D is 45 minutes for 20 cells per wave length and time taken for training the ANNs is 30minutes and testing time is less than one second using a P-IV personal computer. The agreement of ANNs results with the calculated results of the Horn shaped antenna for slot width variations

and slot length variations, makes it possible to realize an universal artificial neural network to test the returnloss of any variations of slot width and slot length of Horn shaped antenna with accuracy.

The calculation of radiation patterns using the ANNs is a new and interesting part of this works that reflects the simplicity and accuracy of the method. Calculation of radiation patterns using tunnel based Artificial Neural Networks can save considerable computational time while giving accurate results.

Table No 8.3: Training data for slot width variation(W_s) ($L_s = 06\text{mm}$).

Slot Width(mm)	Frequency(in Ghz)	Returnloss(dB)
5	5.8	-3.669
5	5.855	-3.773
5	5.91	-3.89
5	5.965	-4.025
5	6.02	-4.185
5	6.076	-4.379
5	6.131	-4.618
5	6.186	-4.921
5	6.241	-5.312
5	6.296	-5.824
5	6.351	-6.49
5	6.406	-7.333
5	6.461	-8.321
5	6.516	-9.352
5	6.571	-10.30
5	6.627	-11.11
5	6.682	-11.83
5	6.737	-12.58
5	6.792	-13.41
5	6.847	-14.38
5	6.902	-15.48
5	6.957	-16.70
5	7.012	-17.99
5	7.067	-19.23
5	7.122	-20.17
5	7.178	-20.57
5	7.233	-20.31
5	7.288	-19.55
5	7.343	-18.57
5	7.398	-17.55
5	7.453	-16.57
5	7.508	-15.67
5	7.563	-14.87
5	7.618	-14.14
5	7.673	-13.48
5	7.729	-12.89
5	7.784	-12.35
5	7.839	-11.86
5	7.894	-11.42
5	7.949	-11.00
5	8.004	-10.62
5	8.059	-10.27

5	8.114	-9.938
5	8.169	-9.63
5	8.224	-9.341
5	8.28	-9.07
5	8.335	-8.816
5	8.39	-8.577
5	8.445	-8.354
5	8.50	-8.145
5.2	5.80	-3.664
5.2	5.855	-3.781
5.2	5.91	-3.92
5.2	5.965	-4.09
5.2	6.02	-4.302
5.2	6.076	-4.577
5.2	6.131	-4.94
5.2	6.186	-5.43
5.2	6.241	-6.098
5.2	6.296	-6.999
5.2	6.351	-8.157
5.2	6.406	-9.497
5.2	6.461	-10.79
5.2	6.516	-11.76
5.2	6.571	-12.35
5.2	6.627	-12.72
5.2	6.682	-13.10
5.2	6.737	-13.60
5.2	6.792	-14.26
5.2	6.847	-15.10
5.2	6.902	-16.08
5.2	6.957	-17.19
5.2	7.012	-18.33
5.2	7.067	-19.38
5.2	7.122	-20.11
5.2	7.178	-20.33
5.2	7.233	-19.99
5.2	7.288	-19.26
5.2	7.343	-18.35
5.2	7.398	-17.39
5.2	7.453	-16.48
5.2	7.508	-15.63
5.2	7.563	-14.85
5.2	7.618	-14.15
5.2	7.673	-13.52
5.2	7.729	-12.94
5.2	7.784	-12.41
5.2	7.839	-11.93

5.2	7.894	-11.49
5.2	7.949	-11.08
5.2	8.004	-10.70
5.2	8.059	-10.35
5.2	8.114	-10.03
5.2	8.169	-9.719
5.2	8.224	-9.433
5.2	8.28	-9.164
5.2	8.335	-8.913
5.2	8.39	-8.678
5.2	8.445	-8.461
5.2	8.5	-8.26
5.4	5.8	-3.682
5.4	5.855	-3.822
5.4	5.91	-3.996
5.4	5.965	-4.22
5.4	6.02	-4.517
5.4	6.076	-4.923
5.4	6.131	-5.488
5.4	6.186	-6.283
5.4	6.241	-7.385
5.4	6.296	-8.841
5.4	6.351	-10.56
5.4	6.406	-12.16
5.4	6.461	-13.14
5.4	6.516	-13.40
5.4	6.571	-13.35
5.4	6.627	-13.34
5.4	6.682	-13.52
5.4	6.737	-13.92
5.4	6.792	-14.52
5.4	6.847	-15.31
5.4	6.902	-16.27
5.4	6.957	-17.34
5.4	7.012	-18.44
5.4	7.067	-19.44
5.4	7.122	-20.13
5.4	7.178	-20.32
5.4	7.233	-19.99
5.4	7.288	-19.28
5.4	7.343	-18.39
5.4	7.398	-17.45
5.4	7.453	-16.55
5.4	7.563	-14.94
5.4	7.618	-14.24
5.4	7.673	-13.61

5.4	7.729	-13.03
5.4	7.784	-12.51
5.4	7.839	-12.02
5.4	7.894	-11.58
5.4	7.949	-11.17
5.4	8.004	-10.79
5.4	8.059	-10.44
5.4	8.114	-10.11
5.4	8.169	-9.801
5.4	8.224	-9.515
5.4	8.28	-9.247
5.4	8.335	-8.998
5.4	8.39	-8.767
5.4	8.445	-8.555
5.4	8.5	-8.363
5.6	5.8	-3.747
5.6	5.855	-3.974
5.6	5.91	-4.286
5.6	5.965	-4.724
5.6	6.02	-5.351
5.6	6.076	-6.256
5.6	6.131	-7.562
5.6	6.186	-9.418
5.6	6.241	-11.96
5.6	6.296	-15.09
5.6	6.351	-17.71
5.6	6.406	-17.81
5.6	6.461	-16.40
5.6	6.516	-15.15
5.6	6.571	-14.39
5.6	6.627	-14.07
5.6	6.682	-14.09
5.6	6.737	-14.37
5.6	6.792	-14.88
5.6	6.847	-15.56
5.6	6.902	-16.38
5.6	6.957	-17.29
5.6	7.012	-18.20
5.6	7.067	-19.00
5.6	7.122	-19.54
5.6	7.178	-19.71
5.6	7.233	-19.47
5.6	7.288	-18.91
5.6	7.343	-18.18

5.6	7.398	-17.38
5.6	7.453	-16.57
5.6	7.508	-15.80
5.6	7.563	-15.08
5.6	7.673	-13.8
5.6	7.729	-13.24
5.6	7.784	-12.72
5.6	7.839	-12.24
5.6	7.894	-11.80
5.6	7.949	-11.39
5.6	8.004	-11.01
5.6	8.059	-10.65
5.6	8.169	-10.01
5.6	8.224	-9.73
5.6	8.28	-9.466
5.6	8.335	-9.223
5.6	8.39	-9.003
5.6	8.445	-8.809
5.6	8.5	-8.644
5.8	5.8	-4.119
5.8	5.855	-4.581
5.8	5.91	-5.271
5.8	5.965	-6.314
5.8	6.02	-7.90
5.8	6.076	-10.31
5.8	6.131	-14.00
5.8	6.186	-19.63
5.8	6.241	-22.99
5.8	6.296	-18.46
5.8	6.406	-13.41
5.8	6.461	-12.34
5.8	6.516	-11.76
5.8	6.571	-11.52
5.8	6.627	-11.54
5.8	6.682	-11.75
5.8	6.737	-12.15
5.8	6.792	-12.71
5.8	6.847	-13.42
5.8	6.902	-14.27
5.8	7.012	-16.37
5.8	7.067	-17.59
5.8	7.122	-18.84
5.8	7.178	-20.00
5.8	7.233	-20.87
5.8	7.288	-21.22
5.8	7.343	-20.96

5.8	7.398	-20.25
5.8	7.453	-19.30
5.8	7.508	-18.30
5.8	7.563	-17.32
5.8	7.618	-16.42
5.8	7.673	-15.59
5.8	7.729	-14.85
5.8	7.784	-14.17
5.8	7.839	-13.55
5.8	7.894	-12.99
5.8	7.949	-12.47
5.8	8.004	-12.00
5.8	8.059	-11.57
5.8	8.114	-11.17
5.8	8.169	-10.80
5.8	8.224	-10.47
5.8	8.28	-10.16
5.8	8.335	-9.889
5.8	8.39	-9.648
5.8	8.445	-9.444
5.8	8.5	-9.286
6	5.8	-4.911
6	5.855	-5.868
6	5.91	-7.303
6	5.965	-9.451
6	6.02	-12.70
6	6.076	-17.95
6	6.131	-28.01
6	6.186	-23.25
6	6.241	-17.50
6	6.296	-14.65
6	6.351	-13.01
6	6.406	-12.01
6	6.461	-11.43
6	6.516	-11.14
6	6.571	-11.08
6	6.627	-11.20
6	6.682	-11.48
6	6.737	-11.90
6	6.792	-12.46
6	6.847	-13.15
6	6.902	-13.97
6	6.957	-14.90
6	7.012	-15.94
6	7.067	-17.06
6	7.122	-18.21

6	7.178	-19.31
6	7.233	-20.18
6	7.288	-20.67
6	7.343	-20.64
6	7.398	-20.16
6	7.453	-19.39
6	7.508	-18.49
6	7.563	-17.58
6	7.618	-16.71
6	7.673	-15.90
6	7.729	-15.15
6	7.784	-14.47
6	7.839	-13.84
6	7.894	-13.27
6	7.949	-12.75
6	8.004	-12.27
6	8.059	-11.83
6	8.114	-11.43
6	8.169	-11.07
6	8.224	-10.73
6	8.28	-10.43
6	8.335	-10.17
6	8.39	-9.952
6	8.445	-9.782
6	8.5	-9.677

Table No. 8.4: Training data for variation of slot length(Ls) (Ws=6mm).

Slot Length(mm)	Frequency(in Ghz)	Returnloss(dB)
6	5.897	-4.369
6	6.026	-6.426
6	6.154	-10.35
6	6.282	-18.91
6	6.41	-24.89
6	6.538	-14.84
6	6.667	-11.81
6	6.795	-10.73
6	6.923	-10.66
6	7.051	-11.25
6	7.179	-12.37
6	7.308	-13.99
6	7.436	-16.17
6	7.564	-18.98
6	7.692	-22.18
6	7.821	-23.48
6	7.949	-21.18
6	8.077	-18.29
6	8.205	-16.05
6	8.333	-14.59
6	8.462	-14.32
6	8.59	-16.95
6	8.718	-27.71
6	8.846	-17.84
6	8.974	-13.05
6	9.103	-10.72
6	9.231	-9.264
6	9.359	-8.214
6.5	5.949	-7.14
6.5	6.013	-8.241
6.5	6.076	-11.078
6.5	6.139	-14.287
6.5	6.203	-18.872
6.5	6.266	-23.638
6.5	6.329	-22.722
6.5	6.392	-15.663
6.5	6.456	-13.37
6.5	6.519	-12.361
6.5	6.582	-11.35
6.5	6.646	-11.538
6.5	6.709	-11.63

6.5	6.772	-12.45
6.5	6.835	-13.187
6.5	6.899	-14.12
6.5	6.962	-14.837
6.5	7.025	-16.21
6.5	7.089	-17.314
6.5	7.152	-18.322
6.5	7.215	-19.08
6.5	7.278	-19.46
6.5	7.342	-20.155
6.5	7.405	-20.888
6.5	7.468	-21.529
6.5	7.532	-20.706
6.5	7.595	-19.88
6.5	7.658	-19.42
6.5	7.722	-18.137
6.5	7.785	-17.038
6.5	7.848	-15.938
6.5	7.911	-15.113
6.5	7.975	-14.56
6.5	8.038	-13.737
6.5	8.101	-13.187
6.5	8.165	-12.636
6.5	8.228	-12.179
6.5	8.291	-11.9962
6.5	8.354	-11.72
6.5	8.418	-11.628
6.5	8.481	-11.353
6.5	8.544	-11.72
6.5	8.608	-11.903
6.5	8.671	-12.27
6.5	8.734	-12.82
6.5	8.797	-13.46
6.5	8.861	-12.27
6.5	8.924	-11.44
6.5	8.987	-10.437
6.5	9.051	-9.154
6.5	9.114	-8.6042
6.5	9.177	-8.054
6.5	9.241	-7.5037
6.5	9.304	-6.863
7	5.949	-8.03
7	6.013	-10.88
7	6.076	-15.56
7	6.139	-23.80
7	6.203	-22.76

7	6.266	-17.14
7	6.329	-14.41
7	6.392	-12.97
7	6.456	-12.25
7	6.519	-11.99
7	6.582	-12.06
7	6.646	-12.39
7	6.709	-12.94
7	6.772	-13.70
7	6.835	-14.63
7	6.899	-15.72
7	6.962	-16.92
7	7.025	-18.17
7	7.089	-19.32
7	7.152	-20.13
7	7.215	-20.36
7	7.278	-19.98
7	7.342	-19.18
7	7.405	-18.20
7	7.468	-17.18
7	7.532	-16.21
7	7.595	-15.32
7	7.658	-14.51
7	7.722	-13.78
7	7.785	-13.12
7	7.848	-12.52
7	7.911	-11.97
7	7.975	-11.47
7	8.038	-11.02
7	8.101	-10.60
7	8.165	-10.23
7	8.228	-9.896
7	8.291	-9.601
7	8.354	-9.353
7	8.418	-9.162
7	8.481	-9.046
7	8.544	-9.037
7	8.608	-9.178
7	8.671	-9.507
7	8.734	-9.965
7	8.797	-10.23
7	8.861	-9.917
7	8.924	-9.152
7	8.987	-8.338
7	9.051	-7.658
7	9.114	-7.119

7	9.177	-6.688
7	9.241	-6.334
7	9.304	-6.032
7	9.367	-5.768

CHAPTER 9

**CONCLUSIONS, FUTURE SCOPE
AND PUBLICATIONS**

9.1 General Conclusions

The principal contribution of this study include the development of new design of probe-fed microstrip patch antennas on thin substrate for wide band width, high gain along with multi frequency operation. Also it includes development of formula for calculation of resonance frequency of designed antenna as well as implementation of Artificial Neural Network code for the calculation of design parameter of these microstrip patch antennas.

The limitation of miniaturization, large bandwidth, High gain, simplicity in design, low cost and accurate computation technique for design of microstrip antenna to be used in wireless environment have been addresses in the thesis. In this thesis, new designs are introduced that can be used for the most sought after probe-fed Microstrip patch antenna on thin substrate.

The Horn shaped Microstrip patch antenna is implemented on thin substrate. This Horn shaped antenna gives wide bandwidth (32%) without any design complexities. With the variation of substrate height from 2mm to 3.175mm, the impedance bandwidth varies from 10.32% to 32% respectively. High gain with large bandwidth is a special feature of this antenna. Variation of slot length and width to control the bandwidth gives flexibility to control the bandwidth for varied applications. For air dielectric, the horn shaped microstrip patch antenna gives wide bandwidth with efficiency of 95% to 97% which is the notable feature of the designed antenna.

The coax fed-inverted-L shaped microstrip patch antenna, parasitically coupled inverted-L microstrip antenna and the parasitic coupled T- shaped microstrip

patch antenna have been designed on thin substrate. Inverted-L and parasitically coupled inverted-L microstrip patch antennas exhibit wider bandwidth. On the other hand the T-shaped microstrip patch antennas shows the dual band of frequency of operation with perfect isolation between them.

The multi-slots hole-coupled microstrip patch antenna on substrate of thickness 2mm has been designed and the characteristics are studied. The multi-slot hole coupled microstrip patch antenna is also a wide band, multi-frequencies antenna. It has the attractive features of simplicity and flexibility of controlling the bandwidth with high isolation between bands of frequencies. And with almost omni directional radiation patterns, the multi slots hole coupled microstrip antenna seems to be a good antenna for wireless communications especially for cellular telephone applications. The achievement of wide bandwidth with a substrate thickness of 2mm is notable feature. The variation of slot parameters, hole size and positions gives the flexibility to shift the frequency and match the impedance, which is an important feature of the referred antenna.

The accurate evaluation of resonant frequency of microstrip patch antenna is of fundamental importance in the microstrip patch antenna design process. To reduce computational effort and time, an alternative method for the determination of resonant frequency have been developed. The generalized method is presented to determine the resonance frequency of slot coupled rectangular microstrip patch antenna. In this implementation a modified formula is used to calculate the edge extension of an equivalent rectangular patch antenna of the slot loaded microstrip patch antenna and then the modified formula is used for calculation of resonance

frequency. The advantage of this method is its simplicity and accuracy without any complicated mathematical functions or operations. Thus, this method can be useful for development of fast CAD algorithm.

The search for techniques that can reduce the computational complexity of modeling of an antenna while giving accurate result is currently a very important research area. The Artificial Neural Networks (ANNs) has been implemented to accurately find the slot length and width of horn shaped antenna for wide band width without involving high experimental cost, time and tedious theoretical calculations. The back propagation algorithm has been used to train the network, which learns using gradient descent method. Again, tunnel based Artificial Neural Networks has been used for determination of radiation pattern of the multi-slot hole-coupled microstrip patch antennas. The tunnel based Artificial Neural Networks can save considerable computational time while giving accurate results. The calculation of radiation pattern using the ANNs is a new and interesting part of the work that reflects the simplicity and accuracy of the method.

9.2 Future Scope

In research, there are always more aspects that can be investigated than what is presented. Here also, there are some aspects of both the new antenna and parameter calculation that can be extended. The new designed presented in this thesis open up the scopes for high gain, wide band and miniaturized microstrip patch antennas for wireless applications. The controlling tools like slot length, width, angle can be further exploited to achieve tunable parameters of microstrip patch antenna as

required in application like medical imaging, cancer detection and smart wireless environment. The idea of implementing artificial neural networks in parameters calculation of microstrip patch antenna invites further exploration of the technique to reduce the complexities in the antenna design and analysis. Integration with optimization techniques such as Genetic algorithm, PSO etc may enhance the efficiency in terms of computational time and accuracy to make the ANN method of antenna design more acceptable specially for the application areas like bio-medical and smart wireless environment.

9.3 Publications of the Scholar

List of Publications of the Scholar Out of the Thesis Work

International Journal Publication:

1. D.K.Neog, Shyam S. Pattnaik, Dhruba C. Panda, Swapna Devi, Bonomali Khuntia and Malay Dutta, "Design of a Wide Band Microstrip Antenna and use of Artificial Neural Network in the Parameter Calculation," *IEEE Antenna and Propagation Magazine*, vol. 47, no. 3, June 2005, pp. 60-65.
2. D. K. Neog, S. S. Pattnaik, M. Dutta, S. Devi, B. Khuntia, D. C. Panda, "Inverted-L shaped and parasitically coupled inverted-L shaped microstrip antennas for wide bandwidth," *Microwave Optical Technology Letters*, USA, Vol.42, No.03, August 5th, 2004, pp. 190-192.
3. D. K. Neog, S. S. Pattnaik, M. Dutta, S. Devi, D. C. Panda, B. Khuntia, "A new wide-band horn-shaped patch antenna," *International Journal of Electronics*, (communicated ref: IJE/2005/143).
4. Dipak. K. Neog, Shyam S. Pattnaik, Dhruba. C. Panda, Mallay Dutta, Swapna Devi and Bonomali Khuntia "Resonance Frequency of E-Shaped Microstrip Patch Antenna," *Microwave Optical Technology Letters*, USA (Accepted for publication, ref: MOP-06-0089).

International Conference Publication

5. D. K. Neog, S. S. Pattnaik, M. Dutta, S. Devi, D. C. Panda and B. Khuntia "A Novel Patch Antenna for Wide Band Generation," Proc. of *International Conference on Antenna Technologies*, ICAT, Ahmedabad, Feb. 21-22, 2005, pp. 345-348.

List of Publications of Scholar

International Journal

- 1 D.K.Neog, Shyam S. Pattnaik, Dhruva C. Panda, Swapna Devi, Bonomali Khuntia and Malay Dutta, “Design of a Wide Band Microstrip Antenna and use of Artificial Neural Network in the Parameter Calculation,” *IEEE Antenna and Propagation Magazine*, vol. 47, no. 3, June 2005, pp. 60-65.
- 2 S. S. Pattnaik, B. Khuntia, D. C. Panda, D. K. Neog, S. Devi, and M. Dutta, “Application of Genetic Algorithm on Artificial Neural Networks to Calculate Resonant Frequency of Tunable Single Shorting Post Rectangular Patch Antenna,” *International Journal of RF and Microwave Computer Aided Engineering*, vol. 15, no. 1, 3rd Dec. 2004, pp. 140-144.
- 3 D. K. Neog, S. S. Pattnaik, M. Dutta, S. Devi, B. Khuntia, D. C. Panda, “Inverted-L shaped and parasitically coupled inverted-L shaped microstrip antennas for wide bandwidth,” *Microwave Optical Technology Letters*, USA, Vol.42, No.03, August 5th, 2004, pp. 190-192.
- 4 Dipak. K. Neog, Shyam S. Pattnaik, Dhruva. C. Panda, Mallay Dutta, Swapna Devi and Bonomali Khuntia “Resonance Frequency of E-Shaped Microstrip Patch Antenna,” *Microwave Optical Technology Letters*, USA (Accepted for publication, ref: MOP-06-0089).
- 5 Dipak Kr. Neog *etal*, “Calculation of Optimized Parameters of Rectangular Microstrip Patch Antenna using Genetic Algorithm” , *Microwave and Optical Technology Letters* vol-37, No-6, 20th June, 2003, pp.431-433.

- 6 B. Khuntia, S. S. Pattnaik, D. C. Panda, D. K. Neog, S. Devi, and M. Dutta, "Genetic Algorithm with Artificial Neural Networks as its Fitness Function to Design Rectangular Microstrip Antenna on Thick Substrate," *Microwave and Optical Technology Letters*, vol. 44, no. 2, 20th Jan. 2005, pp. 144-146,.
- 7 B. Khuntia, S. S. Pattnaik, D. C. Panda, D. K. Neog, S. Devi and M. Dutta, "A Simple and Efficient Approach to Train Artificial Neural Networks by Genetic Algorithm for Calculating Resonant Frequency of RMA on Thick Substrate," *Microwave and Optical Technology Letters*, vol. 41, no. 4, pp. 313-315, 20th May 2004.

International Conference Publication

- 8 D. K. Neog, S. S. Pattnaik, M. Dutta, S. Devi, D. C. Panda and B. Khuntia "A Novel Patch Antenna for Wide Band Generation," Proc. of *International Conference on Antenna Technologies*, ICAT, Ahmedabad, Feb. 21-22, 2005, pp. 345-348.
- 9 S. S. Pattnaik, D. C. Panda, B. Khuntia, S. Devi, and D. K. Neog, "Tunnel Based Artificial Neural Network to Calculate the Radiation Pattern of Cell Phone Antenna in Presence of Human Head," *IEEE-ASPW*, Delhi, 2002, pp.330-334.
- 10 S. Devi D. C. Panda, S. S. Pattnaik, B. Khuntia, and D. K Neog, "Initializing Artificial Neural Networks by Genetic Algorithm to Calculate the ResonantFrequency of Single Shorting Post Rectangular Patch Antenna,"

- IEEE Proceedings Antennas and Propagation Society*, vol. 3, pp 144-147, 2003.
- 11 D. C. Panda, S. S. Pattnaik, B. Khuntia, S. Devi, D. K. Neog, and R. K. Mishra, "Application of NFDTD for the Calculation of Parameters of Microstrip Antenna," *International Conference on Antenna Technologies, ICAT, Ahmedabad, Feb. 21-22, 2005*.
- 12 S. Devi, S. S. Pattnaik, B. Khuntia, D. C. Panda, M. Dutta, and D. K. Neog, "Design of Knowledge Based Continuous Genetic Algorithm to Train Artificial Neural Networks and its Application on Rectangular Microstrip Antenna," *International Conference on Antenna Technologies, Ahmedabad, Feb. 21-22, 2005*.

National Conference Publication

- 13 S. S. Pattnaik, D. C. Panda, B. Khuntia, S. Devi, and D. K. Neog, "Tunnel Based Artificial to Calculate the Radiation Pattern of Commercially Available Cell Phone Antenna in Presence of Human Head Initialized by Genetic Algorithm," *Horizons of Telecommunication, Institute of Radio Physics and Electronics, University of Calcutta, 2003*.
- 14 S. Devi, S. S. Pattnaik, B. Khuntia, D. C. Panda, and D. K. Neog, "Design of Microstrip Antenna using Genetic Algorithm," *National Symposium on Antenna and Propagation(APSYM), Kochi, India, December 2004*.

CHAPTER 10

REFERENCES

References

1. A.K.Skrivervik, J.-F.Zürcher, O.Staub and J.R.Mosig, "PCS Antenna Design: The Challenge of Miniaturization," *IEEE Antennas and Propagation Magazine*, vol.43, No.4, August 2001, pp.12-25.
2. G.A.Deshamps, "Microstrip microwave antennas," *Thrid USAF Symp on Antenna*, 1952.
3. J.Q.Howell, "Microstrip antenna," *IEEE AP-S Int. Simp. Digest*, 1972, pp.177-188.
4. Ramesh Garg, "Progress in Microstrip Antennas," *IETE Technical Review*, Vol.18, Nos.2&3, March-June 2001, pp-85-98.
5. D.M.Pozar, "Microstrip Antennas," *Proc. IEEE*, Vol.80, No.1, January 1992, pp-79-91.
6. Bahl,I.J. and Bhartia,P. "Microstrip Antennas," *Artech house*, Dedham, MA, 1980.
7. C.A.Balanis, "*Antenna Theory: Analysis and Design*," 2nd edition, New York, John Wely and Sons, 2002.
8. J.R.James & P.S.Hall, *Hand Book of Microstrip Antennas*, Vol-1 &2, London, Peter Peregrinus, 1989.
9. G. Kumar and K.P.Roy, *Board Band Microsrip Antenna*, London, Artech House, 2003.
10. K.R.Carver and J.W.Mink, "Microstrip Antenna Technology," *IEEE Transaction on Antenna Propagation*, vol. AP-29, No.1, January, 1981, pp. 2-24.

11. P.Katchi and N.G.Alexxopouls, "On the modeling of electromagnetically coupled microstrip antenna- the printed strip dipole," *IEEE Transaction on Antenna Propagation*, vol.AP-32, 1984, pp. 1179-1186.
12. H.G.Oltman and D.A.Huebner, Electromagnetically coupled microstrip dipoles, *IEEE Transaction on Antenna Propagation*, Vol.AP-29, No.1, January, 1981, pp. 151-157.
13. G.Gronau and I.Wolf, "Aperture coupling of a rectangular microstrip resonator," *Electronics letters*, Vol. 22, May 1986, pp 554-556.
14. H.F.Pues and A.R.Van De Capelle, "Impedance matching technique for increasing the bandwidth of microstrip antennas", *IEEE Transactions on Antennas and Propagation*, Vol.AP-37, No.11, pp.1345-1354, November, 1989.
15. G.L.Mathaei, L. Yong, and E.M.T. Jones, "Microwave filters, Impedance matching networks and coupling structures," *McGraw Hill*, 1964.
16. H.An, B.K.J.C.Nauwelaers and A.R.Van de Capelle, "Broad Band Microstrip Antenna Design with the Simplefied Real Frequency Technique", *IEEE Transactions on Antennas and Propagation*, Vol.42, No.2, February,1994, pp.129-136.
17. D.de Haaij, J.W.Odendaal and J.Joubert, "Increasing the bandwidth of a microstrip patch antenna with a single parallel resonant circuit," *Proceeding of the IEEE africon 2002 conference*, Vol.2, George, South

-
- Africa, October,2002, pp.527-528.
18. J.Y.Wu, C.Y.Huang and K.L.Wong, "Compact broadband circularly polarized square microstrip antenna," *Microwave and Optical Technology letters*, Vol-21, issue-6, May,1999, pp 423-425.
19. K.L.Wong and Y.F.Lin, "Small broad band rectangular microstrip antenna with chip resistor loading," *Electronics Letters*, Vol.33, 1997, pp.1593-1594.
20. Z.D.Ciu, P.S.Hall and D.Wake, "Dual frequency planer inverted F antenna, *IEEE Transactions on Antennas and Propagation*, Vol.AP-45, No.10, October, 1997, pp. 1451-1458.
21. S.K.Pallit, A, Hamedy, "Design and development of wide band and dual band microstrip antenna," *IEE Proc- Microw. Antennas Propa*, Vol.146, No.1, February 1999, pp. 35-39.
22. H.Kuboyama et al, "Post loaded microstrip antenna for pocket size equipment at UHF," *Proc. ISAP*, August 1985, pp.433-436.
23. T.Chakravarty and De, "Design and tunable modes and dual-band circular patch antenna using shorting posts," *IEE Proc- Microw. Antennas Propag.*, Vol.146, No.3, June, 1999, pp. 224-228.
24. A.Mortazawi, T.Itoh and J.Harvey, Editor, "Active antennas and quasi-optical arrays," *IEEE press*, New York, 1999.
25. E. Denlinger, "Radiation from Microstrip Radiators," *IEEE Transactions on Microwave Theory and Techniques*, vol.17, no.4, April 1969, pp. 235-236.
-

-
26. K. P. Ray and G. Kumar, "Improved Method for the Prediction of Resonance Frequency of Triangular Microstrip Antennas," *IETE Journal of Research*, vol. 47, no. 3&4, May-August 2001, pp.161-164.
 27. R. E. Munson, "Conformal Microstrip Antennas and Microstrip Phased Arrays," *IEEE Transaction Antennas and Propagation*, vol.22, no.1, Jan. 1974, pp.74-77.
 28. Y. T. Lo, D. D. Harrison, D. Solomon, G. A. Deschamps, and F. R. Ore, "Study of Microstrip Antennas, Microstrip Phased Arrays, and Microstrip Fed Networks," Rome Air Development Centre, Tech. Rep. Oct. 1977,TR-77-406.
 29. M. Kara, "Empirical Formulas for the Computation of the Physical Properties of Rectangular Microstrip Antenna Elements with Thick Substrates," *Microwave and Optical Technology Letters*, vol.14, no.2, 5thFeb. 1997, pp.115-120.
 30. E. H. Newman and P. Tulyathan, "Analysis of Microstrip Antennas Using Moment Methods," *IEEE Transaction on Antennas and Propagation*, vol. 29, no.1, January 1981, pp.47-53.
 31. H. Pues and C. A. Van De, "Accurate Transmission Line Model for the Rectangular Microstrip Antenna", *IEE Proc. Microwaves, Optics & Antennas*, vol.134, 1984, pp.334-340.
 32. C. Wu, K. Wu, Z. Bi, and J. Litva, "Accurate Characterization of Planar Printed Antennas Using Finite-Difference Time-Domain Method," *IEEE Transaction on Antennas and Propagation*, vol.40,
-

- no.5, May 1992, pp.526-534.
33. W. F. Richards, Y. T. Lo, and D. D. Harrison, "An improved Theory for Microstrip Antennas and Application," *IEEE Transaction Antennas and Propagation*, vol. 29, no.1, Jan. 1981, pp.38-46.
34. E. Chang, S. A. Long, and W. F. Richards, "An Experimental Investigation of Electrically Thick Rectangular Microstrip Antennas," *IEEE Transaction Antennas and Propagation*, vol.34, no.6, June 1986, pp.767-772.
35. D. L. Sengupta, "Resonant Frequency of Tunable Rectangular Patch Antenna," *IEE Electron Letter*, vol.20, 1984, pp.614-615.
36. D. H. Schaubert, F. H Farr, A. R Sindoris, and S. T Hayes, "Post-tuned Microstrip Antennas for Frequency Agile and Polarization-diverse Application," HDL-TM-81-8, US Army Electronics Research and Development Command, Harry Diamond Laboratories, Adelphi, MD 20783, USA.
37. P. K. Agrawal and M. C. Bailey, "An Analysis Technique for Microstrip Antennas," *IEEE Transactions on Antennas and Propagation*, vol.25, no.6, Nov. 1977, pp.756-759.
38. Y. T. Lo, D. Solomon, and W. F. Richards, "Theory and Experiment on Microstrip Antenna," *IEEE Transaction on Antennas and Propagation*, vol. 27, no.2, March 1979, pp.137-145.
39. J. Herault, R. Moini, A. Reineix, and B. Jecko, "A New Approach to Microstrip Antennas Using a Mixed Analysis: Transient-Frequency,"

-
- IEEE Transaction on Antennas and Propagation*, vol.38, no.8, Aug. 1990, pp. 1166-1175.
40. H. An, B. K. J. C. Nauwelers, and A. R. Van de Capelle, "Broadband Microstrip Antenna Design with the Simplified Real Frequency Technique," *IEEE Transaction on Antennas and Propagation*, vol.42, no.2, Feb. 1994, pp.129-136.
41. R. Kastner, E. Heyman, and A. Sabban, "Spectral Domain Iterative Analysis of Single- and Double-Layered Microstrip Antennas Using the Conjugate Gradient Algorithm," *IEEE Transaction on Antennas and Propagation*, vol.36, no.9, Sept. 1988, pp.1204-1212.
42. X. Gang, "On the Resonant Frequencies of Microstrip Antennas," *IEEE Transaction on Antennas and Propagation*, vol.37, no.2, Feb. 1989, pp.245-247.
43. A. E. Gera, "The Radiation Resistance of a Microstrip Element," *IEEE Transaction on Antennas and Propagation*, vol.38, no.4, April 1990, pp. 568-570.
44. J. R. James, P. S. Hall, C. Wood, and A. Henderson, "Some Recent Development in Microstrip Antenna Design," *IEEE Transaction on Antennas and Propagation*, vol.29, no.1, Jan. 1981, pp.124-128.
45. M. D. Deshpande and M. C. Bailey, "Input Impedance of Microstrip Antennas," *IEEE Transaction on Antennas and Propagation*, vol.30, no.4, July 1982, pp. 645-650.
46. R. W. Dearnley and A. R. F. Barel, "A Comparison of Models to
-

-
- Determine the Resonant Frequencies of a Rectangular Microstrip Antenna,” *IEEE Transaction on Antennas and Propagation*, vol.37, no.1, Jan. 1989, pp. 114-117.
47. J. Q. Howell, “Microstrip Antennas,” *IEEE Transaction on Antennas and Propagation*, vol.23, no.1, Jan.1975, pp.90-93.
48. M. C. Bailey and M. D. Deshpande, “Integral Equation Formulation of Microstrip Antennas,” *IEEE Transaction on Antennas and Propagation*, vol.30, July 1982, pp.651-656.
49. K. R. Carver and E. L. Coffey, “Theoretical Investigation of the Microstrip Antenna,” New Mexico State University, Tech. Rep. PT 00929, Jan. 1979.
50. A. G. Derneryd, “A Theoretical Investigation of the Rectangular Microstrip Antenna,” *IEEE Transaction on Antennas and Propagation*, vol.26, July 1978, pp.532-535.
51. W. C. Chew and Q. Liu, “Resonance Frequency of a Rectangular Microstrip Patch,” *IEEE Transaction on Antennas and Propagation*, vol.36, no.8, Aug. 1988, pp.1045-1056.
52. F. Abboud, J. P. Damiano, and A. Papiernik, “Simple Model for the Input Impedance of Coax-fed Rectangular Microstrip Patch Antenna for CAD,” *IEE Proceedings*, vol.135, no.5, Oct. 1988, pp.323-326.
53. K. Araki and T. Itoh, “Hankel Transform Domain Analysis of Open Circular Microstrip Radiating Structures,” *IEEE Transaction on Antennas and Propagation*, vol.29, no.1, Jan. 1981, pp.84-89.
-

-
54. A. Reineix and B. Jecko, "Analysis of Microstrip Patch Antennas Using Finite Difference Time Domain Method," *IEEE Transaction on Antennas and Propagation*, vol.37, no.11, Nov. 1989, pp.1361-1369.
 55. Nassimuddin and A. K. Verma, "Fast and Accurate Model for Analysis of Equilateral Triangular Patch Antenna," *Journal of Microwave and Optoelectronics*, vol.3, no.4, April 2004, pp.99-110.
 56. J. Watkins, "Circular Resonant Structures in Microstrip," *Electronics Letters*, vol. 5, no. 21, 16th Oct. 1969, pp. 524-525.
 57. T. T. Wu, "Theory of the Microstrip," *Journal of Applied Physics*, vol. 28, no. 3, March 1957, pp. 299-302.
 58. J. R. Mosig, "Arbitrarily Shaped Microstrip Structures and Their Analysis with a Mixed Potential Integral Equation," *IEEE Transactions on Microwave Theory and Techniques*, vol. 36, no. 2, Feb. 1988, pp.314-323.
 59. J. R. Mosig, and F. E. Gardiol, "Analytical and Numerical Techniques in the Green's Function Treatment of Microstrip Antennas and Scatterers," *IEE Proceedings*, vol.130, no.2, March 1983, pp. 175-182.
 60. M. Kaddour, A. Mami, A. Gharsallah, A. Gharbi, and H. Baudrand, "Analysis of Multilayer Microstrip Antenna by Using Iterative Method," *Journal of Microwave and Optoelectronics*, vo.3, no.1, April 2003, pp.39-52.
 61. S. Touchard, "Multilayer Microstrip Antennas Study by Using the Spectral Domain Approach," *Onde Electrique*, vol. 73, no.1, Jan.-Feb.

- 1993, pp.15-19.
62. L. Xia, C. Wang, L. Li, P. Kooi, and M. Leong, "Fast Characterization of Microstrip Antenna Resonance in Multilayered Media Using Interpolation/Extrapolation methods," *Microwave and Optical Technology Letters*, vol. 29, no.5, 5th March 2001, pp.342-346.
63. L. I. Basilio, M. A. Khayat, J. Williams, and S. A.Long, "The Dependence of the Input Impedance on Feed Position of Probe and Microstrip Line-Fed patch Antennas," *IEEE Trans. Antennas Propagation*, vol.49, Jan. 2001,pp.45-47.
64. D. H. Schaubert, F. G. Farrar, A. Sindoris and S. T. Hayes, "Microstrip Antennas with Frequency Agility and Polarization Diversity," *IEEE Trans. Antennas Propagation*, vol. 29, Jan. 1981, pp. 118-123.
65. J. S. Dahele and K. F. Lee, "Experimental Study of the Triangular Microstrip Antenna," *IEEE APS Int. Symp. Dig*, 1984, pp. 283-286.
66. R. K Mongia, and A. Ittipiboon, "Theory and Experimental Investigations on Rectangular Dielectric Resonator Antennas," *IEEE Trans. on Antennas and Propagation*, vol. 45, no. 9, Sept. 1995, pp. 1348-1356.
67. N. Kumprasert and W. Kiranon, "Simple and Accurate Formula for the Resonant Frequency of the Circular Microstrip Disk Antenna," *IEEE Trans. on Antennas and Propagation*, vol. 43, no. 11, Nov. 1995,pp. 1331-1335.
68. A. Weng and R. Qinghuo, "Resonance Frequency of Rectangular

-
- Microstrip Patch Antennas,” *IEEE Trans. on Antennas and Propagation*, vol. 36, no. 8, Aug. 1988, pp.1046-1056.
69. E. F. Keuster and D. C. Chang, “A Geometrical Theory for the Resonant Frequencies and Q Factors for Some Triangular Patch antenna,” *IEEE Transaction on Antennas and Propagation*, vol. 31, no.1, 1983, pp. 27-34.
70. S. S. Pattnaik, G. Lazzi, and Om P. Gandhi, “On the Use of Wide-Band, High-Gain Microstrip Antenna for Mobile Telephones,” *IEEE Antenna and Propagation Magazine*, vol.40, no.1, Feb.1998, pp.88-90.
71. Q. Balzano, O. Garay, and T. J. Manning. Jr., “Electromagnetic Energy Exposure of Simulated Users of Portable Cellular Telephones,” *IEEE Veh. Technology*, vol.44, 1995, pp.390-403.
72. P. Bernardi, M. Cavagnaro, and S. Pisa, “Evaluation of the SAR Distribution in the Human Head for Cellular Phones Used in a Partially Closed Environment,” *IEEE Electromagnetic Compatibility*, vol. 38, 1996, pp 357-366.
73. G. Lazzi, S. S. Pattnaik, C. M. Furse and O. P. Gandhi, “Comparison of FDTDComputed and Measured Radiation Patterns of Commercial Mobile Telephones in Presence of the Human Head,” *IEEE Antenna and Propagation Magazine*, vol.46, June 1998, pp. 943-944.
74. G. Lazzi, S. S. Pattnaik, and Om P. Gandhi, “Experimental and FDTD-Computed Radiation Patterns of Cellular Telephones Held in Slanted Operational Conditions,” *IEEE Electromagnetic Compatibility*, vol. 41,
-

-
- no. 2, 1999, pp. 141-144.
75. G. Lazzi and Om P. Gandhi, "Realistically Tilted and Truncated Anatomically Based Models of the Human Head for Dosimetry of Mobile Telephones," *IEEE Electromagnetic Compatibility*, vol.39, Feb. 1999, pp. 55-61.
76. M. Okoniewski and M. A. Stuchly, "A Study of the Handset Antenna and Human Body Interaction," *IEEE Trans Microwave Theory Tech.*, vol. 44, Oct.1996,pp. 1855-1864.
77. K. Ichige and H. Arai, "Concept and Evaluation of a 2-D FDTD Formulation Based on Expanded Wave Equation Approach," *IEICE Trans. Electron.*, vol. E84-c, no. 7, July 2001.
78. Z.N.Chen and M.Y.W.Chia, "Center-fed Microstrip patch antenna," *IEEE Transaction on Antenna Propagation*, vol. 51, No.3, March 2003, pp. 483-487.
79. Frank Zavosh and James T. Aberle, "Design of High Gain Microstrip Antennas," *Microwave Journal*, vol. 42, No. 9, September 1999, pp. 138-148.
80. M. M. Ney, "Method of moments as applied to electromagnetic problem," *IEEE Transaction on Microwave theory and techniques*, vol. MTT-33, No.10, October,1985, pp. 972-980.
81. A.Hoorfar and V. Jamnejad, " Electromagnetic modeling and analysis of wireless communication antennas," *IEEE microwave magazine*, Vol.4, No.1, 2003, pp.51-67.
-

-
82. S.C.Gao, L.W.Li, M.S.Leong, T.S.yeo, "Annalysis of a H-Shaped patch antenna by using FDTD method," *Progress in Electromagnetics Research*, PIER 34, 2001, pp. 165-187.
 83. M.M.Nikolić, A. R.Djordjević and A.Nehrai, "Microstrip Antennas With Suppressed Radiation in Horizontal Directions and reduced Coupling," *IEEE Transaction on Antenna Propagation*, vol. 53, No.11, November 2005, pp. 3450-3476.
 84. J.P.Damiano and A.Papernaik, " Servey of analytical and numerical models for probe-fed microstrip antennas," *IEE Proce-Microwave, Antennas Propag.*, Vol.141, No.1, February,1994,pp. 15-22.
 85. H.Mang and X.Xiaowen, "Full wave analysis and wide-band design of probe-fed Multilayered Cylindrical-Rectangular Microstrip Antennas," *IEEE Transaction on Antenna Propagation*, vol. 52, No.7, July 2004, pp. 1749-1757.
 86. Jean-Francois Zurcher and Fred E. Gardiol, "Boardband Patch Antenna," *London, Artech House*, 1995.
 87. D. M. Pozar and D.H.Schaubert, Eds., "Microstrip Antennas: The analysis and Design of Microstrip antennas and arrays," *New York, IEEE press*, 1995.
 88. Munson,R.E., "Conformed Microstrip Antennas Microstrip Phased Arrays." *IEEE Transactions on Antennas and Propagation*,Vol.22, 1974, pp-74-78.
 89. Hall. S. and C.M. Hall, "Coplanar Corporate Feed Effects in

-
- Microstrip Patch Array Design,” *IEE Proc.*, Pt. H., Vol.135, 1988, pp. 180-186.
90. N.Yaun, T.S.Yeo, X.C.Nie, Y.B.Gan and L.W.Li, “Efficient Analysis of Probe Feed Microstrip Antennas on Arbitarily shaped Finit ground Plane and Substrate,” *0-7803-8883-6/05/\$20.00 ©2005 IEEE* 2005, pp. 134-137.
91. D.M.Pozar , “Microstrip antenna aperture coupled to a microstrip line,” *Electron. Lett.*, Vol. 21, No.2, January,1995, pp.49-50.
92. D.M.Pozar and S.D.Targonski, “Improved coupling for aperture coupled microstrip antenna,” *Electron. Lett.*, Vol.127, No.12, June 1991, pp.1129-1131.
93. D.M.Pozar, “Aperture coupled microstrip subarrays,” *Electron. Lett.*, Vol. 30, No.23, November,1994, pp.1901-1902.
94. X.H.Yang and L.Shafai, “Characteristics of aperture coupled microstrip antennas with various radiating patches and coupling apertures,” *IEEE Transactions on Antennas and Propagation*, Vol.43, No.1, January,1995, pp.72-78.
95. V.Rathi, G.Kumar and K.P.Ray, “Improved coupling for aperture coupled microstrip antennas,” *IEEE Trans. Atnennas Propagat.*, Vol.44, No.8, August,1996, pp.1196-1198.
96. R.Garg, P. Bhartia, I.Bahi and A.Ittipiboon, “Microstrip Design Hand Book,” *Artech House Inc.*, 2001.
97. Q. Rao and R.H.Johnston, “Modified Aperture Coupled Microstrip
-

-
- Atnenna,” *IEEE Transactions on Antennas and Propagation*, Vol.52, No.12, December,2004, pp.3397-3400.
98. D.M.Pozar and B.Kaufmann, “Increasing the Bandwith of a Microstrip Antenna by Proximity Coupling, *Electronics Letters*,” Vol.23, April,1987, pp.368-369.
99. T.N.Chang and Y.C.Wei, “Proximity Coupled Microstrip Reflectarray,” *IEEE Transactions on Antennas and Propagation*, Vol.52, No.2, February,2004, pp.631-635.
100. D.Sanchez-Hernandsez, “A survey of board band microstrip patch antennas, *Microwave Journal*,” September,1996, pp.60-84.
101. D.M.Pozar, “Review of band width enhancement technique of microstrip antennas, in *Microstrip antennas: The analysis and Design of Microstrip Antennas and Arrays*,” D.M.Pozar and D.H.Schaubert, Eds. New york, IEEE press, 1995, pp.157-166.
102. C.Wood, “ Improved band width of microstrip antenna using parasitic elements”, *IEE Proceedings*, Vol.127, Pt. H, No.4, August,1980, pp.231-234.
103. G.Kumar and K.C.Gupta, “ Broad-band microstrip antenna using additional resonators gap coupled to radiating edges”, *IEEE Transactions on Antennas and Propagation*, Vol.AP-32, No.12, December1984, pp.1375-1379.
104. G.Kumar and K.C.Gupta, “Non-radiating edges and four edges gap coupled multiple resonator broad band microstrip antennas”, *IEEE*
-

-
- Transactions on Antennas and Propagation*, Vol.AP-33, No.2, February,1985, pp.173-178.
105. G.Kumar and K.C.Gupta, "Directly coupled multiple resonator wide band microstrip antennas", *IEEE Transactions on Antennas and Propagation*, Vol.AP-33, No.6, June,1985, pp.588-593.
106. R.Garg and V.S.Reddy, "A Broad band coupled strip Microstrip Antenna", *IEEE Transactions on Antennas and Propagation*, Vol.49, No.9, September,2001, pp.1344-1345.
107. R.B.Waterhouse, "Design of probe fed stacked patches", *IEEE Transactions on Antennas and Propagation*, Vol.47, No.12, December1999, pp.1780-1784.
108. C.S Lee, V.Nalbandian, and F. Schwering, "Planner dual-band microstrip antenna", *IEEE Transactions on Antennas and Propagation*, Vol.43, No.8, August, 1995, pp.892-894.
109. N. Herscovici, Z.Sipus and D.Bonefacic, "Circularly Polarized Single-Fed Wide-Band Microstrip Patch", *IEEE Transactions on Antennas and Propagation*, Vol.51, No.6, June 2003, pp.1277-1279.
110. J. Anguera, L.Bcuada, C.Puente, C.Borja and J.Soler, "Stacked H-Shaped Microstrip Patch Antena", *IEEE Transactions on Antennas and Propagation*, Vol.52, No.4, April,2004, pp.983-993.
111. D.M.Kokotoff, J.T.Aberle and R.B.Waterhouse, "Rigorous analysis of probe fed printed annular ring antenna", *IEEE Transactions on Antennas and Propagation*, Vol.47, No.2, February 1999, pp.384-388.
-

112. A.Mitchell, M.Lech, D.M.Kokotoff and R.B.Waterhouse, "Search for high performance probe fed stacked patches using optimization", *IEEE Transactions on Antennas and Propagation*, Vol.51, No.2, February 2003, pp.249-252.
113. G.A.Vandenbosch and A.R.Vande Apelle, " Study of capacitively fed microstrip antenna element", *IEEE Transactions on Antennas and Propagation*, Vol.42, No.12, December1994, pp.1648-1652.
114. G.A.Vandenbosch, "Network model for capacitively fed microstrip element", *Electronics Letters*, Vol.35, No.19, September 1999, pp. 1597-1600.
115. Z.F.Liu, P.S. Kooi, L.W.Li, M.S.Leong and T.S.Yeo, "A method for designing broad-band microstrip antenna in multilayered planar structures", *IEEE Transactions on Antennas and Propagation*, Vol.47, No.9, September 1999, pp.1416-1420.
116. M.A.Gonzalez de Aza, J.Zapata and J.A.Encinar, "Broad band cavity backed and capacitively probe fed microstrip patch arrays", *IEEE Transactions on Antennas and Propagation*, Vol.48, No.5, May 2000, pp.784-789.
117. G.Mayhew-Ridgers, J.W.Odendaal and J.Joubert, " Single layer capacitiv feed for wide band probe-fed microstrip antenna elements", *IEEE Transactions on Antennas and Propagation*, Vol.51, No.6, June 2003, pp.1405-1407.
118. P.S.Hall, "Probe compensation in thick microstrip patches",*Electronics*

-
- Letters*, Vol.23, No.11, May 1987, pp. 606-607.
119. S.K.Palit and A.Hamadi, "Design and development of wideband and dual band microstrip antennas", *IEE proc. Microwave Antennas Propagation*, Vol.146, No.1, February 1999, pp.35-39.
120. T.Huynh and K.F.Lee, "Single-layer single-patch wide band microstrip antenna," *Electron Letters*, Vol.31, No.16, August 1995, pp.1310-1312.
121. F. Yang, X.-X. Zhang, X. Ye and Y. Rahmat-Samii, "Wide Band E_Shaped Patch antennas for wireless communications," *IEEE Transaction on Antenna Propagation*, vol. 49, no.7, July, 2001, pp 1094-1100.
122. Kin-Lu Wong and Wen-Hsiu Hsu, "A Broad-Band Rectangular Patch Antenna With a Pair of Wide Slits," *IEEE Transaction on Antenna Propagation*, vol. 49, no.9, September 2001, pp 1345-1347.
123. Wen-Hsiu Hsu and Kin-Lu Wong, "Broad-Band Probe-Fed Patch Antenna With a U-Shaped Ground Plane for Cross-Polarization Reduction," *IEEE Transaction on Antenna Propagation*, vol. 50, no.3, March, 2002, pp 352-354.
124. Jui-Han Lu, "Bandwidth enhancement design of single layer slotted circular microstrip antennas," *IEEE Transaction on Antenna Propagation*, vol. 51, no.5, May 2003, pp. 1126-1129.
125. R.Chair, C.L.Mak, K.F.Lee, K.M.Luk and A.A.Kishk, "Miniature wide band half U-slot and half E-shaped patch antennas," *IEEE*
-

-
- Transaction on Antenna Propagation*, vol. 53, No.8, August,2005, pp. 2645-2651.
126. K. Uehara and K. Kagoshima, "Rigorous Analysis of Microstrip Phased Array Antennas Using a New FDTD Method," *Electronics Letter*, vol.30, no.2, pp.100-101, 1994.
127. T. Kashiwa, T. Onishi, and I. Fukai, "Analysis of Microstrip Antennas on a Curved Surface using Conformal Grids FD-TD Method," *IEEE Transaction on Antennas and Propagation*, vol.42, no.3,pp.423-427, 1994.
128. M.M.Ney, "Method of moments as applied to electromagnetic problem," *IEEE Transaction on Microwave theory and techniques*, vol.MTT-33, No.10, October 1985, pp. 972-980.
129. A.Hoorfar and V. Jamnejad, " Electromagnetic modeling and analysis of wirless communication antnennas," *IEEE microwave magazine*, Vol.4, No.1, 2003, pp.51.
130. C.A. Balanis, *Advanced Engineering Electromagnetics*, John Wiely & Sons, New Yrok, 1989.
131. E. A. Hammerstad, "Equation for microstrip Circuit Design," *Proc. Fifth European Microwave Conf.*, September 1975, pp.268-272.
132. H.Pues and A Van de Capelle, "Accurate transmission line model for the rectangular microstrip antenna," *IEE Proceedings*, Vol.131, Pt.H, no.6, December 1984, pp.334-340.
133. A.G.Derneryd, "A theoretical investigation of the rectangular

-
- microstrip antenna element," *IEEE Transaction on Antenna Propagation*, vol. AP-26, No.4, July 1978, pp. 532-533.
134. E.H.Van Lil and A.R.Van de Capelle, "Transmission line model for mutual coupling between microstrip antennas," *IEEE Transaction on Antenna Propagation*, vol. AP-32, No.8, August 1984, pp. 816-821.
135. W.F. Richards, "Microstrip antennas," *Chapter 10 in Antenna Handbook: Theory, Applications and Design (Y.T.Lo and S.W.Lee, eds)*, Van Nostand Reinhold Co., New York, 1988.
136. Stutzman, W.L. and Thiele, G.A., "Antenna theory and design," *John Wiley & Sons, Inc*, 1998.
137. Harrington. R.F., "Field computation by Moment Methods," Macmillan, New York, 1968.
138. Kantorovich,L. and Akilov,G., "Functional Analysis in Normed Spaces," Pergamon, Oxford, 1964, pp. 586-587.
139. IE3D Version-7.04, *Zeland Software Inc.*, Fremont, CA.
140. B. Yegnanarayana, "Artificial Neural Networks," Prentice-Hall of India Pvt. Ltd. New Delhi, Ch.8, 2001.
141. T. Chen, H. Chen, and R. Liu, "Approximation Capability in $C(R^n)$ by Multilayer Feedforward Networks and Related Problems," *IEEE Transactions on Neural Networks*, vol.6, no.1, Jan 1995, pp.25-30.
142. K. Hornik, M. Stinchombe, and H. White, "Multilayer Feed-Forward Networks are Universal Approximators," *IEEE Transaction on Neural Networks*, vol.2, 1989, pp.359-366.
-

143. S. Grossberg, "Studies of Mind and Brain: Neural Principles of Learning Perceptron, Development, Cognition, and Motor Control," Boston, Reidel Press, 1982.
144. J. A. Anderson and E. Rosenfeld, "Neurocomputing: Foundation of Research," Cambridge, MA, MIT Press, 1989.
145. J. J. Hopfield, "Neural Networks and Physical Systems with Emergent Collective Computational Abilities," *Proceedings of National Academy Sciences*, vol.79, 1982, pp.2554-2558.
146. Haykin, "Neural Network-A Comprehensive Foundation", 1994.
147. G. L Creech, B .J. Paul, C. Lesniak, T .J. Jenkins and M. C. Calcaterra, "Artificial Neural Networks for Fast and Accurate EM CAD of Microwave Circuits," *IEEE Transaction Microwave Theory Tech*, vol.45, May 1997, pp. 794-802.
148. E. Wang and Q. J. Jhang, "Knowledge Based Neural Models for Microwave Design," *IEEE Trans. Microwave Theory Tech*, vol.45, Dec 1997, pp.2333-2343.
149. R. Mitra and V. Veremey, "On the Application of Neural Networks to Efficient Design of RF and Wireless Circuits," *Wireless Symposium*, San Jose, California, Feb. 22-25 2000.
150. G. Fedi, S. Manetti, G. Pelosi, and S. Selleri, "Profile Corrugated Circular Horns Analysis and Synthesis via an Artificial Neural Network," *IEEE Transaction on Antennas and Propagation*, vol.49, no.11, Nov. 2001, pp.1597-1602.

151. J. Huang, "Theoretical Analysis of ART Neural Networks and their Applications in Frequency Selective Surfaces," PhD Dissertation, University of Central Florida, 1994.
152. G. Washington, "Aperture Antenna Shape Prediction by Feedforward Neural Networks," *IEEE Transaction on Antennas and Propagation*, vol.45, no.4, April 1997, pp.683-688.
153. P. Watson and K. C. Gupta, "EM-ANN models for Microstrip Vias and Interconnects in Dataset Circuits," *IEEE Transaction on Microwave Theory and Techniques*, vol.44,no.12, 1996, pp.2495-2503.
154. M. Vai, M. S. Prasad, "Automatic Impedance Matching with a Neural Network," *IEEE Trans. Microwave Guided Wave Letter*, vol.3, no.10, Oct.1993, pp.353-354.
155. Y. Harcouss, *etal*, "The Use of Artificial Neural Networks in Nonlinear Microwave Devices and Circuit Modeling: An Application to Telecommunication System Design," *International Journal on RF and Microwave CAE*, vol. 9, 1999.
156. K. C. Gupta, R. Garg, R. Chadha, "Computer-Aided Design of Microwave Circuits," Artech House, 1981.
157. G. L. Creech, B. Paul, C. Lesniak, T. Jenkins, R. Lee, and M. Calcaterra, "Artificial Neural Networks for Accurate Microwave CAD Applications," *IEEE Int. Microwave Symposium, Digest*, San Francisco, CA, 1996, pp. 733–736.
158. E. K. Murphy and V. V. Yakovlev, "FDTD-Backed RBF Neural

- Network Technique for Efficiency Optimization of Microwave Structure,” *Proceeding of the 9th ampere conf. On Microwave and RF Heating*, Loughborough, Sept. 2003, pp. 197-200.
159. H. J. Delgado and H. Thursby, “A Novel Neural Network Combined With FDTD for Synthesis of a Printed Dipole Antenna,” *IEEE Transaction on Antennas and Propagation*, vol. 53, no. 7, July 2005, pp.2231-2235.
160. L. Vegni and A. Toscano, “Analysis of Microstrip Antennas Using Neural Networks,” *IEEE Trans. on Magnetics*, vol.33, no.2, pp.1414-1419, March 1997.
161. A. Patnaik and R. K. Mishra, “ANN Techniques in Microwave Engineering”, *Microwave*, March 2000, pp.55-60.
162. A. Patnaik and R. K. Mishra, “Neural Network Based CAD Design of Square Patch Antenna,” *IEEE Transaction on Antenna and Propagation*, vol. 46, no. 12, Dec. 1998, pp. 1890-1891.
163. R. K. Mishra and A. Patnaik, “Designing Rectangular Patch Antenna Using Neurospectral Method,” *IEEE Transaction Antenna and Propagation*, vol.51, no.8, 2003, pp.1914-1921.
164. C. G. Christodoulou and M. Georgiopoulos, “Applications of Neural Networks in Electromagnetics,” *Artech House Publication*, 2001.
165. D. Karaboga, K. Guney, S. Sagiroglu, and M. Erler, “Neural Computation of Resonant Frequency of Electrically Thin and Thick Rectangular Microstrip Antennas,” *IEEE Proc. Microwave Antennas*

-
- Propagation*, vol. 146, 1999.
166. C. Christodoulou and M. Georgiopoulos, "Applications of Neural Networks in Electromagnetics," Oxford: Clarendon, 1999.
167. E. R. Brinholo, J. F. Z. Destro, A. A. C. de Freitas, and N. P. de Alcantara Jr., "Determination of Resonant Frequencies of Triangular and Rectangular Microstrip Antennas, Using Artificial Neural Networks," *Progress in Electromagnetics Research Symposium*, Hangzhou, China, Aug. 22-26, 2005.
168. N. P. Somasiri, X. Chen, and A. A. Rezazadeh, "Neural Network Modeler for Design Optimisation of Multilayer Patch Antennas," *IEE Proceedings Microwaves, Antennas and Propagation*, vol. 151, no. 6, Dec. 2004, pp. 514-518.
169. K. Y. Yezdandoost and D. C. Gharpure, "A CAD Software Tool for the Design and Analysis of Rectangular Microstrip Patch Antenna," *3rd International Conference on Antenna Theory and Techniques*, Sept. 1999.
170. H. El zooghby, C. G. Christodoulou, and M. Georgiopoulos, "Performance of Radial Basis Function Networks for Direction of Arrival Estimation with Antenna Arrays," *IEEE Transaction on Antennas and Propagation*, vol. 45, no. 11, Nov. 1997, pp.1611-1617.
171. Q. J. Zhang and K. C. Gupta, "Neural Networks for RF and Microwave Design," Artech House Publication, Norwood, MA, 2000.
172. K. C. Gupta, "Emerging Trends in Millimeter-Wave CAD," *IEEE*

-
- Transaction on Microwave Theory and Techniques*, vol. 46, 1998, pp. 747-755.
173. F. Wang and Q. J. Zhang, "Knowledge-Based Neural Models for Microwave Design," *IEEE Trans Microwave Theory Tech.*, vol. 45, 1997, pp. 2333-2343.
174. F. Wang, V. K. Devabhaktuni, and Q. J. Zhang, "A Hierarchical Neural Network Approach to the Development of a Library of Neural Models for Microwave Design," *IEEE Trans Microwave Theory Tech.*, vol. 46, 1998, pp.2391-2403.
175. A. Patnaik, R. K. Mishra, G. K. Patra, and S. K. Dash, "An Artificial Neural Network Model for Effective Dielectric Constant of Microstripline," *IEEE Trans Antennas Propagation*, vol. 45, 1997, pp.1697.
176. H. Zaabab, Q. J. Zhang, and M. S. Nakhla, "Device and Circuit Level Modeling using Neural Networks with Faster Training Based on Network Sparsity," *IEEE Trans Microwave Theory Techniques*, vol.45 1997, pp.1696-1704.
177. Cho and K. Gupta, "EM-ANN Modeling of Overlapping Open-ends in Multilayer Microstrip Lines for Design of Bandpass Filters," *IEEE APS International Symposium Digest*, Orlando, FL, July 1999, pp. 2592-2595.
178. J. Bandler, M. Ismail, J. Rayas-Sanchez, and Q. Zhang, "New Directions in Model Development for RF-Microwave Components

-
- Utilising Artificial Neural Networks and Space Mapping,” *IEEE APS International Symposium Digest*, Orlando, FL, July 1999, pp. 2572-2575.
179. G. Antonini and A. Orlandi, “Gradient Evaluation for Neural-Networks-Based Electromagnetic Optimisation Procedures,” *IEEE Trans Microwave Theory Techniques*, vol. 48, 2000, pp. 874-876.
180. Q. J. Zhang, F. Wang, and M. S. Nakhla, “Optimization of High-Speed VLSI Interconnects: A Review,” *International Journal of Microwave Millimeter-Wave*, vol. 7, 1997, pp. 83-107.
181. Q. J. Zhang, “Neuromodeling of Microwave Circuits Exploiting Space Mapping Technology,” *IEEE MTT-S International Microwave Symposium Digest*, Anaheim, CA, June 1999, pp. 149-152.
182. P. M. Watson and K. C. Gupta, “EM-ANN Models for Mmicrostrip vias and Interconnects in Dataset Circuits,” *IEEE Trans Microwave Theory Techniques*, vol. 44, 1996, pp. 2495-2503.
183. P. M. Watson, K. C. Gupta, and R.L. Mahajan, “Development of Knowledgebased Artificial Neural Network Models for Microwave Components,” *IEEE MTT-S International Microwave Symp. Dig*, Baltimore, MD, June 1998, pp. 9-12.
184. P. M. Watson, K. C. Gupta, and R. L. Mahajan, “Applications of Knowledgebased Artificial Neural Network Modeling to Microwave Components,” *International Journal of RF Microwave CAE*, 9th May 1999, pp. 254-260.
185. K. C. Gupta, “EM-ANN Models for Microwave and Millimeter-wave
-

-
- Components,” *IEEE MTT-S International Microwave Symposium Workshop on Application of ANN to Microwave Design*, Denver, CO, June 1997, pp. 17-47.
186. P. Watson and K.C. Gupta, “EM-ANN Models for via Interconnects in Microstrip Circuits,” *IEEE MTT-S International Microwave Symposium Digest*, San Francisco, CA, June 1996, pp. 1819-1822.
187. P. M. Watson and K. C. Gupta, “Design and Optimization of CPW Circuits using EM-ANN Models for CPW Components,” *IEEE Trans Microwave Theory Techniques*, vol. 45, 1997, pp.2515-2523.
188. P. Watson, G. Creech, and K. Gupta, “Knowledge Based EM-ANN Models for the Design of Wide Bandwidth CPW Patch-slot Antennas,” *IEEE APS International Symposium Digest*, Orlando, FL, July 1999, pp. 2588- 2591.
189. G. L. Creech, B. Paul, C. Lesniak, T. Jenkins, R. Lee, and M. Calcaterra, “Artificial Neural Networks for Accurate Microwave CAD Applications,” *IEEE MTT-S International Microwave Symposium Digest*, San Francisco, CA, June 1996, pp. 733-736.
190. Y. Harkouss, J. Rousset, H. Chehade, E. Ngoya, D. Barataud, and J. P. Teyssier, “Modeling Microwave Devices and Circuits for Telecommunications System Design,” *Proceedings IEEE International Conference on Neural Networks*, Alaska, May 1998, pp. 128-133.
191. H. Zaabab, Q. J. Zhang, and M. Nakhla, “Analysis and Optimization of Microwave Circuits & Devices using Neural Network Models,” *IEEE*

-
- MTT-S International Microwave Symposium Digest*, San Diego, CA, May 1994, pp. 393-396.
192. V. K. Devabhaktuni, C. Xi, F. Wang, and Q. J. Zhang, "Robust Training of Microwave Neural Models," *IEEE MTT-S International Microwave Symposium Digest*, Anaheim, CA, June 1999, pp. 145-148.
193. S. Goasguen, S. M. Hammadi, and S. M. El-Ghazaly, "A Global Modeling Approach using Artificial Neural Network," *IEEE MTT-S International Microwave Symposium Digest*, Anaheim, CA, June 1999, pp. 153-156.
194. G. L. Creech, "Neural Networks for the Design and Fabrication of Integrated Circuits," *IEEE MTT-S International Microwave Symposium Workshop on Application of ANN to Microwave Design*, Denver, CO, June 1997, pp. 67-86.
195. G. Fedi, S. Manetti, G. Pelosi, and S. Selleri, "Design of Cylindrical Posts in Rectangular Waveguide by Neural Network Approach," *IEEE APS International Symposium Digest*, Salt Lake City, UT, July 2000, pp. 1054-1057.
196. G. Fedi, A. Gaggelli, S. Manetti, and G. Pelosi, "Direct-Coupled Cavity Filters Design using a Hybrid Feedforward Neural Network-Finite Elements Procedure," *International Journal of RF and Microwave CAE*, 9th May 1999, pp. 287-296.
197. S. Bila, Y. Harkouss, M. Ibrahim, J. Rousset, E. N'Goya, D. Billargeat,

-
- S. Verdeyme, M. Auborg, and P. Guillon, "An Accurate Wavelet Neural-Network-Based Model for Electromagnetic Optimization of Microwave Circuits," *International Journal of RF and Microwave CAE*, 9th May 1999, pp.297-306.
198. S. Verdeyme, D. Billargeat, S. Bila, S. Moraud, H. Blondeaux, M. Aubourg, and P. Guillon, "Finite Element CAD for Microwave Filters," *Proceedings 28th EuMC Workshop*, Amsterdam, Netherlands, Oct. 1998, pp. 12-22.
199. P. Burrascano, S. Fiori, and M. Mongiardo, "A Review of Artificial Neural Networks Applications in Microwave Computer-Aided Design," *International Journal of RF and Microwave CAE*, 9th May 1999, pp. 158-174.
200. S. Wang, F. Wang, V. K. Devabhaktuni, and Q. J. Zhang, "A Hybrid Neural and Circuit-Based Model Structure for Microwave Modeling," *Proc 29th European Microwave Conf*, Munich, Germany, Oct. 1999, pp. 174-177.
201. M. Vai, S. Wu, B. Li, and S. Prasad, "Creating Neural Network Based Microwave Circuit Models for Analysis and Synthesis," *Proc Asia Pacific Microwave Conf*, Hong Kong, Dec. 1997, pp. 853-856.
202. Y. Harkouss, J. Rousset, H. Chehade, E. Ngoya, D. Barataud, and J.P. Teyssier, "The use of Artificial Neural Networks in Nonlinear Microwave Devices and Circuits Modeling: An Application to Telecommunication System Design," *Int JRF and Microwave CAE*,

-
- vol. 9, May 1999, pp. 198-215.
203. Y. Fang, M. C. E. Yagoub, F. Wang, and Q.J. Zhang, "A New Macromodeling Approach for Nonlinear Microwave Circuits Based on Recurrent Neural Networks," *IEEE MTT-S Int Microwave Symp Dig*, Boston, MA, June 2000, pp. 883-886.
204. Christodoulou, A. El Zooghby, and M. Georgiopoulos, "Neural Network Processing for Adaptive Array Antennas," *IEEE APS International Symposium Digest*, Orlando, FL, July 1999, pp. 2584-2587.
205. Charpentier and J. J. Laurin, "An Implementation of a Direction-Finding Antenna for Mobile Communications using a Neural Network," *IEEE Transaction on Antennas and Propagation*, vol. 47, 1999, pp. 1152-1159.
206. S. El-Khamy, M. Aboul-Dahab, and K. Hijjah, "Sidelobes Reduction and Steerable Nulling of Antenna Arrays using Neural Networks," *IEEE APS International Symposium Dig*, Orlando, FL, July 1999, pp. 2600-2603.
207. G. Castaldi, V. Pierro, and I. M. Pinto, "Neural Net Aided Fault Diagnostics of Large Antenna Arrays," *IEEE APS International Symposium Digest*, Orlando, FL, July 1999, pp. 2608-2611.
208. P. R. Chang, W. H. Yang, and K. K. Chan, "A Neural Network Approach to MVDR Beamforming Problem," *IEEE Transaction on Antennas and Propagation*, vol. 40, 1992, pp. 313-322.
209. H. L. Southall, J. A. Simmers, and T. H. O'Donnell, "Direction
-

-
- Finding in Phased Arrays with a Neural Network Beamformer,” *IEEE Transaction on Antennas and Propagation*, vol.43,1995,pp. 1369-1374.
210. M. Vai and S. Prasad, “Automatic Impedance Matching with a Neural Network,” *IEEE Microwave Guided Wave Letters*, vol. 3, 1993, pp. 353-354.
211. M. Vai and S. Prasad, “Microwave Circuit Analysis and Design by a Massively Distributed Computing Network,” *IEEE Transaction on Microwave Theory and Techniques*, vol. 43, 1995, pp. 1087-1094.
212. M. M. Vai, S. Wu, B. Li, and S. Prasad, “Reverse Modeling of Microwave Circuits with Bi-directional Neural Network Models,” *IEEE Transaction on Microwave Theory and Techniques*, vol. 46, 1998, pp. 1492-1494.
213. P. M. Watson, C. Cho, and K. C. Gupta, “Electromagnetic-Artificial Neural Network Model for Synthesis of Physical Dimensions for Multilayer Asymmetric Coupled Transmission Structures,” *International Journal of RF and Microwave CAE*, 9th May 1999, pp.175-186.
214. Wang, V.K. Devabhaktuni, C. Xi, and Q.J. Zhang, “Neural Network Structures and Training Algorithms for RF and Microwave Applications,” *International Journal of RF and Microwave CAE*, 9th May 1999, pp.216-240.
215. Q. Zhang, F. Wang, and V. Devabhaktuni, “Neural Network Structures for EMMicrowave Modeling,” *IEEE APS International Symposium*
-

-
- Dig*, Orlando, FL, July 1999, pp. 2576-2579.
216. S. S. Pattnaik, D. C. Panda, B. Khuntia, and S. Devi, "Calculation of Parameters of Microstrip Antenna Using Artificial Neural Networks," *Proceedings APSYM*, Cochin University, 2002, pp. 27-31.
217. S. S. Pattnaik, D. C. Panda, and S. Devi, "Input Impedance of Rectangular Microstrip Patch Antenna Using Artificial Neural Networks," *Microwave and Optical Technology Letters*, vol. 32, no. 5, 5th March 2002, pp.381-383.
218. S. Devi, D. C. Panda, and S. S. Pattnaik, "A Novel Method of Using Artificial Neural Networks to Calculate Input Impedance of Circular Microstrip Antenna," *Proceedings IEEE Antennas and Propagation Society International Symposium*, vol. 3, June 2002, pp.462 – 465.
219. S. S. Pattnaik, D. C. Panda, and S. Devi, "Input Impedance of Circular Microstrip Antenna Using Artificial Neural Networks," *IETE Technical Review*, vol. 19, no. 3, Mar-June 2002, pp.125-127.
220. S. S. Pattnaik, D. C. Panda, and S. Devi, "Tunnel Based Artificial Neural Networks Technique to Calculate the Resonant Frequency of Thick Substrate Microstrip Antenna," *Microwave and Optical Technology Letters*, vol. 34, no. 6, 20th Sept. 2002, pp.460-462.
221. S. S. Pattnaik, D. C. Panda, and S. Devi, "Radiation Resistance of Coax-Fed Rectangular Microstrip Patch Antenna Using Artificial Neural Networks," *Microwave and Optical Technology Letters*, vol. 34, no. 1, 5th July 2002, pp.51-53.
-

-
222. S. Devi, D. C. Panda, S. S. Pattnaik, B. Khuntia, and D. K Neog, "Initializing Artificial Neural Networks by Genetic Algorithm to Calculate the Resonant Frequency of Single Shorting Post Rectangular Patch Antenna," *IEEE Antennas and Propagation Society, AP-S International Symposium (Digest)*, vol. 3, 2003, pp 144-147.
223. D. K. Neog, S. S. Pattnaik, D. C. Panda, S. Devi, B. Khuntia, and M. Dutta, "Design of a Wide Band Microstrip Antenna and use of Artificial Neural Networks in the Parameter Calculation," *IEEE Antenna and Propagation Magazine*, vol.47, no.3, June2005, pp.60-65.
224. S. S. Pattnaik, B. Khuntia, D. C. Panda, D. K. Neog, S. Devi, and M. Dutta, "Application of Genetic Algorithm on Artificial Neural Networks to Calculate Resonant Frequency of Tunable Single Shorting Post Rectangular Patch Antenna," *International Journal of RF and Microwave Computer Aided Engineering*, vol. 15, no. 1, Dec. 2004, pp. 140-144.
225. S. S. Pattnaik, D. C. Panda, B. Khuntia, S. Devi, and D. K.Neog, "Tunnel Based Artificial Neural Network to Calculate the Radiation Pattern of Cell Phone Antenna in Presence of Human Head," *Proceedings IEEE-ASPW*, Delhi, 2002, pp.330-334.
226. S. S. Pattnaik, D. C. Panda, B. Khuntia, S. Devi, and D.K.Neog, "Tunnel Based Artificial to Calculate the Radiation Pattern of Commercially Available Cell Phone Antenna in Presence of Human Head Initialized by Genetic Algorithm," *Horizons of*

-
- Telecommunication, Institute of Radio Physics and Electronics, University of Calcutta, 2003.*
227. R. K. Mishra and A. Patnaik, "Design of Circular Microstrip Antenna using Neural Network," *IETE Journal of Research*, vol. 44, nos. 1–2, Jan.–Apr. 1998, pp. 35–39.
228. D. C. Panda, S. S. Pattnaik, B. Khuntia, S. Devi, D. K. Neog, and R. K. Mishra, "Application of NFDTD for the Calculation of Parameters of Microstrip Antenna," *International Conference on Antenna Technologies, ICAT, Ahmedabad, Feb. 21-22, 2005.*
229. S. S. Pattnaik, B. Khuntia, D. C. Panda, D. K. Neog, and S. Devi, "Calculation of Optimized Parameters of Rectangular Microstrip Patch Antenna Using Genetic Algorithm," *Microwave and Optical Technology Letters*, vol. 23, no. 4, 20th June 2003, pp. 431-433.
230. R. J. Schalkoff, "Artificial Neural Networks," McGraw-Hill Companies. Inc., 1997.
231. B. L. Kalam and S. C. Kwasny, "Why tanh: Choosing a Sigmoidal Function," *IEEE Int. Conf on Neural Networks*, vol.4, 1992, pp.578-581.
232. S. I. Amari, "Mathematical Foundation of Neurocomputing," *IEEE Proceedings*, vol. 78, no.9, 1990, pp.1443-1463,.
233. K. Hornik, M. Stinchcombe, and H. White, "Multilayered Feed-Forward Networks are Universal Approximators," *IEEE Trans. Neural Networks*, vol.2, 1989, pp.359-366.
234. T. Chen, H. Chen, and R. Liu, "Approximation Capability in $C(\mathbb{R}_n)$ by

-
- Multilayer Feedforward Networks and Related Problems,” *IEEE Transaction on Neural Networks*, vol.6, no.1, Jan.1995, pp.25-30.
235. Y. Lee, S. H. Oh, and M. W. Kim, “The Effect of Initial Weights on Premature Saturation in Backpropagation Learning,” *IEEE Proceedings, International Joint Conference on Neural Networks*, vol. I, 1991, pp. 765-770.
236. H. Lari-Najafi, M. Nasiruddin, and T. Samad, “Effect of Initial Weights on Backpropagation and its Variations,” *IEEE International Conference on Systems, Man and Cybernetics*, 1989, pp. 218-219.
237. G. P. Drago and S. Ridella, “Spastically Controlled Activation Weight Initialization SCAWI,” *IEEE Transaction on Neural Networks*, vol.3, no.4, 1992, pp. 627-631.
238. L. Breiman, “Bagging Predictors,” *Machine Learning*, vol. 24, 1996, pp. 123-140.
239. L. Breiman, “Combining Predictors, in Combining Artificial Neural Nets: Ensemble and Modular Multi-Net Systems,” A.J.C. Sharkey (ed.), *Springer*, London, 1999, pp 31-50.
240. D. E. Rumelhart, G. E. Hinton, and R. J. Williams, “Learning Internal Representations by Error Propagation,” *Parallel Distributed Processing*, Cambridge, MA, MIT Press, vol. I, 1986, pp. 318-362.
241. P. J. Werbos, “Beyond Regression: New Tools for Prediction and Analysis in the Behavioural Sciences,” PhD Thesis, Harvard University.

-
242. K. Hornik, M. Stinchcombe, and H. White, "Multilayer Feed Forward Networks are Universal Approximators," *Neural Networks*, vol. 2, no. 5, 1989, pp. 359-366.
 243. G. Cybenko, "Approximation by Superpositions of a Sigmoidal Function. Mathematics of Control," *Signals, and Systems*, vol. 2, no. 4, 1989, pp.303-314.
 244. E. J. Hartman, J. D. Keeler, and J. M. Kowalski, "Layered Neural Networks with Gaussian Hidden Units as Universal Approximations," *Neural Computation*, vol. 2, no. 2, 1990, pp.210-215.
 245. V. Rao and H. Rao, "C++ Neural Networks and Fuzzy Logic," BPB, New Delhi, pp.336, 1996.
 246. P. R. Chowdhury, Y. P. Singh, and R.A. Chansarkar, "Dynamic Tunneling Technique for Efficient Training of Multilayer Perceptrons," *IEEE Transactions on Neural Networks*, vol. 10, no.1, Jan.1998, pp.48-55.
 247. K. Deb, "Optimization for Engineering Design, Algorithm and Examples," New Delhi, India: Prentic-Hall of India, 1995.
 248. I.Papapolymerous, R.F.Drayton, and L.P.B. Katehi," Micromachined patch antennas," *IEEE Transactions on Antennas and Propagation*, Vol. 46, Feb.1998, pp.275-283.
 249. N.Herscovici,"New considerations in the design of microstrip antennas", *IEEE Transactions on Antennas and Propagation*, Vol. 46, June1998, pp.807-812.

-
250. A.K.Skrivervik, J.-F. Zurcher, O.Staub and J.R Mosig, "PCS Antenna Design: The Challenge of Miniaturization", *IEEE Antennas and Propagation Magazine*, Vol. 43, No.03, August, 2001, pp.12-25,.
 251. S.M.Rao, D.R.Wilton, and A.W.Glission, "Electromagnetic scattering by surfaces of arbitrary shape," *IEEE Transactions on Antennas and Propagation*, vol. 30, May. 1982, pp 409-418.
 252. X.X.Zhang and F.Yang, "The study of slit cut on the microstrip antenna and it s applications," *Microwave Optical Techn. Lett.*, vol.18, no.4, July. 1998, pp. 297-300.
 253. K. Sarabandi and R. A. Azadegan, "Design of an efficient miniaturization UF planar antenna," *IEEE Transactions on Antennas and Propagation*, Vol. 51, No. 6, June-2003, pp. 1270-1276.
 254. Zhi Ning Chen and Y. W. M. Chia, "Radiation pattern of a probe-fed L-shaped plate antenna," *Microwave And Optical Technology Letters*, Vol. 27, No. 6, Dec-20, 2000, pp. 410-413.
 255. Zhi Ning Chen, "Radiation pattern of a probe-fed L-shaped plate antenna," *Microwave And Optical Technology Letters*, Vol. 27, No. 6, Dec-20, 2000, pp. 410-413.
 256. D.K.Neog, S.S.Pattnaik, M.Dutta, S.Devi, B.Khuntia and D.C.Panda, "Inverted-L shaped and parasitically coupled inverted-L shaped microstrip patch antennas for wide bandwidth", *Microwave and Optical Technology Letters*, Vol.42, No.3, August, 2004, pp 190-192.
 257. D. R Jahagirdar and R. D. Stewart, "Non-leaky conductor backed

- coplanar wave guide-fed rectangular microstrip patch antenna.” *IEEE Microwave and Guided-Wave Letters*, vol. 8, no. 3, March 1998, pp.115-117.
258. S. M. Deng, M. D. Wu and P. Hsu, “Analysis of coplanar waveguide-fed microstrip antenna.” *IEEE Transactions on Antennas and Propagation*, vol. 43, no. 7, July 1995, pp.734-737.
259. XinYun, Elise C. Fear, Ronald H. Johnston, “Compact Antenna for Radar Based Breast Cancer Detection”, *IEEE Transactions on Antennas and Propagation*, Vol. 53, August, 2005, pp 2374-2380.
260. D.Pozar, “Input impedance and mutual coupling of rectangular microstrip antenna”, *IEEE Transactions on Antennas and Propagation*, Vol. 30, Jun 1982, pp 1191-1196.
261. M.Despanday, D. Shively, and C.R.Cockrell, “Resonant frequencies of irregularly shaped microstrip antennas using method of moments,” NASA Tech. Paper 3386, 1993.
262. D.Yau, N.V. Shuley and L.O.McMillan, “Characteristics of microstrip leaky wave antenna using the method of moments”, *IEE Proc-Microw. Antennas Propagation*, Vol. 146, No. 5, October 1999, pp 324-328,.
263. J.S.Dahele and K.F.Lee, “On the resonant frequencies of the triangular patch antenna”, *IEEE Transactions on Antennas and Propagation*, Vol. AP-35, January 1987, pp 100-101.
264. R.Garg and S.A.Long, “An improved formula for the resonant

-
- frequencies of the triangular microstrip patch antenna”, *IEEE Transactions on Antennas and Propagation*, Vol. AP-36, 1989, pp 570.
265. R.Singh, A.De and R.S.Yadav, “On the resonant frequency of the triangular microstrip patch radiator”, The 3rd Asia Pasific Microwave Conference Proceedings, Tokyo, pp 289-291, 1990.
266. N.Kumprasert and W. Kiranon, “Simple and accurate formula for the resonant frequency of the equilateral triangular microstrip patch antenna”, *IEEE Transactions on Antennas and Propagation*, Vol. AP-42, No.8, 1994, pp 1178-1179.
267. Kerim Guney, “Comments on – on the resonant frequencies of microstrip antennas, *IEEE Transactions on Antennas and Propagation*, Vol.42, No.9, 1994, pp 1363-1365.
268. M.Kara, “ Closed-Form Expression for the Resonant frequency of rectangular Microstrip Antenna Elements with Thick Substrates”, *Microwave and Optical Technology Letters*, Vol.12, No.3, June1996, pp 131-136.
269. P. Mythill and A. Das, “Simple approach to determine resonant frequencies of microstrip antenna”, *IEE Proc- Microw. Antennas Propagation*, Vol. 145, No. 2, April 1998, pp 159-162.
270. Rajanish and T.S.Vedavathy, “Resonant frequency of higher order modes for circular microstrip antenna”, Asia Pasific Microwave Conference (APMC'99), 1999, pp 936-940.
271. K.P.Ray and Girish Kumar, “Determination of the resonant frequency
-

- of microstrip antennas”, *Microwave and Optical Technology Letters*, Vol.23, No.2, October, 1999, pp 114-17.
272. G. Angiulli and M. Versaci, “Resonant frequency evaluation of microstrip antennas using a neural-fuzzy approach”, *IEEE Transaction on Magnetics*, Vol.39, No.3, 2003, pp 1333-1336.
273. J.R.James, P.S. Hall and C. Wood, “Microstrip Antenna Theory and Design”, Peter Peregrinus Ltd, London, 1981.
274. A.F.Sheta, A.Mohra and S.F.Mahmoud, “Multi-band operation of a compact H-shaped microstrip antenna”, *Microwave and Optical Technology Letters*, Vol.35, No.5, December, 2002, pp 363-367.
275. D.K.Neog, S.S.Pattnaik, M.Dutta, D.C.Panda, S.Devi and B.Khuntia, “A novel patch antenna for wide band generation”, *Proceeding of international conference on antenna technologies*, 2005, pp 345-348.
276. H. Yamashita, N. Kowata, V. Cingoski, and K. Kaneda, “Direct Solution Method for Finite Element Analysis Using Hopfield Neural Network,” *IEEE Transactions on Magnetics*, vol. 31, no. 3, pp. 1964-1967, 1995.
277. J. Takeuchi and Y. Kosugi, “Neural Network Representation of Finite Element Method,” *Neural Networks*, vol. 7, pp.389-395, 1994.
278. T. S. Low and B. Chao, “The use of Finite Elements and Neural Networks for the Solution of Inverse Electromagnetic Problem,” *IEEE Transactions on Magnetics*, vol. 28, no. 5, pp. 2811-2814, 1992.
279. S. Sagiroglu and K. Gunney, “Calculation of Resonant Frequency for

- an Equilateral Triangular Microstrip Antenna with use of Artificial Neural Networks,” *Microwave and Optical Technology Letters*, vol. 14, no. 2, 1997, pp.89-93.
280. D. T Davis, C. H. Chan, and J. N. Hwang, “Frequency Selective Surface Design using Neural Networks Inversion Based on Parameterized Representation,” *IEEE Symposium on Antennas and Propagation*, London, Canada, June, pp.200-203,1991.
281. J. N. Hwang, C. H. Chan, and R. J. Marks II, “Frequency Selective Surface Design Based on Iterative Inversion of Neural Networks,” *Proceedings International Joint Conference on Neural Networks*, San Diego, CA, pp. 139-144, June 1990.
282. M. Alberti, “A Hopfield Network Based Adaptation Algorithm for Phased Antenna Arrays,” *Proceedings of IEEE Workshop on Neural Networks in Signal Processing*, pp.555-564, 1994.
283. H. L. Southall, J. A. Simmers, and T. H. O’Donnell, “Directional Finding Phased Arrays with a Neural Network Beamformer,” *IEEE Transaction on Antenna and Propagation*, vol. 43, no. 12, pp.1369-1374, 1995.
284. A. H. El Zooghby, C. G. Christodoulou, and M. Georgiopoulos, “Neural Network Based Adaptive Beamforming for One- and Two-Dimensional Antenna Arrays,” *IEEE Transaction on Antenna and Propagation*, vol. 46, no. 12, pp. 1891-1893,1998.
285. A. H. El Zooghby, C. G. Christodoulou, and M. Georgiopoulos, “A

-
- Neural Network-based Smart Antenna for Multiple Source Tracking,”
IEEE Transaction on Antenna and Propagation, vol. 48, no. 5, pp.768-776, May 2000.
286. Pichitpong Soontornpipit, Cynthia M Furse and You Chung Chung, “Miniaturized biocompatible microstrip antenna using genetic algorithm,” *IEEE Transaction on Antennas and Propagation*, June 2005, pp.1939-1945.
287. Pichitpong Soontornpipit, Cynthia M Furse and You C.Chung, “Design of implantable microstrip antenna for communication with medical implants,” *Special issue of IEEE Transaction on Microwave Theory and Techniques on Medical Applications and Biological Effects of RF/Microwaves*, September 2004.
288. C.Furse, “Design of an antenna for pacemaker communication,” *Microwaves and RF*, March 2000, pp.73-76.
289. C. M. Furse, Y. Cui, G. Lazzi, and O. P. Gandhi, "Use of PML Boundary Conditions for Wireless Telephone Simulations," *Microwave and Optical Technology Letters*, Vol.15, no.2, pp.95-98, June 5 1997.
290. O.Gandhi, G.Lazzi, C.Furse, "Electromagnetic Absorption in the Human Head and Neck for Mobile Telephones at 835 and 1900 MHz," *IEEE Transactions on Microwave Theory and Techniques*, Vol. 44, pp. 1884-1897, 1996.
291. K. Gosalia and G. Lazzi, "Reduced Size, Dual Polarized Microstrip
-

-
- Patch Antenna for Wireless Communications," to be printed in IEEE Transactions on Antennas and Propagation, Nov. 2003.
292. G. Lazzi, O.P. Gandhi, and D. Sullivan "Use of PML Absorbing Layers for the Truncation of the Head Model in Cellular Telephone Simulations," IEEE Transactions on Microwave Theory and Techniques, Special Issue on Biological Effects and Medical Applications of RF/Microwaves, pp.2033-2039, Nov. 2000.
293. O.P. Gandhi, G. Lazzi, A.D. Tinniswood, and Q.S. Yu, "Numerical and Experimental Methods for Determination of SAR and Radiation Patterns of Handheld Wireless Telephones," Bioelectromagnetics, Vol. 20, pp. 93-101, March 1999.
294. O.P.Gandhi, G.Lazzi, and C.M.Furse, "Electromagnetic Absorption in the Human Head and Neck for Mobile Telephones at 835 and 1900 Mhz," IEEE Transactions on Microwave Theory and Techniques, Vol.44, pp.1884-1897, Oct. 1996.